Importance of *AtAOX1a* during oxidative stress in *Arabidopsis thaliana* and *Saccharomyces cerevisiae*

Thesis submitted for the award of the degree of

DOCTOR OF PHILOSOPHY

BY

ABHAY PRATAP VISHWAKARMA

(Enrollment No. 08LPPH21)

DEPARTMENT OF PLANT SCIENCES
SCHOOL OF LIFE SCIENCES
UNIVERSITY OF HYDERABAD
HYDERABAD-500 046, INDIA

Oct 2015

DEPARTMENT OF PLANT SCIENCES
SCHOOL OF LIFE SCIENCES
UNIVERSITY OF HYDERABAD
HYDERABAD-500 046, INDIA

DECLARATION

I hereby declare that the work presented in this thesis entitled **"Importance of *AtAOX1a* during oxidative stress in *Arabidopsis thaliana* and *Saccharomyces cerevisiae*"**, has been carried out by me under the supervision of Dr. K.P.M.S.V. Padmasree in the Department of Plant Sciences, School of Life Sciences, University of Hyderabad and this work has not been submitted for any degree or diploma of any other University or Institute. The work is plagiarism free.

Abhay Pratap Vishwakarma
(Candidate)
Enrol. No. 08LPPH21

Dr. K. P. M. S. V. Padmasree
(Supervisor)

DEPARTMENT OF PLANT SCIENCES
SCHOOL OF LIFE SCIENCES
UNIVERSITY OF HYDERABAD
HYDERABAD-500 046, INDIA

CERTIFICATE

This is to certify that **Mr. Abhay Pratap Vishwakarma** has carried out the research work embodied in the present thesis entitled **"Importance of *AtAOX1a* during oxidative stress in *Arabidopsis thaliana* and *Saccharomyces cerevisiae*"**, for the degree of Doctor of Philosophy under my supervision in the Department of Plant Sciences, School of Life Sciences, University of Hyderabad.

Dr. K.P.M.S.V. Padmasree
(Supervisor)
Department of Biotechnology and Bioinformatics

Head
Department of Plant Sciences

Dean
School of Life Sciences

DEDICATED TO MY MOTHER

Acknowledgements

With great pleasure I express my deep sense of gratitude to my supervisor **Dr. K.P.M.S.V. Padmasree** for her constant support, encouragement and guidance. She has been liberal and always let me work the way I liked. Association with her through these years has given me an opportunity to understand and learn key research and professional skills.

I am grateful to my doctoral committee members, **Prof. A.S. Raghavendra** and **Dr. Sarada Devi Tetali** for their valuable suggestions throughout my doctoral work and also for allowing me to use their lab facilities.

Thanks are due to **Prof. Ch. Venkat Ramana**, Head, Department of Plant Sciences and **Prof. P. Reddanna**, Dean, School of Life Sciences, for providing necessary facilities for my research. I extend my thanks to former Heads of Department, **Prof. Appa Rao Podile** and **Prof. Attipalli R. Reddy** and the former Deans, **Prof. A.S. Raghavendra**, **Prof. M. Ramanadham**, **Prof. Aparna Dutta Gupta** and **Prof. R.P. Sharma.**

I am extremely grateful to **Prof. Renate Scheibe** for a kind gift of Arabidopsis seeds.

I am grateful to **Prof. P.B. Kirti** for his guidance in yeast work and also for extending his lab facilities.

I thank **Prof. B. Senthilkumaran** and **Mrs. Leena** for their help and suggestions in Real time PCR study.

I am thankful to **Prof. P. Prakash Babu** and his research scholar **Dr. Suraj** for helping me in antibody generation.

I thank **Ms. Nalini** and **Mrs. Monica** for their technical support in using confocal and proteomics facilities respectively.

I also thank all the **faculty members** of School of Life Sciences.

I am thankful to my former labmates **Dr. Dinakar** and **Dr. Prasad** for their help and guidance in learning the basic lab techniques during my early days of joining. I extend my thanks to present labmates **Srinivas**, **Swathi**, **Mohan**, **Lokya**, **Swaroop**, **Shankar**, **Mariyamma** and **Kalyani** for enjoyable company.

I extend my thanks and appreciation to Lab attendants **Mr. Arun** and **Mr. Prashant** for his help in lab and greenhouse.

I thank all **research scholars** from **Prof. A.S. Raghavendra**, **Prof. P.B. Kirti** and **Dr. Sarada Devi** laboratory for their help and co-operation in utilizing the respective lab facilities.

I am highly grateful to my friends from campus, **Suresh**, **Das**, **Abhay kumar**, **Ahan**, **Naveen**, **Pawan**, **Anirudh**, **Rakesh**, **Kapil**, **Sai Krishna**, **Shivendra**, **Soorat**, **Dilip**, **Deepankar**, **Israr**, **Sumit**, **Kamal**, **Prateek**, **Zahoor** and **Debashree** for their affection and support throughout my research tenure.

It's time to thank all my non-HCU friends, **Pradeep**, **Swatantra**, **Govind**, **Vivek**, **Amit**, **Rahul**, **Chitrank**, **Virendra**, and **Ritu.** They were behind me in all ups and downs and supported me till now and forever. Thank you all for being there with me.

I am thankful to all the **non teaching staff** members of Department of Plant Sciences and School of Life Sciences for their help in official work.

I gratefully acknowledge the **UOH-BBL**, **DBT-CREBB-JRF** and **CSIR-SRF** for research fellowship.

I am thankful to **DBT-CTEP** for providing me travel grant and **UoH-DST-PURSE grant** for per diem to attend an International conference organized at Baku, Azerbaijan.

I also acknowledge **UGC**, **CSIR**, **DBT**, **DST**, **DBT-CREBB**, **DST-FIST**, **UGC-SAP** and **UPE** for research funding to the laboratory, Department and School of Life Sciences.

My special thanks to my **parents**, **brother**, **sisters**, **bhabhi** and **jiju** for their patience, constant support and confidence on me.

Abhay

TABLE OF CONTENTS

List of Abbreviations

AA	=	antimycin A
AL	=	actinic light
AOX	=	alternative oxidase
aox1a	=	mutant lacking alternative oxidase 1a
ADH	=	alcohol dehydrogenase
CEF-PSI	=	cyclic electron flow around photosystem I
COX	=	cytochrome c oxidase
DCPIP	=	dichlorophenolindophenol
DEPC	=	diethylpyrocarbonate
ETR	=	electron transport rate
Fv/Fm	=	maximum quantum yield of photosystem II
H_2DCF-DA	=	2',7'-dichlorodihydrofluorescien diacetate
HL	=	high light
IPTG	=	isopropyl-β-D-thiogalactopyranoside
KCN	=	potassium cyanide
LEF	=	linear electron flow
MDA	=	malondialdehyde
MDH	=	malate dehydrogenase
mETC	=	mitochondrial electron transport chain
NPQ	=	non-photochemical quenching
OAA	=	oxaloacetic acid
PCD	=	programmed cell death
PCR	=	polymerase chain reaction
PMS	=	phenazine methosulfate
PPFD	=	photosynthetic photon flux density
PSI	=	photosystem I
PSII	=	photosystem II
PTOX	=	plastid terminal oxidase
PQ	=	plastoquinone

PQH2	=	plastoquinol
PVDF	=	polyvinylidene difluoride
qP	=	photochemical quenching
ROS	=	reactive oxygen species
SDS-PAGE	=	sodiumdodecyl sulfate polyacrylamide gel electrophoresis
SHAM	=	salicyl hydroxamic acid
SP	=	saturation pulse
TBA	=	thiobarbituric acid
TBOOH	=	tertiary butyl hydroperoxide
TCA	=	trichloroacetic acid
UCP	=	uncoupling protein
UQ	=	ubiquinone
WT	=	wild-type
WWC	=	water-water cycle
Y(I)	=	quantum yield of PSI
Y(II)	=	quantum yield of PSII

Chapter 1

Introduction and Review of Literature

Higher plants are sessile in nature. Therefore, they are often challenged by several biotic and abiotic stresses, which may lead to oxidative stress due to an imbalance between production and detoxification of free radicals at the cellular level. On the other hand, being aerobic, plants are also prone to undergo oxidative stress. Mitochondria and chloroplasts are the main source of reactive oxygen species (ROS) generation, because any over reduction of ubiquinone (UQ)/plastoquinone (PQ) enhance the probability of electron leakage and once these leaky electrons react with O_2, it leads to generation of ROS. Under such circumstances alternative oxidase (AOX) pathway has been found very promising enzyme as it catalyzes cyanide-resistant respiration and prevents over-reduction of the cyanide-sensitive cytochrome oxidase (COX) pathway and thereby generation of ROS. During this process, AOX plays a significant role in oxidizing the UQ pool without ATP generation under several biotic/abiotic stresses. An analog of AOX called as plastid terminal oxidase (PTOX) has also been found in chloroplast, and it is known to oxidize the PQ pool. Thus, it is suggested that AOX plays an important role in energy balance, minimizing ROS levels and is also capable of playing various physiological roles under stress conditions. The present study is centered on AOX and its importance during oxidative stress caused by high light stress or restriction of electron transport through COX pathway.

1. Alternative Oxidase

AOX is not only confined to plant kingdom but also has been found in archaea, yeast, some protists and animals. Initially, it was identified in thermogenic plants of the Araceae family (Meeuse 1975). Due to higher AOX catalysed respiration these thermogenic plants are able to warm up their reproductive tissues independent from ambient temperature and thus provide the favorable conditions for floral development (Watling et al., 2006;

Wagner et al., 2008; Miller et al., 2011). Later, it was found in several lower organisms including yeasts studied till date, but exceptionally absent in *Saccharomyces cerevisiae* and *Schizosaccharomyces pombe* (McDonald et al., 2009; Neimanis et al., 2013; Rogov et al., 2014).

1.1. Structure and regulation of AOX

AOX is located in the inner membrane of mitochondria. Genome sequencing studies revealed that the position of four glutamate and two histidine residues were conserved in the amino acid sequence of AOX (Siedow et al., 1995). It was found that these residues act as ligands in the diiron active site. Therefore, the AOX was assigned to diiron carboxylate protein family (Moore et al., 1995; Berthold et al., 2002; Berthold and Stenmark, 2003). Site-directed mutagenesis studies further confirmed the essential nature of these amino acids as well as identifying other residues (e.g., tyrosine) essential for AOX activity (Albury et al., 2002; Moore and Albury, 2008). EPR spectroscopy studies revealed that the active site for the reduction of oxygen to water comprise a binuclear iron center (Berthold et al., 2002; Moore et al., 2008), while other studies have identified the residues important for ubiquinol binding (Moore and Albury, 2008; Albury et al., 2010). A crystal structure of AOX from *Trypanosome brucei* revealed that the oxidase is an integral interfacial membrane protein with nonhaem diiron carboxylate active site buried within a four helix bundle and exists as a homodimer. The active site is ligated by four glutamate residues and a highly conserved Tyr220 is responsible for its catalytic activity. Further, two hydrophobic cavities occur per monomer which bind with ubiquinol and Tyr220 for catalytic cycle and O_2 reduction (Moore et al., 2013; Shiba et al., 2013; Young et al., 2013).

Two types of AOX can be phylogenetically distinguished based on their regulatory mechanism. First, the plant-type AOX, which exist as a nonfunctional covalent homodimer and activated in the presence of soluble reductants (e.g. thioredoxin and

glutathione) and α-keto acids (Umbach and Siedow, 1993; Rhoads et al., 1998). Second, the fungi-type AOX, which exists as a monomer and regulated by nucleotide monophosphates (Sakajo et al., 1997; Rogov et al., 2014). The monomer structure of fungal AOX was first revealed by Joseph-Horne et al. (2000). They found that the conserved cysteine residues responsible for dimerization of AOX in plants were absent in fungal AOX.

1.2. Composition of mitochondrial respiratory apparatus and role of AOX in oxidizing ubiquinol

The respiratory apparatus of plant mitochondria is divided into four different components: (a) TCA cycle, responsible for oxidative decarboxylation of organic acids leading to reduction of NAD(P) and FAD, and substrate-level phosphorylation of ADP to ATP; (b) the classical oxidative phosphorylation coupled to NAD(P)H and $FADH_2$ oxidation; (c) rotenone-insensitive type-2 NAD(P)H dehydrogenases and the non-energy conserving AOX; (d) the set of carriers and channels that provide the substrates and cofactors for these processes from the cytosol and those that facilitate release of the products of respiration to the rest of the cell (Millar et al., 2011).

Mitochondrial electron transport chain (mETC) is composed of five complexes. Complex I (NADH dehydrogenase) catalyzes the oxidation of matrix NADH to reduce the UQ **(Fig. 1.1)**. In plants, so far 49 subunits have been separated from Complex I by combinations of native and denaturing electrophoresis. However, 32 subunits showed high similarity to mammalian Complex I components while 17 subunits were found to be unique to plants (Heazlewood et al., 2003; Klodmann et al., 2010). The cytoplasmic male-sterile mutants (CMSII) impaired in Complex I function showed an increase in AOX catalysed respiration, antioxidant capacity and decrease in ROS levels, suggesting that plants can survive without Complex I (Dutilleul et al., 2003). In contrast, it was also

observed that CMSII mutants impair the AOX engagement and modulated redox homeostasis during elicitor (harpin) induced cell death in tobacco (Vidal et al., 2007).

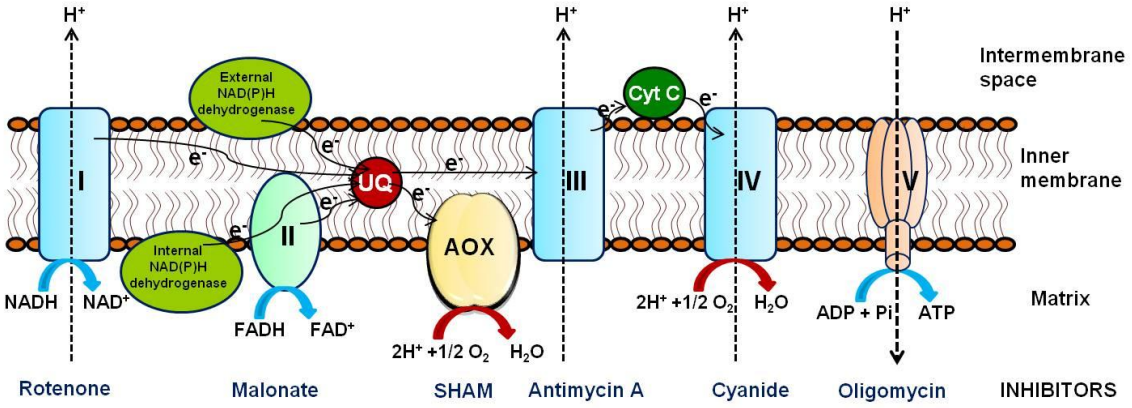

Fig.1.1. A diagrammatic representation of plant mitochondrial electron transport chain. The inner mitochondrial membrane houses the several Complexes (I, II, III, IV and V). The respective inhibitor has been shown below each complex. A continuous arrow shows the flow of electrons while dotted arrow indicates the flow of protons. Abbreviations: Q-ubiquinone, Cyt C-cytochrome C, SHAM-salicylhydroxamic acid.

Complex II (succinate dehydrogenase) oxidizes FADH with subsequent reduction of UQ. Complex II is composed of four core subunits i.e. SDH1, SDH2, SDH3 and SDH4 (Figueroa et al., 2002). The essentiality of Complex II has been demonstrated in gametophyte development in Arabidopsis (León et al., 2007). Complex III is UQ-cytochrome c oxidoreductase. Using blue native/sodium dodecyl sulphate-polyacrylamide gel electrophoresis (BN/SDS-PAGE), ten subunits have been separated in Arabidopsis (Meyer et al., 2008). Complex IV (cytochrome c oxidase; COX) is a terminal oxidase, consisting of 14 subunits. Eight proteins were found to be homologous with other organisms, whereas six subunits represented the plant specific COX subunits (Millar et al., 2004).

Electron transport via complexes I, III and IV is coupled with proton translocation (4, 4 and 2 H^+, respectively) from mitochondrial matrix to the intermembrane space (IMS), resulting in generation of electrochemical proton gradient. Complex V (ATP synthase) catalyzes the oxidative phosphorylation where the energy stored in

electrochemical proton gradient is converted to ATP in the mitochondrial matrix. Plant mETC is specially featured with two dehydrogenases (external and internal) and cyanide-insensitive terminal oxidase i.e. AOX (Schonbaum et al., 1971; Vanlerberghe and McIntosh 1997; Møller, 2001). The external and internal dehydrogenases are known to reduce the UQ. In contrast, both COX and AOX oxidize the UQ with simultaneous reduction of O_2 to H_2O. However, when the electrons flow through the AOX pathway that branches at the level of UQ, the proton pumping at Complex III and IV is avoided and energy is simply dissipated as heat (Millenaar and Lambers 2003).

1.3. Capacity and activity of AOX

As described above, AOX is non-proton pumping terminal oxidase and bypasses the proton-pumping complexes III and IV. Thus, electron flow through AOX dramatically decreases the energy yield of respiration. The maximum possible flux of electrons to AOX is known as AOX capacity, also considered as an analogous estimation of AOX enzyme activity. The AOX capacity of a tissue, isolated mitochondria or protoplasts can be estimated by the addition of a COX pathway inhibitor such as cyanide (CN), followed by addition of AOX inhibitor such as *n*-propyl gallate or salicylhydroxamic acid (SHAM). Thus, the capacity of AOX is generally measured in terms of O_2 uptake resistant to the COX pathway inhibitor and sensitive to the AOX pathway inhibitor (Møller et al., 1988; McDonald et al., 2002). But, in this method AOX capacity cannot be measured in a steady state before the addition of inhibitors. Also, the actual flux of electrons to AOX remains unknown. However, actual electron flux depends upon the partitioning of electrons between AOX and complex III as both utilizes the common substrate (ubiquinol). Therefore, to understand the electron partitioning between AOX and COX, Guy et al. (1989) have used oxygen isotope discrimination technique, where AOX and COX discriminated heavy O_2 ($^{18}O^{16}O$). This technique has been applied to measure the AOX activity in leaf tissue, isolated mitochondria as well as at field level

(Nagel et al., 2001; Kornfeld et al., 2012). However, one major limitation of the isotope discrimination method is that it can be executed only in dark conditions. Hence, this method is not applicable to measure the AOX activity during photosynthesis. These constraints can be eliminated by the usage of transgenic and mutant plants with modified AOX capacity as they provide an alternate and more reliable way to estimate the importance of AOX during photosynthetic metabolism (Florez-Sarasa et al., 2011; Yoshida et al., 2011b; Gandin et al., 2012; Zhang et al., 2014).

1.4. Physiological role of AOX

1.4.1. Role of AOX in minimizing ROS and RNS generation

The generation of ROS is an inevitable consequence of aerobic respiration. The mitochondrion is a major source of ROS generation and mainly depends on the reduction state of ETC components. Complexes I and III are the major sites of ROS generation in mETC (Møller, 2001; Murphy, 2009). In case of animals, the reduction state of mETC is mainly dependent upon the electron flow, membrane potential, and oxidative phosphorylation. Thus, when ADP is readily available and being phosphorylated to ATP, dissipation of the proton gradient decreases the membrane potential and consequently less O_2^- is generated (Møller, 2001). Unlike animals, plants have much-complicated regulation of electron flow, oxidative phosphorylation, and ROS generation, since the electron flow through AOX does not contribute to a membrane potential. Thus, AOX is capable of preventing the over-reduction of the mETC and O_2^- production by keeping the continuous electron flow, even when ADP is limiting (Purvis, 1997).

Recent studies have shown the direct evidence of electron leakage and thereby increased ROS levels in AOX-deficient Arabidopsis and tobacco leaves (Strodtkötter et al., 2009; Cvetkovska and Vanlerberghe, 2012). Apart from limiting ROS, the role of AOX was also revealed in minimizing the RNS levels. In mitochondria, the single electron leaked from ETC reacts with NO_2^-, which leads to the generation of NO

(Planchet et al., 2005; Gupta et al., 2010, 2011). The transgenic tobacco lines deficient in AOX showed elevated O_2^- and NO levels when compared to WT. Furthermore, in the presence of AA, WT plants exhibited dramatic increase in O_2^- and NO levels in contrast to AOX overexpression lines (Cvetkovska and Vanlerberghe, 2013).

1.4.2. Role of AOX in signaling

In last one decade mitochondria are emerged as a signaling organelle due to its ability to influence cellular processes such as nuclear gene expression (retrograde regulation), cellular redox, ROS and programmed cell death in response to several stress and developmental stages (Clifton et al., 2006; Noctor et al., 2007; Rhoads et al., 2006; Rhoads and Subbaiah, 2007; Schwarzländer and Finkemeier, 2013). Unlike metabolic pathways, signaling pathways are often associated with an amplification of the signal by second messengers. Signaling molecules such as ROS, RNS, salicylic acid and ethylene are found to be strongly connected with mitochondrial metabolism (especially AOX), suggesting a link between AOX and signaling events (Clifton et al., 2006; Van Aken et al., 2009; Li et al., 2013b; Cvetkovska and Vanlerberghe, 2012; Vanlerberghe, 2013). Interestingly, knockdown of AOX in *Nicotiana tabacum* resulted in increased NO level, which in turn has altered the size of guard cell and stomatal movement (Cvetkovska et al., 2014). Furthermore, to maintain the oxygen homeostasis and ROS levels, the AOX activity was also found to be modulated according to the availability of cellular oxygen (Gupta et al., 2009). On the other hand, AOX catalyzed respiration and/or its activity are known to be induced against a wide range of abiotic and biotic stresses, suggesting that AOX can be used as a functional marker for yield stability and plant breeding studies under stress conditions (Arnholdt-Schmitt et al., 2006).

1.4.3. Role of AOX in developmental growth and fruit ripening

The role of AOX in the overall growth of plants and fruit ripening is poorly understood. On the one hand, theoretical views implicate that enhanced AOX catalyzed respiration

reduces the ATP levels, which is crucial for growth. On the other hand, few studies have demonstrated the AOX dependent increase in growth and yield under stress conditions. Perhaps, under such situations AOX allows efficient carbon use, total respiratory activity and maintenance of redox and ROS homeostasis (Fiorani et al., 2005; Sieger et al., 2005; Ho et al., 2007).

The role of AOX in fruit ripening was proposed long ago on behalf of increased transcript levels of AOX during fruit ripening in mango (Considine et al., 2001). However, clear evidence is still lacking in this regard. Transgenic tomato plants with low AOX expression lines showed delayed ripening; reduced carotenoids, respiration, and ethylene production accompanied by down-regulation of ripening-associated genes (Xu et al., 2012a). Further, treatment of mature green tomatoes with n-propyl gallate (nPG; inhibitor of AOX pathway) resulted in delayed ripening by at least 7 days. Additionally, they also suggested nPG as a safe and potential inhibitor for climacteric fruits ripening like tomato (Xu et al., 2012b). More recently, Perotti et al. (2014) discussed the involvement of AOX and mitochondrial uncoupling protein in fruit ripening of both climacteric and non-climacteric type fruits. Climacteric and non-climacteric fruits are categorized based on the engagement of respiration and ethylene during the ripening process. Climacteric fruits show a sharp increase in respiration rate and ethylene content at the onset of ripening. Whereas ripening of non-climacteric fruits are independent of respiration and ethylene is not required. Further, engagement of AOX and uncoupling proteins (UCPs) were found in regulating the ethylene peak during different ripening stages of papaya fruit (Oliveira et al., 2015).

1.5. Protective role of AOX during biotic and abiotic stress

1.5.1. Biotic stress

Since, plants are sessile and cannot escape from pathogen invasion, they possess several efficient defense mechanisms. Thus, despite the presence of several microorganisms such

as bacteria, nematodes, virus and fungi in the close vicinity, diseases occur rarely to plants as they activate separate defense mechanisms depending on the type of pathogen invaded (Garcia-Brugger et al., 2006). There are three major signaling pathways, which are involved in pathogen recognition and defense response, i.e. salicylic acid (SA), jasmonic acid (JA) and ethylene. The SA-dependent response is triggered by biotrophic pathogens, whereas JA/ethylene-dependent defense responses are activated on the invasion of necrotrophic pathogens (Thomma et al., 2001).

An increase in the respiratory rates of a plant is a widespread phenomenon during plant-pathogen interaction. The AOX catalyzed respiration has been found to be frequently induced during plant-pathogen interaction (Simons et al., 1999; Hanqing et al., 2010; Lee et al., 2011). Recent experiments of Garcia et al. (2013) demonstrated that infection of Arabidopsis with *Botrytis cinerea* leads to cyanide accumulation, which has further strengthened the reason behind AOX induction during plant-pathogen interaction. Beside, plant-pathogen interaction also leads to accumulation of O_2^-, H_2O_2 and NO (oxidative burst) other than SA, JA, and ethylene. These signaling molecules and oxidative burst promote the hypersensitive response (HR), which enhances the induction of AOX (Alvarez, 2000; Delledonne, 2005; Amirsadeghi et al., 2007; Koornneef and Pieterse, 2008; Cvetkovska and Vanlerberghe, 2013). Earlier, Chivasa et al. (1997) demonstrated the AOX mediated induction of SA, which interferes with replication of tobacco mosaic virus (TMV) and thereby prevent from viral infection. But, transgenic tobacco plants with altered level of AOX did not show any difference in viral resistance and suggested that AOX is not a critical component in viral resistance, but may play a role in HR (Ordog et al., 2002). However, an increase in AOX transcript was observed in *Nicotiana tabacum* when infected with tobacco necrosis virus (TNV) or TMV (Künstler et al., 2007). Further, several studies have demonstrated that infection with bacterial pathogens and their elicitors can strongly induce the AOX at the protein or transcript level in leaf tissue and cell suspensions (Lacomme and Roby, 1999; Krause and Durner,

2004; Vidal et al., 2007; Kiba et al., 2008). Despite the several studies conducted to date, the shreds of evidence reported are not enough to establish a critical defensive role of AOX in response to biotic stress, particularly against viral pathogens.

1.5.2. Abiotic stress

(a) Light stress

Plants are often encountered by high light stress, which is harmful to plants and lead to damage of the photosynthetic apparatus. In order to protect themselves from high light, plants have evolved several defense systems including water-water cycle, cyclic electron flow around photosystem I, thermal dissipation and antioxidant enzymes (Asada, 2000; Li et al., 2000; Müller et al., 2001; Ort and Baker, 2002; Raghavendra and Padmasree, 2003; Kramer et al., 2004). Since the last decade, several studies have revealed the importance of respiratory components, particularly AOX as an extra-chloroplastic defense system against photoinhibitory light (Noguchi and Yoshida, 2008; Yoshida et al., 2007, 2008, 2010; Zhang et al., 2010; Xu et al., 2011). High light stress causes an imbalance between production and utilization of NAD(P)H and over-reduction of chloroplastic electron transport chain that lead to the generation of ROS. In this connection, the role of AOX is well known in oxidising the excess reducing equivalents and minimizing the ROS levels in order to support the efficient photosynthesis (Raghavendra and Padmasree, 2003; Yoshida et al., 2008; Zhang et al., 2014). Several studies have demonstrated an increase in AOX catalyzed respiration, protein and transcript level on exposure to high light stress. On the other hand, plants deficient in AOX showed susceptibility against high light stress (Yoshida and Noguchi, 2009; Florez-Sarasa et al., 2011; Yoshida et al., 2011a,b; Zhang et al., 2011; Garmash et al., 2015).

(b) Temperature stress

The role of AOX is vastly studied in response to temperature stress, particularly low temperature. Several studies have shown a remarkable increase in AOX transcript and/or

protein and ROS level, when plants are exposed to low temperature (Vanlerberghe and McIntosh, 1992; Djajanegara et al., 2002; Grabelnych et al., 2004; Fiorani et al., 2005; Sugie et al., 2006; Campbell et al., 2007; Armstrong et al., 2008; Watanabe et al., 2008; Umbach et al., 2009; Lei et al., 2010; Wang et al., 2011, 2012; Gandin et al., 2014b; Grabelnych et al., 2014; Tang et al., 2014). Using oxygen isotope fractionation technique, Ribas-Carbo et al. (2000) revealed a significant increase in electron partitioning towards AOX in chilling exposed maize cultivar Z7. However, this study suggested that increased AOX respiration acts as a marker for chilling stress rather than providing tolerance.

Besides, AOX showed temperature-sensitive plasticity to floral reflectance in *Plantago lanceolata*. Genotypes grown at low temperature exhibited higher AOX content and floral reflectance plasticity than warm-grown plants (Umbach et al., 2009). Similarly, Searle et al. (2011a,b) demonstrated that field-grown alpine grasses had higher AOX protein levels during the cold season. The impact of AOX was also revealed in shoot acclimation in response to low temperature. In Arabidopsis, AOX overexpression lines showed a 30% increase in leaf area and 33% larger rosette size, whereas anti-sense lines showed a reduction in leaf area by 27% and 25% in rosette size when compared to wild-type plants on exposure to 12 °C (Fiorani et al., 2005). In watermelon, inhibition of the AOX pathway during low temperature (10 °C) resulted in down-regulation of several genes responsible for stress and defense response, signal transduction, protein fate and synthesis (Li et al., 2012). On the other hand, overexpression of AOX in *Oryza sativa* showed a significant decrease in lipid peroxidation and ion leakage in response to cold stress (Li et al., 2013a).

In a recent study, the inhibition assay in coral symbiont culture showed a significant increase in AOX pathway in response to thermal stress (Oakley et al., 2014). Overexpression of AOX1a in rice showed a thermotolerance at both acute exposures (41-45 °C for 10 min) and chronic exposure (37 °C for 8 d). In contrast, wild-type and

antisense lines showed a decrease in the root, shoot growth and phenotypic damage (Murakami and Toriyama, 2008).

(c) Salt stress

Salt stress is a widespread adverse condition, which leads to dysfunction of mETC resulting in increased mitochondrial ROS and lipid peroxidation, and the induction of mitochondrial and peroxisomal antioxidative defense systems in plants (Mittova et al., 2003, 2004). The induction of AOX transcript and/or protein under salt stress is reported in several plant species suggesting its role in improving the tolerance against salinity (Hilal et al., 1998; Kreps et al., 2002; Seki et al., 2002; Andronis and Roubelakis-Angelakis, 2010; Marti et al., 2011; Mhadhbi et al., 2013). In plants, during salt stress ethylene and NO are produced as a primary signal response, but they are also known as ROS inducers. In Arabidopsis callus, ethylene-mediated induction of the AOX pathway was hypothesized, which acts in the scavenging of H_2O_2 level in response to salt stress (Wang et al., 2010). In rice, on exposure to salt stress AOX catalyzed respiration was found to be increased by 50% of total respiration and also revealed the correlation between up-regulation of *AOX1a* and increasing H_2O_2 concentration (Feng et al., 2010). Furthermore, AOX overexpression lines in Arabidopsis ameliorated the growth inhibition as well as balanced the Na^+ and K^+ balance in response to salinity (Smith et al., 2009).

(d) Drought stress

Drought stress mainly affects the carbon balance, particularly, photosynthesis and respiration due to occurrence of stomatal and biochemical limitations (Flexas et al., 2006; Atkin and Macherel, 2009; Lawlor and Tezara, 2009). In this context, AOX has been recognized as safeguard against drought stress to optimize the photosynthesis and respiratory processes, which was evident through an increase in AOX catalyzed respiration or its protein/transcript level in response to drought stress (Seki et al., 2002; Bartoli et al., 2005; Giraud et al., 2008; Vassileva et al., 2009; Li et al., 2013b). During

combined stress of drought and heat, AOX induction was accompanied by an increase in the transcript level related to glycolysis and the pentose phosphate pathway, suggesting the utilization of sugars under such conditions (Rizhsky et al., 2002). Besides, on exposure to severe drought and high irradiance, knockdown of AOX in tobacco plants exhibited increase in ROS and cellular damage with concomitant decrease in ROS scavenging defense system. These results suggested that deficiency of AOX severely compromised the capacity of recovering compared to WT plants (Wang and Vanlerberghe, 2013). In *Vigna unguiculata*, the tolerant cultivar Vita 3 showed an increase in AOX protein and its respiratory capacity in the presence of polyethylene glycol (PEG) induced drought stress (Costa et al., 2007). Furthermore, AOX overexpression lines of *Nicotiana tabacum* showed better maintenance of photosynthesis and respiration against drought stress suggesting that AOX catalyzed respiration acts as an electron sink and prevents the loss of chloroplast ATP synthase for efficient photosynthetic performance (Dahal et al., 2014, 2015). These results suggest that AOX plays a protective role in response to drought stress, particularly to support metabolism in the light.

(e) Metal stress

Metals are essential micronutrients or macronutrients required for proper growth and metabolism of plants. A few of them (Cu, Zn, Mn and Fe) act as a cofactor for several proteins and enzymes such as superoxide dismutase, ascorbate oxidase, cytochrome oxidase, plastocyanin and polyphenol oxidase. But, their excess amount leads to the oxidative challenge that can be toxic to plants (Yruela, 2005; Sagardoy et al., 2009; Ravet and Pilon, 2013). Furthermore, heavy metals (e.g. Cd, As, Pb and Hg) are known as menacing phytotoxicant even at very low concentration.

Pádua et al. (1999) demonstrated that the exposure of sycamore cell suspension to Cu leads to induction of protein and enzymatic activity of AOX. Since, metals have a

property of donating/accepting the electrons, their abundance in cells often generates the ROS and lead to oxidative stress. Aluminum (Al) has been shown to repress mitochondrial respiration and induction of ROS generation, which was further validated by loss of complex I and complex III activities (Li and Xing, 2011; Panda et al., 2013). In this study, Al-dependent increase in AOX catalyzed respiration was revealed, perhaps a response by the cell to prevent mETC dysfunction (Li and Xing, 2011). Furthermore, AOX overexpression lines of tobacco cells showed the tolerance against Al mediated oxidative stress by altering the respiratory capacity (Panda et al., 2013). In addition, redox inactive heavy metal like Cd possesses strong affinity with oxygen, nitrogen and sulfur atoms, which in turn can inhibit the protein activity or displacement of natural metal centers (Cuypers et al., 2010). In recent years, AOX is introduced as a primary defense in response to Cd-induced oxidative challenge (Castro-Guerrero et al., 2008; Keunen et al., 2013, 2015). Upon Cr(VI) exposure, AOX involves in metabolic interconnectivity among respiration, carbohydrate and phenolics, which results in metabolic adaptation to support the tolerance of Salvinia minima against Cr(VI) stress (Prado et al., 2013).

(f) Ozone stress

Ozone is a well-known phytotoxic air pollutant, which causes the visual changes such as chlorosis, necrosis, biomass and yield including a decrease in the photosynthetic potential (Dizengremel et al., 2008; Bagard et al., 2008; Betzelberger et al., 2012). Further a significant reduction in the COX pathway capacity was observed in tobacco leaves on exposure to ozone (Ederli et al., 2006). The loss in the COX pathway activity was attributed to a transient increase of NO, a potential inhibitor of COX. Also, the loss in COX pathway capacity was accompanied by an increased AOX expression and capacity, which depends upon both the increase in NO (Ederli et al., 2006) and a protein phosphorylation event (Pasqualini et al., 2012). The increase in AOX expression and

respiration rate was also revealed in higher plants under acute ozone exposure (Dizengremel, 2001; Tosti et al., 2006).

1.6. Role of AOX in optimizing photosynthesis

Photosynthesis and respiration are the most crucial processes as they regulate the carbon and energy metabolism in the plants. Photosynthesis is a reductive process known to occur in chloroplasts, in which light energy is converted into carbohydrates in the presence of CO_2 and water while oxygen is liberated concomitantly as a by-product. Respiration is an oxidation process occurring in the mitochondria, where carbohydrates are metabolized through glycolysis, oxidative pentose phosphate (OPP) pathway and tricarboxylic acid (TCA) cycle. These pathways generate reducing equivalents and ATP molecules. These reducing equivalents are then used to support biosynthetic reactions or can be oxidized by mETC. In last three decades, an intensive research on this fundamental connection between photosynthesis and respiration leads to the recognition of chloroplasts and mitochondria as interdependent organelles and the biochemical reactions were turned out to mutually beneficial to each other occur in these organelles (Raghavendra et al., 1994; Hoefnagel et al., 1998; Raghavendra and Padmasree, 2003; Noguchi and Yoshida, 2008; Dinakar et al., 2010a,b). During this interaction several crosstalk occurs between both organelles, in which cyclic electron transport, malate valve and mETC play a crucial role in maintaining the energy balance and redox homeostasis (Scheibe et al., 2005; Yoshida et al., 2007; Kramer and Evans, 2011; Talla et al., 2011; Hebbelmann et al., 2012; Bailleul et al., 2015). During light, the reducing power generated by chloroplasts is several magnitudes higher than its consumption by Calvin cycle. The over-accumulation of reducing power ($NADPH/NADP^+$) causes inhibition of electron flow from PSII to PSI, which results in over reduction of PQ pool and consequently ROS generation. The excess ROS can damage the thylakoid membrane and photosynthetic apparatus. Malate dehydrogenases (MDHs) associated with malate valve

play an important role in preventing the over energization of chloroplast and ROS generation. In chloroplasts, MDH can convert the oxaloacetic acid (OAA) into malate at the expense of NADPH and malate can be transported to cytosol or mitochondria/peroxisomes through the operation of malate valve. During this process cytosolic/mitochondrial/peroxisomal MDH converts malate to OAA and NAD(P)H is produced, which is further oxidized by mETC components. Thus, mitochondria play a vital role in maintaining the energy balance and keeping photosynthesis active (Raghavendra and Padmasree 2003; Noguchi and Yoshida, 2008; Zhang et al., 2010; Xu et al., 2011; Yoshida et al., 2011b; Zhang et al., 2011; Gandin et al., 2012; Zhang et al., 2014). In this connection, further experimental evidences of participation of malate valve and MDH in optimizing photosynthesis by AOX pathway during oxidative stress are discussed in **chapter 4 and 5**. Moreover, inhibition of the AOX pathway using mutant/transgenic or metabolic inhibitors (SHAM or propyl gallate) resulted in significant reduction in photosynthetic O_2 evolution, photosynthetic yield, thermal dissipation and damage in the D1 protein in response to light stress. In contrast, AOX overexpression lines showed enhanced photosynthetic O_2 evolution, yield and thermal dissipation when compared to wild-type plants during light stress (Giraud et al., 2008; Dinakar et al., 2010a; Florez-Sarasa et al., 2011; Zhang et al., 2011).

1.6.1. Special features of photosystem I and photosystem II

Photosynthesis is accomplished by a series of reactions that occurs mainly in the chloroplast. During photosynthesis the oxidation of H_2O, reduction of $NADP^+$ in thylakoid membrane is catalyzed by photosystem II (PSII) and photosystem I (PSI), respectively (Nelson and Yocum 2006). PSI and PSII absorb the photons at a wavelength of 700 nm and 680 nm, respectively. The numbers associated with photosystems indicate the order in which they were discovered, not the order of electron transfer. A quantitative measurement of total number of chlorophyll associated with PSI and PSII revealed that

approximately 10-20% more chlorophyll was associated with PSI (in agreement of more number of quanta captured by PSI) when compared to PSII (Albertsson, 2001; Joliot and Joliot, 2002).

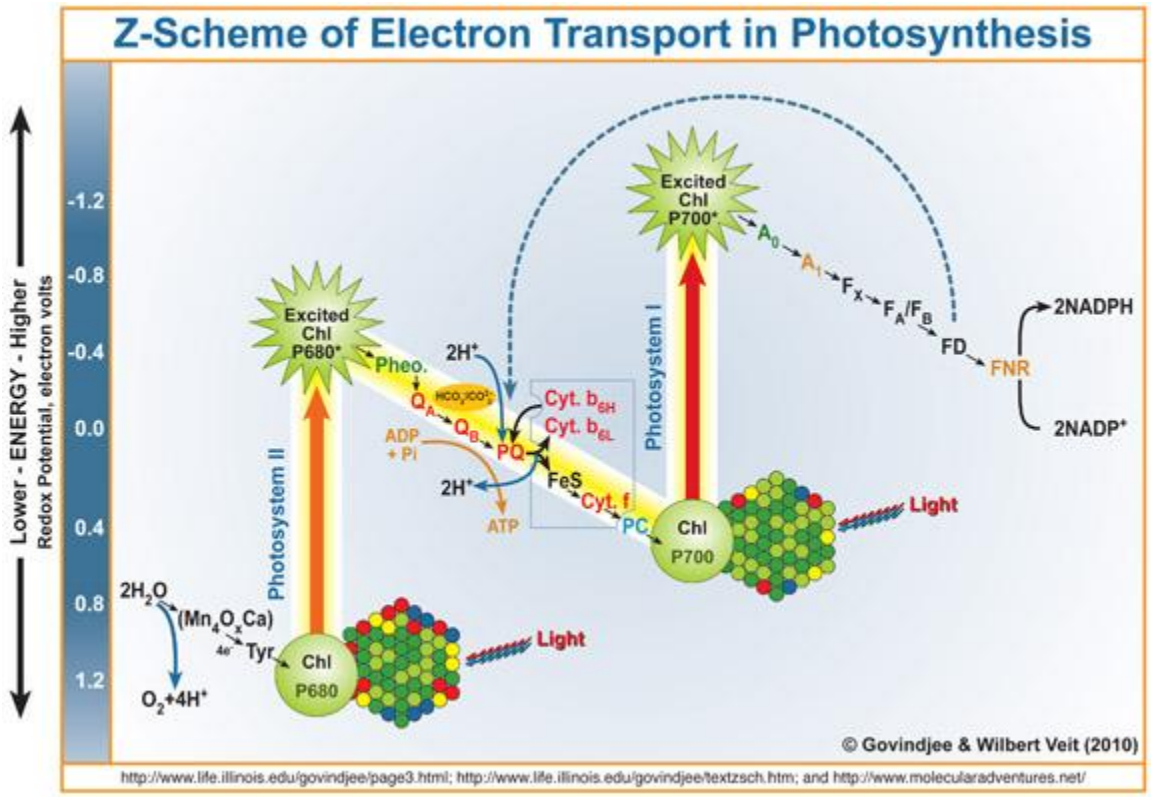

Fig. 1.2. Diagrammatic representation of electron transport system in chloroplasts (adapted from Govindjee and Wilbert Veit 2010 available at http://www.life.illinois.edu/govindjee/Z-Scheme.html).

PSI and PSII are connected in series with cytochrome b6f complex (Cyt bf). The electron flow between PSI and PSII is recognized through two routes. First, linear electron flow (LEF) that starts from water and ends up at ferredoxin with ultimate reduction of $NADP^+$. This route involves several components (P680, phaeophytin, Q_A, Q_B, PQ, Cyt bf, plastocyanin, P700 and Fd), which are arranged in Z-shape due to differences in their redox potential, hence it is also known as Z-Scheme (Hill and Bendall, 1960; Allen, 2003; Govindjee and Wilbert Viet, 2010; **Fig. 1.2**). Second, cyclic electron flow around

PSI (CEF-PSI), which starts from PQ and recycled from Fd to PQ without NADPH formation. In both pathways, the electron transport is coupled to proton translocation that occurs across the thylakoid membrane and lead to generation of a proton gradient (ΔpH). This ΔpH is utilized in ATP synthesis (Shikanai, 2007, 2014). In addition to ATP synthesis, the increase in ΔpH during excess light leads to acidification of thylakoid lumen and thereby induces the thermal dissipation (Müller et al., 2001).

CEF-PSI is consisted of two redundant pathways: the major pathway depends on proton gradient regulation 5 (PGR5) and PGR5-like photosynthetic phenotype 1 (PGRL1) proteins, whereas the minor pathway is mediated by chloroplast NADH dehydrogenase (NDH) complex (Munekage et al., 2004; Peng et al., 2011). In higher plants, the main pathway of CEF-PSI depends on PGR5, which was identified in *pgr5* mutant of *Arabidopsis*. CEF-PSI is also essential for balancing the ATP/NADPH ratio, thermal dissipation and CO_2 assimilation (Munekage et al., 2002; Shikanai, 2007; Munekage et al., 2008). Furthermore, the knockdown of *PGR5* in rice caused a 50% decrease in PGRL1 protein level, which suggests the role of PGR5 in accumulation of PGRL1 (Nishikawa et al., 2012). In NDH-dependent pathway, NDH oxidizes NADPH and reduces the PQ pool like complex I does in mitochondria (Ogawa, 1991). This pathway is predominant in cyanobacteria and involved in multiple processes by modifying its subunit compositions (Zhang et al., 2004; Shikanai, 2007).

1.6.2. Defense mechanism associated with chloroplasts and their relation with AOX

a) Xanthophyll cycle and Non-photochemical quenching

Under excess light, violaxanthin is converted to zeaxanthin via an intermediate antheraxanthin and this reaction is reversed during low light conditions. This reversible reaction of two xanthophylls is known as xanthophyll cycle and occurs throughout the plant kingdom (Demmig-Adams and Adams, 1996; **Fig. 1.3**). Using chlorophyll fluorescence approach, several studies demonstrated the zeaxanthin-dependent increase

in energy dissipation (Demmig et al., 1987; Demmig-Adams, 1990; Gilmore and Yamamoto, 1991). During high light exposure, chloroplasts are prone to photooxidative damage and accumulate ROS. In chloroplasts, ROS formation occurs via two pathways: (1) electron transfer to O_2 at the acceptor side of PSI and PSII, resulting in formation of O_2^- and subsequently H_2O_2 by action of SOD (Mehler, 1951; Jahns and Holzwarth, 2012); and (2) electron transfer from triplet chlorophyll ($^3Chl^*$) to O_2, which leads to formation of $^1O_2{}^*$.

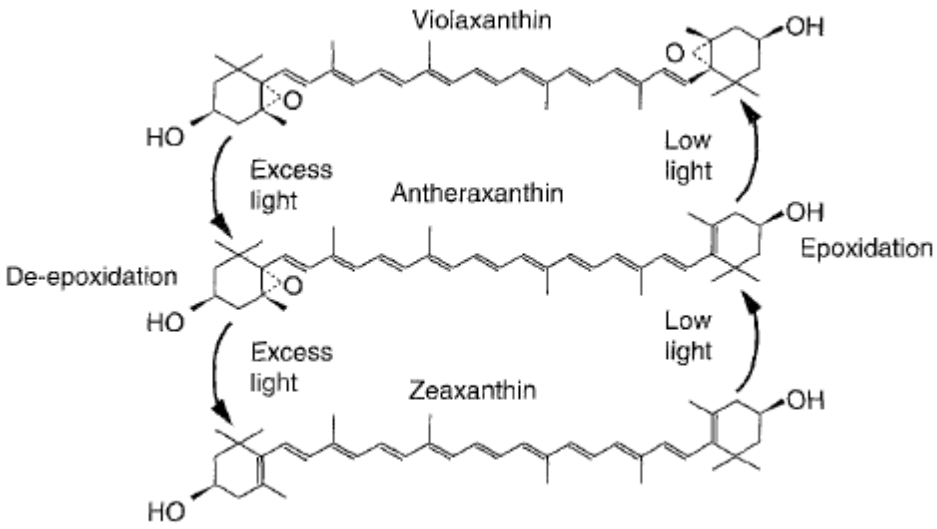

Fig. 1.3. A scheme of the xanthophyll cycle in plants and its regulation during excess or low light. On exposure to high light, violaxanthin is converted to zeaxanthin by stepwise removal (de-epoxidation) of two oxygen and this reaction is reversed (epoxidation) under low light. De-epoxidation occurs within minutes, whereas epoxidation is a slow process and takes minutes to hours (adapted from Demmig-Adams and Adams 1996).

Lutein is most abundant xanthophyll attached to light harvesting complex II (LHCII), and plays a crucial role in deactivating the $^3Chl^*$ and $^1O_2{}^*$, and thereby the reduction of ROS formation (Krieger-Liszkay et al., 2008; Triantaphylidès and Havaux, 2009). Lutein-deficient mutants (*lut1* and *lut2*), epoxy xanthophyll-deficient (*aba1*) and *lut2aba1* double mutant showed a reduction in ΔpH-dependent non-photochemical quenching NPQ and altered the stoichiometry and antenna size of PSII (Lokstein et al., 2002). These

observations suggest the engagement of xanthophylls in modulating the NPQ of PSII during excess light energy (Lokstein et al., 2002; Jahns and Holzwarth, 2012).

b) Plastid terminal oxidase

PTOX is known as an analog of AOX which is localized in the thylakoid membrane of photosynthetic species including higher plants and algae (Carol and Kuntz, 2001; Joët et al., 2002). Similar to AOX (ubiquinol oxidase), PTOX transfers the electron from plastoquinol (PQH2) to molecular oxygen and thus prevent the over-reduction of the PQ pool (Aluru and Rodermel, 2004; Sun and Wen, 2011; McDonald et al., 2011). The engagement of PTOX is also suggested in chlororespiration and synthesis of photoprotective carotenoids, which prevents the over-reduction of chloroplastic ETC (Peltier and Cournac, 2002; Nawrocki et al., 2015). PTOX was found to be up-regulated in several higher plants and algae under various abiotic stress conditions such as heat, drought, cold, high light and salinity (Sun and Wen, 2011).

c) Water-water cycle

In 1951, Mehler discovered the photoreduction of O_2 to H_2O_2 in thylakoids, which revealed that chloroplasts not only oxidize water to evolve O_2 but also reduce O_2 to H_2O. Later, this cycling of water was termed as water-water cycle (WWC). In this cycle, O_2^- was identified as the primary product of the photoreduction of O_2, which was scavenged by chloroplastic Cu/Zn-superoxide dismutase (Cu/Zn-SOD) and thereby prevents the inactivation of PSI complex (Asada et al., 1974; Asada, 1999; Asada, 2000). Disorder of WWC leads to generation of •OH radical, which is unavoidable in aged leaves. Polyols and mannitol were found as efficient scavenger of •OH radicals (Shen et al., 1997). The knockdown of SOD (a key enzyme of WWC) in *Arabidopsis* caused a decrease in overall growth and development. Additionally, the chloroplast size, chlorophyll content and photosynthetic activity were also diminished (Rizhsky et al., 2003). The *rbcS* antisense lines of *Oryza sativa* showed a rapid increase in electron flux through WWC and NPQ at

20% O_2. However, with increasing CO_2 assimilation, the electron flow through WWC and NPQ was decreased. In 2% O_2, CEF-PSI remained high and contributed to NPQ. These results suggest the physiological function of both WWC and CEF-PSI in maintaining the balance between Calvin cycle and energy dissipation for optimal photosynthesis (Makino et al., 2002; Miyake, 2010).

1.7. Various roles of AOX in microbes and animals

Due to its unique characteristic of performing cyanide-resistant respiration, the role of AOX is also studied in lower organisms, animals and human cell lines. The host cells, which do not possess native AOX like bacteria, viruses, animals and humans, were heterologously transformed to validate its function. Various physiological roles of AOX have been described below.

1.7.1. Cyanide-insensitive respiration and cell growth

Respiration is a crucial phenomenon known to enhance the chronological life span in yeast (Barros et al., 2004). Hemes are essential components for the activity of COX-catalyzed respiration. A *hemA E. coli* strain (SASX41B) was incapable of performing COX-catalyzed aerobic respiration. But, when this strain was complemented with cDNA encoding *AOX* from *A. thaliana* resulted in aerobic respiration as well as cyanide-insensitive respiration. Moreover, upon treatment with KCN or SHAM, cells transformed with AOX showed higher growth (OD_{600}) in comparison to the empty vector (Kumar and Söll, 1992). Expression of AOX from *Sauromatum guttatum* to *Schizosaccharomyces pombe* resulted in increased AOX catalyzed respiration and overall growth. The possible reason behind this was suggested as the higher engagement of AOX (Affourtit et al., 1999). Similarly, cloning of AOX (from *Aspergillus niger*) in the host strain *Lactococcus lactis* enhanced the biomass and nisin (an antibacterial peptide) production in response to oxidative stress (Papagianni and Avramidis, 2012).

Any defects in mETC lead to a large number of diseases (e.g. deafness, diabetes, epilepsy ischemia and Parkinson's disease) in human. This could be due to lack of several redox-active proteins (e.g. AOX and rotenone-insensitive internal NADH dehydrogenase) in mETC (Rustin and Jacobs, 2009; Schiff et al., 2012). Interestingly, heterologous expression of AOX in human cells from skunk cabbage showed a significant decrease in ROS production and also AOX was induced by pyruvate. Hence, in this study functional expression of AOX was suggested as an artificial alternative respiration that can be used as a therapy for various mitochondrial diseases (Matsukawa et al., 2009). AOX expression from *Ciona intestinalis* compensate cytochrome c oxidase deficiency in human cells and mouse as well as enhanced the growth and tolerance level against viral infection (Dassa et al., 2009; El-Khoury et al., 2013, 2014).

1.7.2. Defense response

During plant-pathogen interactions cyanide is produced by plants as a defensive mechanism to inhibit the pathogen's respiration and growth. In plants, cyanide can be detoxified by the enzyme β-cyanoalanine synthase (CYS). In Arabidopsis *cys-c1* showed increased susceptibility to necrotrophic fungus *Botrytis cinerea* (Garcia et al., 2013). On the other hand, pathogens possessing AOX might be more offensive in nature. In pathogenic fungi, *Aspergillus fumigatus* and *Sclerotinia sclerotiorum* presence of AOX ensure their survival and growth inside the host in response to oxidative stress (Tudella et al., 2004; Xu et al., 2012c).

The *in vivo* characterization of AOX in *Histoplasma capsulatum* (human pathogenic fungi) exhibited induction of AOX at both mRNA and protein level in response to H_2O_2 or antimycin. These results indicated that AOX can play an important role in the survival of this pathogen in humans (Johnson et al., 2003). Similarly, in *Paracoccidioides brasiliensis* AOX was found to handle its survival against oxidative stress imposed by immune cells in human (Ruiz et al., 2011).

The present study has been designed to unravel the physiological importance of AOX during various oxidative stresses in *A. thaliana* and *S. cerevisiae*. The approach and objectives of the present work are described in the forthcoming chapter.

***

Chapter 2

Approach and Objectives

Photosynthesis and respiration are the most important metabolic processes known to modulate the carbon and energy metabolism of plants. Conventionally chloroplasts and mitochondria were considered as autonomous organelles as they possess their own genetic material. But, in the last two decades the interactions between chloroplasts and mitochondria have been extensively studied at physiological, biochemical and molecular level, which demonstrated that both organelles mutually benefit each other by exchanging the metabolites to maintain the cellular redox homeostasis under various abiotic stresses (Lambers, 1982; Saradadevi and Raghavendra, 1992; Raghavendra and Padmasree, 2003; Noctor et al., 2004; Yoshida et al., 2006; Xu et al., 2011). Though, chloroplasts and mitochondria have their own defense system such as antioxidative system and heat dissipation machinery, but any disturbance(s) in either organelle affect the metabolism of another one, indicating that self-defense systems and/or energy regulation machinery are not sufficient at individual level.

The various components of mETC are regulated by complex mechanism during biotic/abiotic stress (depending on the type and strength of stress), which modulate the energy level and reduction state of the mETC. AOX has been found to be increased at the transcript or protein level compared to any mitochondrial genes during a wide range of stress conditions (Clifton et al., 2006). Several studies have demonstrated a simultaneous increase in malate valve related enzymes and AOX during high light, which indicates that the reducing equivalents generated in chloroplasts were efficiently transported by malate valve and subsequently oxidized by AOX to protect the thylakoid membrane from damage and to sustain photosynthesis (Yoshida et al., 2007; Dinakar et al,. 2010b; Zhang et al., 2010; Zhang et al., 2014). However, the biochemical or physiological interactions

that take place at the PSI and PSII level with AOX are either due to its induction or a direct role in oxidizing excess reducing equivalents is yet to be elucidated.

In addition to plants, the role of AOX is also revealed in survival of pathogenic fungi such as *Histoplasma capsulatum* and *Aspergillus fumigatus* inside the host under stress conditions (Johnson et al., 2003; Tudella et al., 2004). Similar to plants, the AOX mutant of pathogenic yeast *Cryptococcus neoformans* showed susceptibility to oxidative stress (Akhter et al., 2003). Thus, AOX plays several roles inside and outside the mitochondria over a wide range of stress conditions including higher plants to microbes.

The previous studies from our laboratory have demonstrated that AOX plays a significant role in optimizing photosynthesis under various abiotic stresses such as high light, osmotic and temperature stress using mesophyll cell protoplasts of *Pisum sativum* (Dr. Ch. Dinakar Thesis, 2008; Dinakar et al., 2010a,b). The present study is designed to investigate the role of AOX in optimizing photosynthesis including photochemical reactions at PSI and PSII as well as its impact on cellular redox homeostasis during oxidative stresses (photooxidative or chemically induced). To minimize the ambiguity of AOX pathway inhibitors, knockout mutant of *aox1a* and wild-type plants of *Arabidopsis thaliana* have been used in the present study. On the other hand, previous studies on *Saccharomyces cerevisiae* demonstrated that any increase in respiration and redox ratio of NAD^+/NADH decreased the mitochondrial ROS and concomitantly increased its life span (Barros et al., 2004; Lin et al., 2002, 2004). Accordingly, *Saccharomyces cerevisiae* (devoid of AOX) is used in the present study to investigate the role of *AtAOX1a* in increasing the respiratory tolerance and its role in alleviating oxidative stress.

In context to the above scenario, the objectives of the present work are set as follows:

1. To identify the physiological role of AOX1a in photosynthesis under high light stress in *Arabidopsis thaliana*.
2. To examine the importance of AOX1a in optimizing photosynthesis during restriction of electron transport through cytochrome oxidase pathway in *Arabidopsis thaliana*.
3. To validate the importance of AOX pathway in alleviating oxidative stress using *Saccharomyces cerevisiae* as a model organism.

Rationale for Model plant (*Arabidopsis thaliana*) or organism (*Saccharomyces cerevisiae*) used in the present study

Arabidopsis thaliana is a well-known model plant due to its unique features such as: small size (20 cm tall), short life cycle, grow successfully throughout the year without any seasonal hindrance, self-fertilization, diploid genome, small genome size (157 Mb), completely sequenced, availability of several T-DNA insertion mutants at Arabidopsis Resource Centre (Nottingham, UK) [Meinke et at., 1998; Bennett et al., 2003; Koornneef and Meinke, 2010]. In Arabidopsis, AOX is encoded by five genes namely *AOX1a*, *AOX1b*, *AOX1c*, *AOX1d* and *AOX2*. *AOX1a* transcript has been found to be dramatically induced under several stress conditions compared to other *AOX* genes (Saisho et al., 1997; Clifton et al., 2006). Therefore, in the present study, we used T-DNA insertion line of *aox1a* **(Fig. 2.1)**.

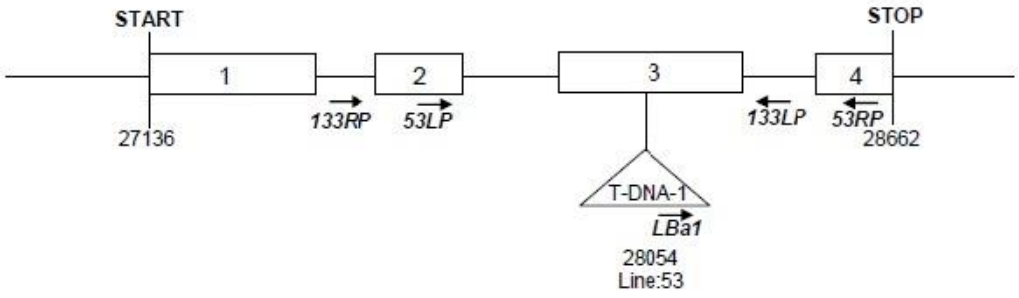

Fig. 2.1. A schematic diagram demonstrating the T-DNA insert in *aox1a*, Salk_084897 (Line 53) of *A. thaliana*. The insertion of T-DNA is localized in third exon. Seeds were obtained from Arabidopsis Biological Resource Centre (www.arabidopsis.org/abrc) and homozygous lines for *aox1a* mutant were characterized by Strodtkötter et al., 2009.

Leaves were plucked from 10-12 weeks old plants and cut into 0.25 cm^2 leaf discs. Leaf discs offer an easy and suitable material for exposing to several stresses under laboratory conditions and allow conducting the physiological, biochemical and molecular experiments as they closely mimic the in vivo environment of higher plants. Further, leaf discs are more suitable than whole leaf for the following reasons: (i) maintenance of constant leaf area, particularly in oxygraph and chlorophyll fluorescent studies; (ii) permeability or uptake of chemicals (inhibitors) through symplast is much easier and efficient through cut edges; (iii) low amount of inhibitors are economic and sufficient for effective results. To study the role of AOX1a in sustaining photosynthesis under photooxidative stress or chemically induced oxidative stress, the leaf discs from WT and *aox1a* were exposed to 700 µmoles m^{-2} s^{-1} and 20 µM antimycin A (AA; inhibitor of COX pathway at complex III), respectively. The impact of AOX1a was assessed through comparison of several physiological and biochemical parameters between WT and *aox1a*.

S. cerevisiae is another model organism that was used in the present study to assess the role of AOX1a in alleviating oxidative stress. *S. cerevisiae* contains some unique features such as single cell eukaryotic organism, rapid cell cycle (90 min at 30 °C), hence can be cultured easily, small genome size (12.1 Mb), completely sequenced, can be transformed that allows the addition or deletion of genes through homologous recombination (Botstein et al., 1997; Carmona-Gutierrez et al., 2010). In spite of having well-developed respiratory system, *S. cerevisiae* does not contain AOX homolog. The absence of AOX in *S. cerevisiae* offers to study the *in vivo* role of AOX. In the present study, *S. cerevisiae* has been transformed with *AtAOX1a* to characterize the function of AtAOX1a in alleviating oxidative stress. The *S. cerevisiae* cells transformed with empty vector were taken as control. The oxidative stress was generated through the external addition of H_2O_2 and tertiary-butyl hydroperoxide (t-BOOH).

***

Chapter 3

Materials and methods

3.1 Plant materials and growth conditions

Arabidopsis thaliana L. Heynh ecotype Columbia, Col-0 (WT) and *aox1a* (SALK_084897) were grown in soilrite mix. The seeds were sown on soil with Murashige and Skoog medium **(Table 3.1)** followed by stratification at 2-4 °C in dark for 3-4 d before transferring them to growth chamber. The plants were grown in an air-conditioned room at 22-24 °C with photosynthetic photon flux density (PPFD) of 50-60 µmol photons m^{-2} s^{-1} under light and dark cycles of 8 and 16 h, respectively. Leaves from 10 to 12 week-old plants **(Fig. 3.1)** were used for preparing leaf discs.

3.2 Light treatment

Leaf discs (ca. 0.25 cm^2) prepared from leaves with a sharp paper punch under water from either sides of the midrib, were placed in a petri dish containing distilled water. Leaf discs were subjected to 50, 250, 500 and 700 µmol photons $m^{-2}s^{-1}$ for 6 h at 25 °C. The illumination was provided by halogen lamps (230 V/150 W; Philips Comptalux). A water jacket was used between the light source and the sample to prevent heating. A small fan was also used to blow air over the petri dishes and thereby dissipate the heat generated by lamps, and prevent any increase of temperature due to heat.

3.3 Antimycin A treatment

Leaf discs (ca. 0.25 cm^2) prepared from leaves as described above, were placed in a petri dish containing 0, 5, 10, 20, 30 and 40 µM antimycin A (AA) in distilled water with 0.01 % Tween-20 and exposed to 50 µmol photons m^{-2} s^{-1} for 6 h at 25 °C.

Table 3.1. The composition of nutrient solution used for growing Arabidopsis plants.

Macronutrients	Concentration (mM)	Micronutrients	Concentration (µM)
KNO_3	5.0	$FeSO_4.7H_2O$	50 (in 50 mM Na_2EDTA)
$KH2PO_4$	2.5	$MnSO_4.4H_2O$	60
$MgSO_4$	2.0	$ZnSO_4.4H_2O$	7
$Ca(NO_3)_2$	2.0	$CuSO_4.5H_2O$	0.1
		H_3BO_3	49
		KI	4.5
		$Na_2MoO_4.2H_2O$	1
		$CoCl_2$	0.1

Fig.3.1. Phenotypic appearance of 12-week-old plants of wild type (cv. Columbia) and *aox1a* mutant of *Arabidopsis thaliana* grown in a controlled growth chamber at a photoperiod of 8 h light (50 µmol photons m^{-2} s^{-1}) and 16 h dark at 22-24 °C .

3.4 Measurement of respiration and photosynthesis in leaf discs

The rates of respiratory O_2 uptake and photosynthetic O_2 evolution of leaf discs were monitored using a Clark-type oxygen electrode (LD-2, Hansatech Instruments Ltd., King's Lynn, UK). Leaf discs were kept on the topmost capillary nylon mesh and 200 µl of 1.0 M bicarbonate buffer (pH 9.0) was sprinkled homogeneously, which generates ca. 5% (v/v) CO_2 in the electrode chamber (Walker, 1988). Oxygen level in electrode chamber was calibrated each time as per manufacturer's instructions before measurement of respiratory and photosynthetic rates. Soon after calibration, the traces of O_2 uptake were monitored for 5 min in dark and subsequently the traces of O_2 evolution were monitored for 10 min **(Fig. 3.2)**.

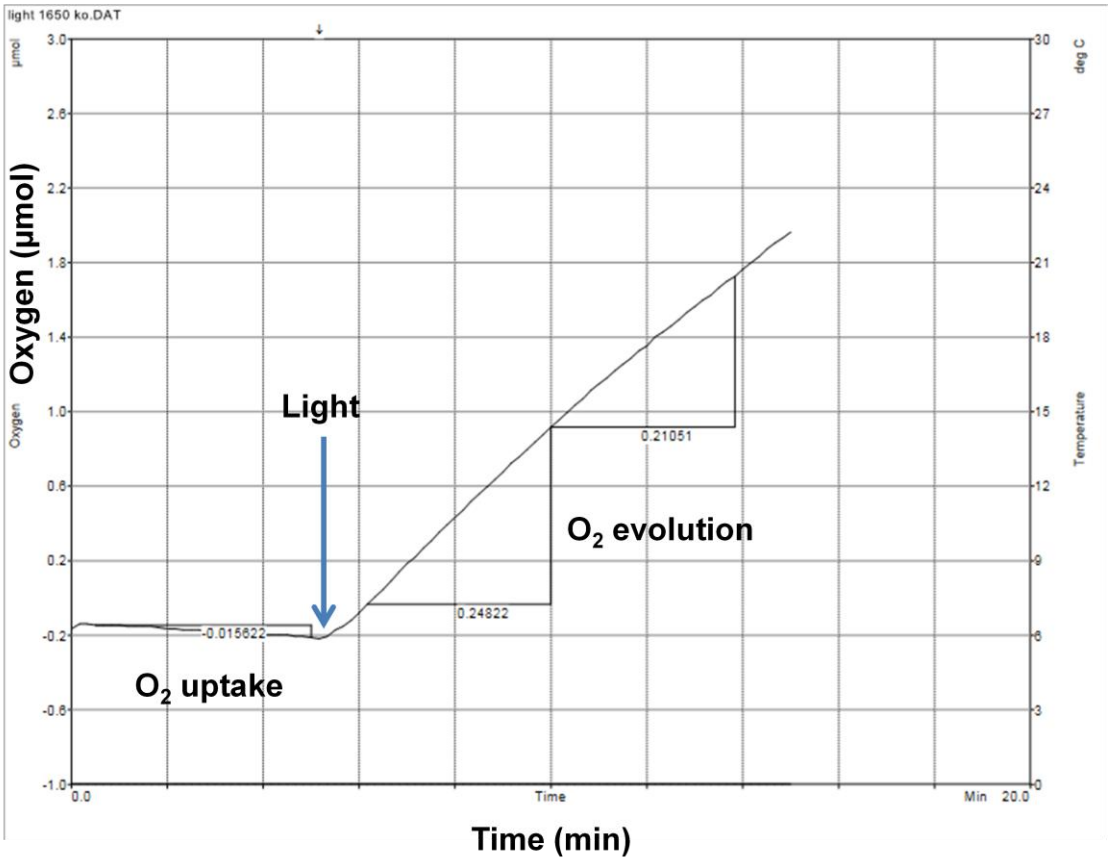

Fig. 3.2. A typical recorder trace of respiratory O_2 uptake and photosynthetic O_2 evolution by leaf discs of *A. thaliana*.

3.5 Chlorophyll fluorescence and P700 measurement

Chlorophyll fluorescence and P700 were measured at 25 °C using a Dual-PAM-100 fluorometer (Heinz Walz GmbH, Germany). After AA treatment leaf discs were incubated in dark for 30 min. The minimum fluorescence (Fo) and maximum fluorescence (Fm) were measured in a dark-adapted sample with a saturation pulse (SP) of 3000 µmol photons $m^{-2}s^{-1}$ for 800 ms. After a delay of 40 s, actinic light (AL) of 126 µmol photons $m^{-2}s^{-1}$ was switched on along with SP of 3000 µmol photons $m^{-2}s^{-1}$ for 800 ms, followed by repetitive application of SPs at every 20 s for 5 min. With each SP the relative changes in yield, photochemical and non-photochemical quenching and electron transport rate were recorded **(Fig. 3.3)**. The changes in chlorophyll fluorescence parameters were monitored using automated induction curve for 5 min. Based on Fo, Fm, F' and Fm' the chlorophyll fluorescence parameters were automatically calculated by Dual-PAM-100 software.

P700 was measured using dual wavelength (difference of intensities of 875 nm and 830 nm pulse-modulated measuring light reaching photodetector) as described in Klughammer and Schreiber (2008). The maximum P700 signal (Pm) was determined by application of SP in presence of Far-Red light and zero P700 signal (Po) was determined after complete reduction of P700, induced by cessation of SP and Far-Red light **(Fig. 3.4)**. Pm' is maximum P700 signal in presence of AL and SP. Based on Po, Pm and Pm' values, yield of PSI [Y(I)] and reduction state of P700 were automatically calculated by Dual-PAM-100 software.

3.6 Measurement of pyridine nucleotides from leaf tissue

The total cellular pools of NAD(H) and NADP(H) were measured according to Queval and Noctor (2007). The reduced and oxidized forms of pyridine nucleotides are distinguished by preferential destruction in acid/base.

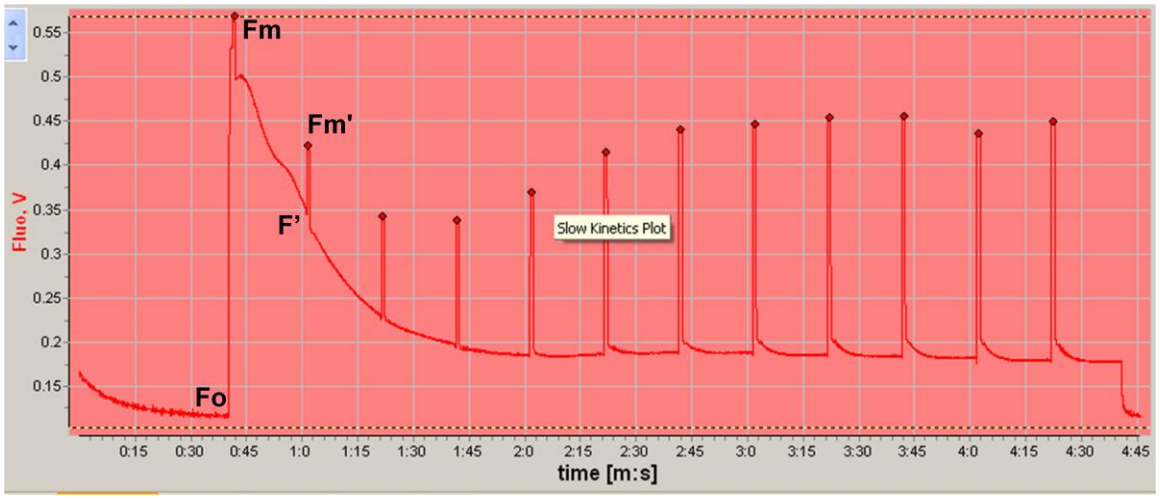

Fig. 3.3. A typical induction curve recording depicts the pattern of chlorophyll fluorescence versus time. Fo - minimal fluorescence from dark adapted samples; Fm - maximal fluorescence from dark adapted samples; F' - minimal fluorescence from light adapted samples and Fm' - maximal fluorescence from light adapted samples. During each application of SP, a new Fo' and Fm' were obtained.

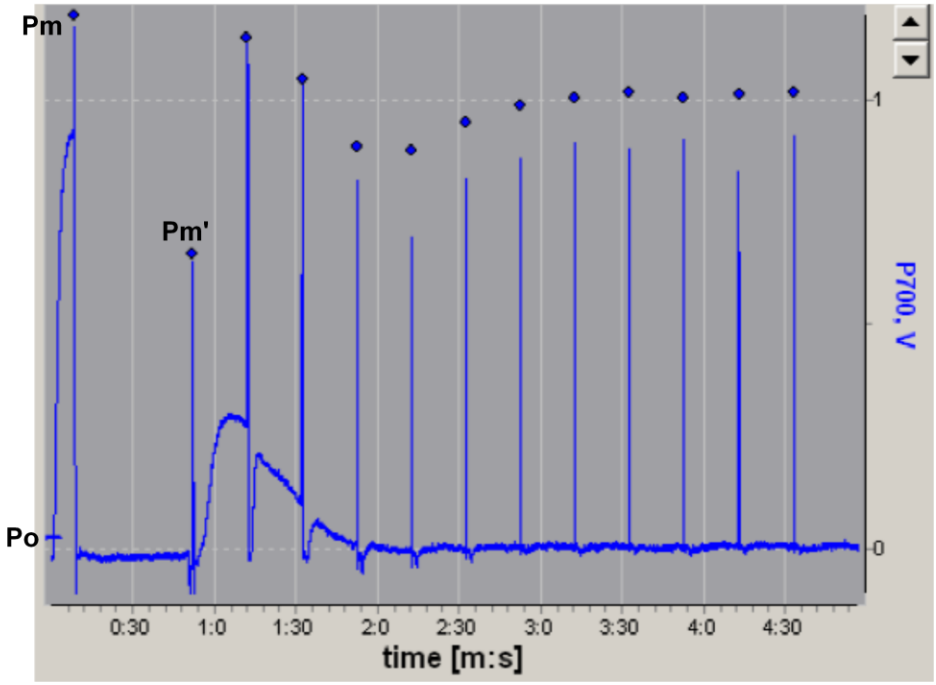

Fig. 3.4. A typical induction curve recording depicts the pattern of P700 versus time. Po - minimal P700 signal from dark adapted samples; Pm - maximal P700 signal from dark adapted samples and Pm' - maximal P700 signal from light adapted samples. During each application of SP, a new Pm' were obtained.

Therefore, leaf discs (100 mg) were finely ground in liquid nitrogen and extracted either into 1.0 ml of 0.2 N HCl for measuring NAD^+ and $NADP^+$ or 0.2 M NaOH for measuring NADH and NADPH. Pyridine nucleotides were quantified by monitoring phenazine methosulfate-catalyzed reduction of dichlorophenolindophenol **(Fig. 3.5)**.

For assay of NAD^+ and NADH, the reaction was started by the addition of ethanol in presence of alcohol dehydrogenase. The reaction medium contains 20 µl neutralized supernatants, 0.1 ml of 100 mM HEPES (pH 7.5) containing 2 mM EDTA, 20 µl of 1.2 mM DCPIP, 10 µl of 20 mM PMS, 25 µl double distilled water and 10 µl of ADH (2500 U ml^{-1}). The reaction was started by the addition of 15 µl of absolute ethanol and decrease in absorbance was read at 600 nm for 3 min.

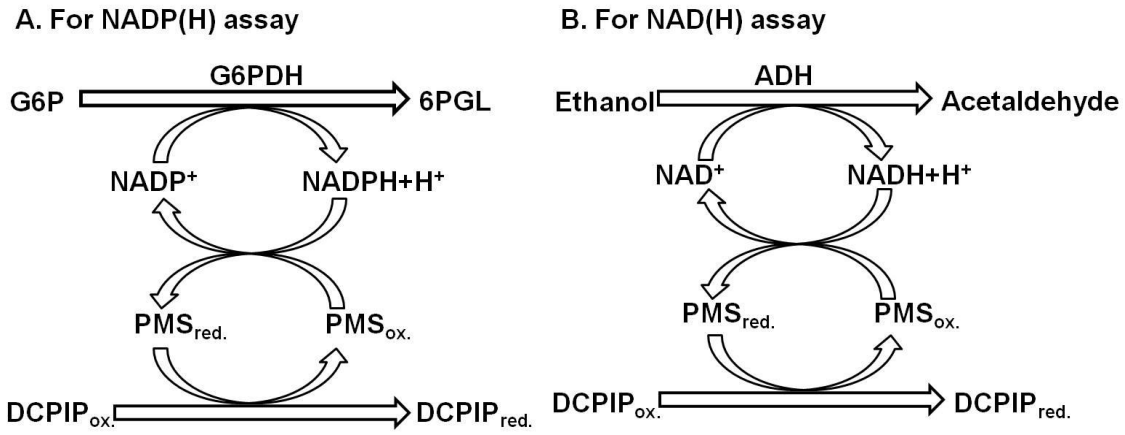

Fig.3.5. A model describing the reaction mechanism during estimation of NADP(H) and NAD(H) content. Abbreviations: ADH – alcohol dehydrogenase; DCPIP – dichlorophenolindophenol; G6P – glucose-6-phosphate; G6PDH – glucose-6-phosphate dehydrogenase; ox. – oxidized; PMS – phenazine methosulphate; red. – reduced.

For assay of $NADP^+$ and NADPH, G6PDH was freshly prepared by centrifugation of an $(NH_4)_2SO_4$ suspension and resuspension of the pellet to 200 Uml^{-1} in 100 mM HEPES (pH 7.5) containing 2 mM EDTA. Aliquots of 30 µl neutralized supernatant were introduced into plate wells containing 0.1 ml of 100 mM HEPES (pH 7.5) containing 2 mM EDTA, 20 µl of 1.2 mM DCPIP, 10 µl of 20 mM PMS, 10 µl of 10 mM glucose 6-phosphate, and 30 µl water. The reaction was started by the addition of 10 µl G6PDH and

decrease in absorbance was read at 600 nm for 3 min. The concentrations of corresponding pyridine nucleotides were calculated using relevant standard curve as shown in **Fig. 3.6** (0-40 pmole).

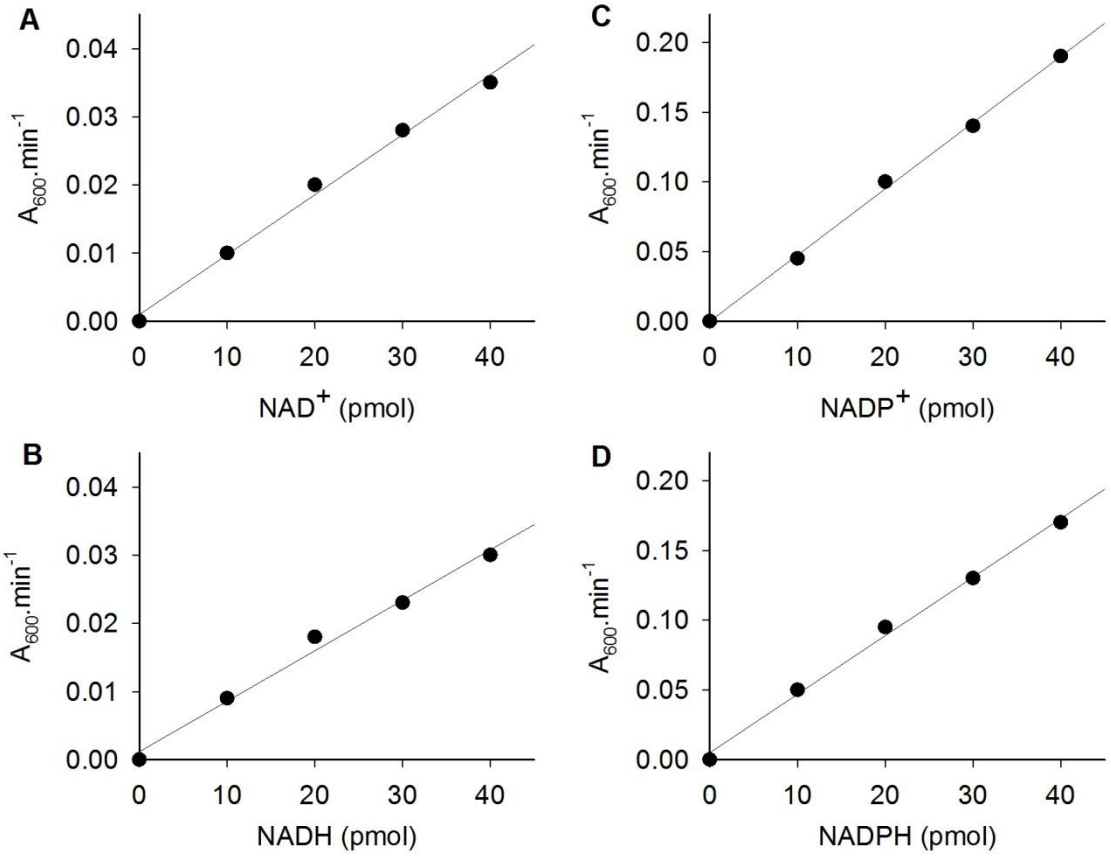

Fig.3.6. Typical standard curve for plate reader assay of pyridine nucleotides. Rates of absorbance change at 600 nm versus concentration of NAD^+ (A), NADH (B), $NADP^+$ (C) and NADPH (D).

3.7 Measurement of ascorbate and dehydroascorbate levels in leaf tissue

The ascorbate (Asc) and dehydroascorbate (DHA) contents were measured according to Foyer et al. (1983). Leaf discs (150 mg) were ground on ice bath using a mortar and pestle in 3 ml of 2.5 M $HClO_4$. The extract was adjusted to pH 5.6 by stepwise addition of 1.25 M K_2CO_3. The resulted precipitate was removed by centrifugation at 10,000 rpm for 10 min at 4 °C. The supernatant was used to estimate the Asc, DHA and Asc/DHA.

An aliquot of 100 µl of supernatant was added to 900 µl of 0.1 M sodium phosphate buffer (pH 5.6) and absorbance was read at 265 nm (A). Ascorbate oxidase (2.5 U, Roche Applied Science, Mannheim, Germany) was added to the above mixture and absorbance at 265 nm was measured (B). A fresh aliquot containing 100 µl of supernatant was incubated with 15 mM reduced glutathione prepared in 150 µl of 0.1 M Tricine–KOH buffer pH 8.5 for 15 min at room temperature. The volume was then made upto 1 ml with 0.1 M sodium phosphate buffer (pH 5.6) and the absorbance was read at 265 nm (C). Asc was measured as the difference of A-B, while DHA was measured as the difference of C-A.

3.8 Estimation of adenylate content

ATP and ADP content were estimated according to Padmasree and Raghavendra (1999a). Leaf tissue (100 mg) was homogenized in liquid nitrogen and extracted in 3% $HClO_4$. The samples were centrifuged at 10,000 rpm for 10 min at 4 °C and resulting supernatants were neutralized with KOH and left on ice for 30 min. The neutralized samples were further centrifuged as described above and the cleared supernatant was used for estimation of ATP and ADP. The levels of ATP were measured using enzymatic assays coupled to NADPH formation, while ADP levels were measured by coupling to NADH utilization, respectively.

3.9 Detection of ROS in leaf tissue

Total cellular ROS levels in leaf discs were monitored using a fluorescent dye, 2, 7-dichlorofluorescein diacetate (H_2DCF-DA). This non-polar compound is converted to membrane-impermeable polar derivative H_2DCF by cellular esterases and is rapidly oxidized to highly fluorescent DCF by intracellular H_2O_2 and other peroxides. Stocks of H_2DCF-DA (1 mM) were made in ethanol and stored in the dark at –20 °C. After the treatment with high light or AA, leaf discs were vacuum-infiltrated using a needle-less

plastic syringe with 25 µM H_2DCF-DA in 10 mM Tris-HCl (pH 7.4). Excess dye was removed with repeated washings, and the samples were immediately observed under a laser-scanning confocal microscope (TCSSP-2, AOBS 4 channel UV and visible; Leica, Germany) at λex 488 nm and λem 525 nm (Dinakar et al., 2010a).

3.10 H_2O_2 measurement in leaf tissue

Estimation of H_2O_2 content was done according to Velikova et al. (2000). Leaf tissue (100 mg) was homogenized in 0.1% TCA over an ice bath. Homogenate was centrifuged at 12,000 rpm for 15 min, 4 °C and supernatant was used for assay. The assay reaction contain 250 µl of supernatant, 250 µl of 10 mM potassium phosphate buffer (pH 7.0) and 500 µl of 1.0 M KI. The absorbance was read at 390 nm and the concentration of H_2O_2 was calculated using relevant standard as shown in **Fig. 3.7** (0-100 µmol H_2O_2).

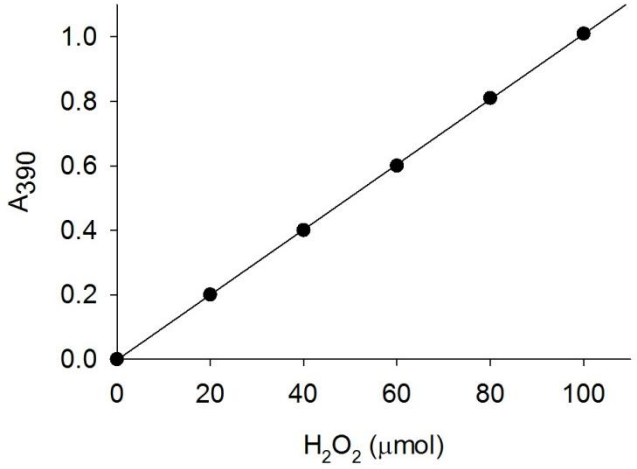

Fig.3.7. Typical standard curve for H_2O_2 demonstrate the absorbance at 390 nm versus concentration of H_2O_2.

3.11 Lipid peroxidation assay in leaf tissue

The thiobarbituric acid test, that quantifies malondialdehyde (MDA) as an end product was used to determine lipid peroxidation according to Heath and Packer (1968). Briefly, 100 mg of leaf tissue was homogenized in 500 µl of 0.1% trichloroacetic acid (TCA) solution on ice. The homogenate was centrifuged at 12,000 rpm for 10 min at 4 °C and

the supernatant was collected. Subsequently, 1.5 ml of 20% TCA containing 0.5% TBA was added to 500 µl of supernatant and boiled in a water bath for 30 min. The reaction was stopped by cooling on ice and centrifuged for 5 min at 12,000 rpm at 4 °C. The absorbance of the supernatant was measured at 532 nm and corrected for non-specific absorbance at 600 nm. The MDA content was calculated using the extinction coefficient of MDA-thiobarbituric acid complex ($\varepsilon = 155\ mM^{-1}\ cm^{-1}$).

3.12 Total RNA isolation and cDNA synthesis from leaf tissue

Total RNA was extracted from leaf tissue using TRI Reagent (Sigma-Aldrich, USA) according to manufacturer's instructions. Approximately 100 mg leaf tissue was ground in liquid nitrogen as fine powder and 1.0 ml of TRI reagent was added. Subsequently, the mixture was vortexed and incubated for 15 min at 25 °C. Thereafter, 200 µl of chloroform were added and incubated for 15 min at 25 °C. After vortexing, samples were centrifuged at 13,000 rpm for 15 min at 4 °C. The uppermost aqueous phase containing total RNA was transferred into a fresh tube containing an equal volume of isopropanol. Mixtures were thoroughly vortexed and further centrifuged as described above. Supernatants were discarded and the precipitated RNA pellets were washed at 4 °C using 1 ml of 75% ethanol for 5 min at 8,000 rpm. Resulting pellets were allowed to air-dry for 10-15 min, then resuspended in sterile DEPC-treated water. Concentration and quality of each RNA sample was analyzed using NanoDrop ND-1000 spectrophotometer (NanoDrop Technologies). One µg of total RNA with an A_{260}/A_{280} ratio of 1.9 – 2.0 was used for first-strand cDNA synthesis using iScript™ cDNA synthesis kit (BioRad, USA) according to the manufacturer's instructions.

3.13 Quantitative reverse transcriptase PCR (qRT-PCR) analysis from leaf tissue

Primers for real-time PCR were designed using Primer Express software (Applied Biosystems) such that at least one of the primers spanned the junction of two exons or intron-exon boundary, giving a single cDNA PCR product precluding amplification of

genomic DNA **(Table 3.2)**. The PCR mixture contained 5 µl of diluted cDNA, 10 µl of 2x SYBR Green PCR Master Mix (Takara bio Inc., Shiga, Japan), and 1.0 pmole of specific primers (synthesized by Eurofins Pvt. Ltd., India) in a final volume of 20 µl. Real-time PCR was carried out after pre-incubation at 95 °C for 10 min followed by 40 cycles of denaturation at 95 °C for 15 s and annealing/extension at 60 °C for 1 min using 7500 Fast Real-Time PCR machine (Applied Biosystems, USA). *UBQ5* was used as housekeeping gene. Cycle threshold (C_T) values were obtained from the exponential phase of PCR amplification. Comparative C_T method was used to analyze the results (Livak and Schmittgen 2001). In this method, genes of interest (GOI) were normalized against UBQ5 (housekeeping gene) expression, generating a ΔC_T value (ΔC_T = GOI C_T−UBQ5 C_T). The relative expression was then calculated according to the equation $2^{-\Delta\Delta CT}$ and WT was used as a calibrator.

Table 3.2 A list of primers corresponding to *A. thaliana* used for real-time PCR study.

Gene name	**Accession no.**	**Primer sequence (5' > 3')**	**Amplicon length (bp)**
UBQ5	AT3G62250	F- CCAAGCCGAAGAAGATCAAG R- ATGACTCGCCATGAAAGTCC	149
CSD1	AT1G08830	F- TGAACTCAGCCTGGCTACTGG R- AGCCACACACCAGAAGATACACAC	164
CAT1	AT1G20630	F- TGGGATTCAGACAGGCAAGAACG R- GTTTGGCCTCACGTTAAGACGAGT	162
CAT2	AT4G35090	F- CGAGGTATGACCAGGTTCGT R- AGGGCATCAATCCATCTCTG	178
sAPX	AT4G08390	F- CCTCCGGAGGGTATCGTTATCTA R- ACAGCCAGAAACATTGTCCAAAAGG	162
tAPX	AT1G77490	F- TGGAGAAGCAGGAGGACAGT R- GCAGCCACATCTTCAGCATA	177

cAPX	AT1G07890	F- GCATGGACATCAAACCCTCT R- AGCAAACCCAAGCTCAGAAA	213
ChlMDH	AT5G58330	F- ACCTCACTGGAGAGGGCATTG R- AATGTGGCTGTGCTCTGTACAGC	135
MMDH1	AT1G53240	F- TTGCCTCGAAGGTGAGGTTGG R- GAGGTGGCAACTCTAGCTGGA	204
ICDH	AT1G54340	F- TGATCCACGGAGCCAAGGTTAG R- CATGCAATAGCCCCTTTTCAGGCT	221
COX15	AT5G56090	F- AGTGGTTTAGAGGGCCACCG R- TCAGCTGGTGGTTCAGGCAT	146
AOX1A	AT3G22370	F- CTTCCAGAGGAGATATGGATGTCGA R- TGCATTCTCTCATTCTCTGCTTCCTC	165
PFK4	AT5G61580	F- GAGCAATACCGAGTAACGCATCAG R- TTGTCACTTCCGTCACCTGAG	156
UGP1	AT3G03250	F- GCCGTGGTCGAGAACAAGAACAT R- CTTGCTTTGCTGTGCCACTTGT	144
G6PD6	AT5G40760	F- AAGGTTGCGTGGGAGATCTTCAC R- GGAGGGATCCAGATATAGCCGTGAG	161
GDCH	AT2G35370	F- GCTCACAGAATCACCTGGCTTGATC R- AGAGAAACCCTCCTAGTGAGCAGC	163
GOX1	AT3G14420	F- ACAGGAGAGGATGCAAGGATAGCG R- CCAATGAGAATACCACTGGTCTTC	247

3.14 Bacterial and yeast strains

Escherichia coli DH5α cells were grown at 37 °C in 2% Luria Bertani media and were used for the maintenance of cloned plasmids. *Saccharomyces cerevisiae* cells were grown either in YPD medium (1% w/v yeast extract, 2% w/v peptone and 2% w/v dextrose) or SC-URA^{-} minimal medium (0.67% w/v yeast nitrogen base without amino acids, 2%

w/v glucose as carbon source and amino acids) at 30 °C. Protein expression was induced using 2% galactose as sole carbon source.

3.15 Plasmid DNA vectors

pET28a(+) (Novagen, USA)

pET28a(+) is a bacterial expression vector which carries T7 lac promoter, N-terminal His tag, thrombin cleavage site and C-terminal His tag. In the present study, pET-28a(+) is used for expressing AtAOX1a. This vector has a bacterial selectable marker for kanamycin.

pYES2 (Invitrogen™, USA)

pYES2 is a *S. cerevisiae* expression vector used for expressing AtAOX1a recombinant proteins. It has β - lactamase gene for ampicillin based bacterial selection and *URA3* gene for selection in *S. cerevisiae*.

3.16 Cloning of *AtAOX1a* in *E. coli*

a) PCR amplification of *AtAOX1a*

Total RNA isolation from *Arabidopsis* WT leaves and cDNA synthesis was done as described in **section 3.12**. The cDNA encoding for *AtAOX1a* mature protein comprising of 297 amino acid residues was amplified using Phusion DNA polymerase (Clontech) with forward primer: 5'-GAGAATTCGCTAGCACGATCACTCTGG-3' and reverse primer: 5'-GGCTCGAGTCAATGATACCCAATTGGAG-3'. The underlined nucleotides indicate *Eco*RI and *Xho*I restriction sites in forward and reverse primers, respectively. PCR thermal cyclic condition includes initial denaturation at 98 °C for 3 min, followed by 30 cycles of 98 °C for 10s, 60 °C for 30s, 72 °C for 30s and a final extension at 72 °C for 5 min. An aliquot (10-20 µl) from the amplified mix was run on 1% agarose gel to check for amplification.

b) Purification of DNA fragments from the agarose gel

After PCR amplification or restriction digestion, DNA bands were excised from the agarose gel and purification was done using QIAquick Gel Extraction Kit according to manufacturer's instructions (QIAGEN).

c) Restriction digestion

DNA digestion was carried out in a reaction volume of 20 µl at 37 °C for 3 h. The reaction mixtures contains 300-400 ng of plasmid DNA (pET28a vector) or insert DNA (amplified *AtAOX1a*), 2X reaction buffer, 5 U of restriction enzyme (New England Biolabs) per 1µg of DNA to be digested and sterile water.

d) Ligation

For plasmid DNA constructs, DNA insert was ligated using T4 DNA Ligase (Takara). The reaction mixture was made in a total volume of 20 µl comprising 1X of ligation buffer, linear digested plasmid DNA and insert DNA (1:3 ratio) and 1 U of T4 DNA Ligase. The reaction mixture was incubated in a water bath at 16 °C for 16 h.

e) Preparation of *E. coli* competent cells and transformation

A single colony of *E. coli* DH5α or BL21(DE3)pLysS cells was inoculated into 5 ml of LB broth and incubated overnight with constant shaking at 37 °C. One ml of the overnight culture was further grown in 50 ml of 2% LB broth with constant shaking until OD_{600} = 0.5. The cells were then cooled on ice for 10 min and centrifuged at 4,000 rpm for 5 min at 4 °C. The resulting pellet was suspended in 40 ml ice-cold 100 mM $CaCl_2$ and incubated on ice for 20 min and further centrifuged as described above. Finally, the pellet was resuspended in 2 ml ice-cold 100 mM $CaCl_2$ and 15% (v/v) sterile glycerol followed by immediate freezing in liquid nitrogen and finally stored at –80 °C in aliquots of 200 µl.

One µl of the plasmid DNA (10–50 ng/µl) or the ligated plasmid DNA construct (ligation mixture) was added to competent cells, gently mixed and incubated on ice for 30 min. The cells were subjected to heat shock at 42 °C for 90 s followed by immediate

incubation in ice for 1 min. LB broth (0.8 ml) was added to the treated cells and further incubated at 37 °C with shaking at 200 rpm for 1 h. Aliquots (100–200 µl) of the transformed cells were spread on LB agar plates (2% Luria Bertani and 1% Agar powder) containing 50 µg/ml kanamycin followed by incubated at 37 °C for overnight.

f) Plasmid DNA isolation from *E. coli*

For plasmid isolation, transformed *E. coli* colonies (DH5α/pLysS) were inoculated in 5 ml of LB broth in presence of 50 µg/ml kanamycin antibiotic and allowed to grow overnight with shaking at 200 rpm at 37 °C. The culture was harvested by centrifugation at 8,000 rpm at room temperature for 3 min and plasmid isolation was done using QIAprep® Spin Miniprep kit (QIAGEN) according to the manufacturer's protocol.

g) DNA sequencing

Positive clones having desired inserts were sent for sequencing to Eurofins Genomics Pvt. Ltd., India. Forward sequencing was done using T7 primer (5'-TAATACGACTCACTATAGGG-3'), whereas reverse sequencing was done using *AtAOX1a* reverse primer (5'-GGCTCGAGTCAATGATACCCAATTGGAG-3'). Sequencing was based on Sanger's sequencing method i.e. dideoxy chain termination method. The obtained sequences were matched by aligning with *AtAOX1a* DNA sequence (AT3G22370) using ClustalW2 multiple sequence alignment tool.

3.17 Expression, purification and confirmation of recombinant protein (pETAtAOX1a)

The expression of AtAOX1a in *E. coli* BL21(DE3)pLysS was induced by the addition of 0.1 mM isopropyl-β-D-thiogalactopyranoside (IPTG) at 28 °C for 4 h in LB medium supplemented with 50 µg/ml kanamycin. The culture was harvested by centrifugation and subjected to the lysis buffer (50 mM Tris-HCl pH 8.0, 150 mM NaCl, 15 mM Imidazole and 1 mM PMSF) for protein extraction.

Protein was separated on 12.5% sodiumdodecyl sulfate polyacrylamide gel electrophoresis (SDS-PAGE) according to Laemmli (1970). The resolving gel was polymerized using 375 mM Tris-HCl buffer pH 8.8, 10% or 12.5% acrylamide, 0.1% SDS, 0.05% ammonium per sulphate (APS) and N,N,N',N'-tetramethylethylenediamine (TEMED). The stacking gel was made of 125 mM Tris-HCl (pH 6.8), 4% acrylamide, 0.1% SDS, 0.04% APS and TEMED. The crude protein was mixed with sample buffer (250 mM Tris-HCl pH 6.8, 8% SDS, 50% glycerol, 10% β-mercaptoethanol and 0.04% bromophenol blue) and boiled at 100 °C for 3 min followed by loading on to gel. Electrophoresis was performed initially at 60V (until the dye migrates into the resolving gel) and then at run at 120 V. The protein expression was visualized by coomassie staining of gel.

After expression, recombinant AtAOX1a protein was purified under denaturing conditions using Ni-NTA column. Protein extract was loaded on to a Ni-NTA column equilibrated with lysis buffer pH 8.0 (8 M Urea, 10 mM Imidazole, 0.1 M NaH_2PO_4 and 0.01 M Tris base) followed by reloading of flow through to allow for sufficient binding of His6-tagged AtAOX1a to Ni-NTA. The column was washed twice with 10 ml of wash buffer pH 6.3 (8 M Urea, 50 mM Imidazole, 0.1 M NaH_2PO_4 and 0.01 M Tris base) and finally eluted in 5 ml of elution buffer pH 4.5 (8 M Urea, 250 mM Imidazole, 0.1 M NaH_2PO_4 and 0.01 M Tris base). Flow through, wash and elution fractions were run on 12.5% SDS-PAGE and visualized by coomassie stain. The purified protein was cut out of the gel with a sharp, sterile surgical blade and eluted in Milli-Q water and subjected to tryptic digestion, followed by matrix assisted laser desorption ionization time-of-flight mass spectrometry (MALDI-TOF/TOF) analysis for further confirmation as AtAOX1a.

3.18 Antibody generation

The purified pET/AtAOX1a protein band (equivalent to one milligram) was cut out of the gel and lysed into 0.5 ml of phosphate buffered saline pH 7.4 (137 mM NaCl, 2.7 mM

KCl, 10 mM Na_2HPO_4 and 2 mM KH_2PO_4). The solution was mixed with 0.5 ml of Freund's incomplete/complete adjuvant at a protein concentration of 1 mg/ml. The first dose of protein with Freund's incomplete adjuvant was injected subcutaneously to an adult rabbit (Newzealand white male rabbit) followed by three subsequent doses of protein with Freund's complete adjuvant given at regular interval of 10 days. After 40 days, the blood was collected from a rabbit's ear vein and resulting serum was used as polyclonal antibody. Animal ethics approval number is UH/IAEC/KPMS/2014-1/24.

3.19 Cloning and of *AtAOX1a* in yeast

a) PCR amplification of *AtAOX1a* and DNA purification

Total RNA isolation from *Arabidopsis* WT leaves and cDNA synthesis was done as described in **section 3.12**. The cDNA encoding for *AtAOX1a* mature protein comprising of 354 amino acid residues, was amplified using Phusion DNA polymerase (Clontech) with forward primer: 5'-GGGAATTCTGATGATGATAACTCGCGGTGG-3' and reverse primer: 5'-GGCTCGAGTCAATGATACCCAATTGGAG-3'. The underlined nucleotides indicate *Eco*RI and *Xho*I restriction sites in forward and reverse primers, respectively. PCR thermal cyclic condition includes initial denaturation at 98 °C for 3 min, followed by 30 cycles of 98 °C for 10s, 60 °C for 30s, 72 °C for 30s and a final extension at 72 °C for 5 min. An aliquot from the amplified mix was run on 1% agarose gel to check for amplification. The amplified DNA bands were excised from gel and purified as described in **section 3.16b**.

b) Restriction digestion and ligation

DNA digestion was carried out in a reaction volume of 20 µl at 37 °C for 3 h. The reaction mixtures contains 300-400 ng of plasmid DNA (pYES2 vector) or insert DNA (amplified *AtAOX1a*), 2X reaction buffer, 5 U of restriction enzyme (New England Biolabs) per 1µg of DNA to be digested and sterile water. For plasmid DNA constructs, DNA insert was ligated as described in **section 3.16d**.

c) Transformation in DH5α cells and plasmid isolation

The ligated product was transformed in DH5α cells as described in section **3.16e**. Further plasmid isolation was performed as described in section **3.16f**. However, in this case ampicillin (100µg/ml) antibiotic was used in place of kanamycin, as pYES2 vector has ampicillin resistant gene.

d) DNA sequencing

Positive clones having desired inserts were sent for sequencing to Eurofins Genomics Pvt. Ltd., India. Forward sequencing was done using T7 primer (5'-TAATACGACTCACTATAGGG-3'), whereas reverse sequencing was done using CYC1 primer (5'-GTCACGCTTACATTCACGC-3'). Sequencing was based on Sanger's sequencing method i.e. dideoxy chain termination method. The obtained sequences were matched by aligning with *AtAOX1a* DNA sequence (AT3G22370) using ClustalW2 multiple sequence alignment tool.

e) Preparation of *S. cerevisiae* competent cells and transformation

A single colony of yeast (INVSc1) was inoculated in 5 ml of YPD broth and was incubated overnight at 30 °C with shaking at 200 rpm. Secondary inoculation was done in 40 ml of YPD broth so that the final required OD_{600} after two generation (3h) reaches 0.5. The following equation was used to calculate the volume of overnight culture to be used for inoculation:

$V1 \times OD_{600}$ of overnight culture $\times (2)^{2\ (generations)}$ = Final Volume × Final OD_{600} (required)

$V1 \times 2.5 \times 4 = 40\ ml \times 0.5$

V1= 2.0 ml.

Thus, 2 ml of the primary inoculum was added to 40 ml of YPD broth. The culture was incubated at 30 °C (200 rpm) for 3 h or more until OD_{600} reaches 0.5 to 0.7. Immediately the culture was placed in ice and then centrifuged at 3500 rpm for 5 min at 4 °C. The harvested cells were resuspended in 10 ml of ice-cold sterile water followed by further

centrifugation at 3500 rpm for 5 min at 4 °C. The pellet was finally resuspended in 300µl of ice-cold freshly prepared lithium solution (10 mM Tris-HCl ph7.5, 1.0 mM EDTA and 100 mM lithium acetate pH7.5) to make the cells competent, and kept on ice.

Cloned plasmid DNA sample (5–10 µg) was mixed with 10 µg of carrier i.e. Salmon Sperm DNA (Sigma-Aldrich, USA) to make a final volume not exceeding 20 µl. Later, 200 µl of freshly prepared competent cells were added to the above mixture followed by immediate addition of 1.2 ml of freshly prepared PEG 2000 (Sigma-Aldrich, USA) solution. The mixture was incubated at 30 °C for 30 min at 200 rpm. Thereafter, cells were subjected to heat shock at 42 °C for 15 min followed by centrifuged at 14,000 rpm for 6 s. The PEG supernatant was then removed carefully and the pellet was resuspended in 200 µl of 1X TE buffer followed by spreading on SC-URA^{-} agar plates containing 2% glucose and 100 µg/ml ampicillin.

3.20 Recombinant protein (pYES2AtAOX1a) expression in *S. cerevisiae*

For protein expression, liquid cultures were grown overnight in 5 ml of SC-URA^{-} medium containing 2% galactose. Protein extraction was done according to Laskar et al. (2011). The culture was further inoculated in same medium until the OD_{600} reaches 0.5. The culture pellet was washed with distilled water followed by 500 µl of 20% TCA. The pellet was resuspended in 200 µl of 20% TCA containing 100 mg acid washed glass beads and vortexed at 4 °C for 30 min. The TCA precipitated proteins were further washed with 5% TCA and dissolved in 60 µl of 1× sample buffer along with 6.66 µl of 1.0 M DTT and 33 µl of 1.0 M Tris HCl (pH 9.0). The protein samples were boiled for 3-5 min followed by centrifugation at 13,000 rpm for 5 min at 25 °C and resulting supernatant was subjected to 12% SDS-PAGE (as described in **section 3.17**).

For immunodetection, proteins were transferred from gel to polyvinylidene difluoride (PVDF) membrane under semi-dry conditions (Towbin et al., 1979). PVDF membrane was cut equivalent to size of gel and activated by sequential incubation in

methanol, water and transfer buffer (25 mM Tris-HCl pH 8.3, 192 mM glycine and 20% methanol). Gel and PVDF membrane were sandwiched by three layers of Whatman No. 3 chromatography papers (presoaked with transfer buffer). The entire sandwich was kept on semi-dry western blot unit and a power supply was given at 0.8 mA per cm^2 area (TE 77 PWR, Semi-dry transfer unit, Amersham Biosciences). The transfer of protein was confirmed by Ponceau S staining (0.2% Ponceau S stain prepared in 3% trichloroacetic acid). The PVDF membrane was blocked with 5% non-fat milk powder prepared in Tris-Buffered Saline (TBS) containing 25 mM Tris-HCl pH 7.5 and 150 mM NaCl. The blocking was allowed for 1 hr at room temperature. The membrane was washed with TBS-Tween (25 mM Tris-HCl pH 7.5, 150 mM NaCl, and freshly added 0.2% Tween 20) for 30 min (3 x 10 min). PVDF membrane was treated for 1 h with a polyclonal antibody against AOX1a (1:1000 dilution) followed by washing with TBS-Tween (3 x 10 min) and treated with goat anti-Rabbit IgG alkaline phosphatase conjugate (1:3000) for 1-2 h. The membrane was finally washed with TBS-Tween and blot was developed using BCIP/NBT (5-bromo-4-chloro-3-indolyl phosphate/nitro-blue-tetrazolium chloride) solution (Bangalore Genei, India).

3.21 Respiration measurement in *S. cerevisiae* cells

The respiratory oxygen uptake measurements were performed using a Hansatech oxygraph (Hansatech Instruments Ltd., United Kingdom). A total of 30 ml of cells was harvested from exponentially grown cultures (OD_{600} = 0.7 to 1.0) by centrifuging at 5000 rpm for 5 min at 4 °C. The cell pellet was resuspended in SC-URA^- minimal medium at a density of approximately 20 OD_{600} units. An aliquot of 25 µl of this cell suspension was added to the oxygraph chamber and brought to final reaction volume of 1 ml with SC-URA^- minimal medium and subsequently, O_2 consumption was measured for 10 min at 25 °C (Agrimi et al., 2011; Dalal et al., 2014).

3.22 Growth of *S. cerevisiae* in liquid media and phenotypical analysis

From the overnight grown primary culture, secondary inoculation was given and the cultures were grown in SC-URA^{-} minimal medium containing 2% galactose up to an OD_{600} of 0.5 and subsequently diluted to an OD_{600} of 0.2 with the same media. Cells were treated with 1 mM KCN and change in growth was recorded up to 6 h by monitoring the OD_{600} at an interval of 2 h duration.

Further, diluted culture (OD_{600} = 0.2) was incubated with 2 mM H_2O_2 or 0.25 mM tertiary-butyl hydroperoxide (t-BOOH) for 4 h at 30 °C. Thereafter, 2.5 µl of control (without inhibitor) and treated (H_2O_2/t-BOOH) cultures were spotted on YPD plates at different dilutions (10^{-1}, $10^{-1.5}$, 10^{-2}, $10^{-2.5}$ and 10^{-3}). Plates were incubated at 30 °C and photographed after 48 h. Similarly, viability of cells was examined with fluctuation assay by plating 500 numbers of controls/treated cells (1.0 OD_{600} = 3×10^7 cells) on YPD plates. After 48 h of growth, colonies were counted manually and cell survival rate in treated samples was determined as a percent of respective controls (Dalal et al., 2014).

3.23 Measurement of pyridine nucleotide content in *S. cerevisiae* cells

The extraction and estimation of NAD and NADH were done according to Queval and Noctor (2007) with minor modifications. Cultures grown in 10 ml of SC-URA^{-} minimal medium (OD_{600} = 0.5 to 0.7) were exposed to oxidative stress by incubating with 2 mM H_2O_2 or 0.25 mM t-BOOH for 75 min at 30 °C in dark. Cells were centrifuged and resuspended in 0.2 N HCl for NAD^+ extraction and 0.2 M NaOH for NADH extraction, respectively. Subsequently, 100 mg of acid washed glass beads (Sigma, USA) were added to each sample and vortexed for 5 min with intermittent cooling. Finally, the samples were centrifuged at 10,000 rpm for 10 min at 4 °C. The supernatant was boiled for 1 min and rapidly cooled on ice. For measurement of NAD, the pH of supernatant was set between 5.0 and 6.0 using 0.2 M NaH_2PO_4 and 0.2 M NaOH. For measurement of

NADH the final pH of supernatant was set between 7.0 and 8.0 by the addition of 0.2 N HCl as described in Queval and Noctor (2007). The assay involves phenazine methosulfate (PMS) catalysed reduction of dichlorophenolindophenol (DCPIP) in the presence of alcohol dehydrogenase (ADH) and ethanol as described in **section 3.6**.

3.24 Detection of ROS in *S. cerevisiae* cells

The intracellular ROS level was measured according to Jang et al. (2004). The cultures were grown in SC-URA$^-$ minimal medium containing 2% galactose. Cells were harvested from cultures showing OD_{600} between 0.5 and 0.7 by centrifugation at 5000 rpm for 10 min at 4 °C. The pellet was washed twice with fresh SC-URA$^-$ minimal medium and resuspended in the same medium to attain a final OD_{600} of 10. The cells were treated with 2 mM H_2O_2 or 0.25 mM t-BOOH for 10 min followed by incubation with 100 µM 2′, 7′- dichlorodihydrofluorescein diacetate (H_2DCF-DA, Sigma) for 5 min in the dark at 25 °C. After treatment, the cells were washed twice with SC-URA$^-$ minimal medium to remove the excess dye. Thereafter, 10 µl of cell suspension were added onto a glass slide and imaged immediately under a laser-scanning confocal fluorescence microscope (LSM 710 NLO ConfoCor 3; Carl Zeiss, Germany). The excitation and emission wavelengths used for DCF fluorescence were 488 nm and 530 nm, respectively.

3.25 RNA isolation and cDNA synthesis from *S. cerevisiae* cells

Cultures were grown in 10 ml of SC-URA$^-$ minimal medium upto an OD_{600} = 1.0 and subsequently exposed to oxidative stress using 2 mM H_2O_2 or 0.25 mM t-BOOH for 75 min at 30 °C. Total RNA was isolated using acid phenol method (Schmitt et al., 1990). Briefly, cells were harvested by centrifugation at 10,000 rpm (4 °C) for 5 min and resuspended in 400 µl of 50 mM sodium acetate (pH 5.3) and 10 mM EDTA. Supernatant was transferred to 1.5 ml tube and 40 µl of 10% SDS was added. Mixture was vortexed and equal volume of phenol was added, vortexed and incubated at 65 °C for 4 min. The

mixture was rapidly cooled on ice for 5 min followed by centrifugation at 12,000 rpm for 10 min at 4 °C. The aqueous layer was mixed with 400 µl chloroform, vortexed and further centrifuged as described above. The extracted aqueous phase was precipitated by adding 1/10th volume of 3 M sodium acetate (pH 5.2) and 2.2 volume of chilled ethanol. The RNA pellet was washed with 70% ethanol and dissolved in 30 µl DEPC treated water. First strand cDNA was synthesized with 2 µg of total RNA using SuperScript® III (Invitrogen) according to manufacturer's instructions.

3.26 Quantitative reverse transcriptase polymerase chain reaction (qRT-PCR) analysis from *S. cerevisiae* cells

Changes in transcript levels were measured using Mastercycler® ep realplex4 (Eppendorf, Germany). Primers used in the present study are listed in **Table 3.3**. Reaction mixture contains 2 µl of cDNA (50 ng), 10 µl of 2x SYBR Green PCR Master Mix (Takara Bio Inc., Shiga, Japan), 0.5 µl of specific primers (0.1 pmole) and 7.0 µl of sterilized water. The thermal cycling conditions were 95 °C for 10 min, followed by 40 cycles at 95 °C for 20 s and 59 °C for 35 s.

Table 3.3 A list of primers corresponding to *S. cerevisiae* used for real time PCR study.

Gene	Accession no.	Primer Sequence (5'>3')	Amplicon length (bp)
SOD1	YJR104C	F- TGGTTGTGTCTCTGCTGGTC R- TAACGACGCTTCTGCCTACA	191
SOD2	YHR008C	F- CAAGCTGGACGTTGTTCAAA R- AGATCTTGCCAGCATCGAAT	191
GPX2	YBR244W	F- TTTGGGGTTCCCATGTAATC R- ACCTGCTTTTTGGCTTTTCA	172
TSA2	YDR453C	F- TTTGTCCCATTGGCTTTTTC R- ACCGTCTTTTCTGGGAAGGT	159
ACT1	YFL039C	F- CGTTCCAATTTACGCTGGTT R- GAAGTCCAAGGCGACGTAAC	184

Cycle threshold (C_T) values were obtained from the exponential phase of PCR amplification. Comparative C_T method was used to analyze the relative gene expression levels (Livak and Schmittgen, 2001). In this method, the gene of interest (GOI) was normalized against actin (*ACT1*) expression, generating a ΔC_T value (ΔC_T = GOI C_T − ACT1 C_T). Relative expression was then calculated according to the equation $2^{-\Delta\Delta CT}$ where pYES2 was used as a calibrator.

3.27 Statistical analysis

The data presented are the average values of results (±SE) from three to four independent experiments conducted on different days. Triplicates were run in each independent experiment. The differences between treatments were analyzed by one-way ANOVA, Tukey test of multiple comparison analysis using Sigma Plot 11.0 software (San Jose, CA, USA).

***

Chapter 4

Physiological role of AOX1a in optimizing photosynthesis under high light stress in *Arabidopsis thaliana*

4.1 Introduction

Light is an essential component for photosynthesis and thereby determines plant growth. But, excess light leads to over-reduction of the chloroplastic electron transport carriers, which results in the generation of ROS and thereby serious damage of the photosynthetic machinery. Since, plants are sessile in nature, and therefore to cope with excess light, they evolved multiple direct or indirect strategies such as (i) thermal dissipation of light energy brought about by the conformational changes in PSII, (ii) operation of the xanthophyll cycle, (iii) dissipation of excess chloroplastic reducing equivalents through operation of malate-oxaloacetate (malate-OAA) shuttle and involvement of external/internal mitochondrial NAD(P)H dehydrogenases, AOX and uncoupling proteins of mitochondrial respiratory chain, and (iv) photorespiration (Vanlerberghe, 2013; Raghavendra and Padmasree, 2003; Noguchi and Yoshida, 2008; Yoshida and Noguchi, 2009; Voss et al., 2013).

The importance of AOX in dissipating excess chloroplastic reducing equivalents to optimize and protect photosynthesis from photoinhibition has gained much interest and attention since past two decades (Dinakar et al., 2010a; Raghavendra and Padmasree, 2003; Noguchi and Yoshida, 2008; Padmasree and Raghavendra, 1999b; Zhang et al., 2010; Dinakar et al., 2010b; Yoshida et al., 2011b; Florez-Sarasa et al., 2011; Xu et al., 2011). The role of AOX in optimizing photosynthesis was demonstrated either by restricting the electron transport through the AOX pathway using specific metabolic inhibitors such as SHAM and propyl gallate (Dinakar et al., 2010a; Padmasree and Raghavendra, 1999a,b; Yoshida et al., 2006; Zhang et al., 2011), or using overexpression/antisense or mutant lines of AOX and monitoring photosynthetic

metabolism (Zhang et al., 2010; Florez-Sarasa et al., 2011; Strodtkötter et al., 2009; Chai et al., 2010). In these studies, the involvement of the malate-OAA shuttle to transfer reducing equivalents from the chloroplast to mitochondrial AOX was demonstrated indirectly by increased levels of NADP-malate dehydrogenase (NADP-MDH), NAD-malate dehydrogenase (NADMDH), citrate synthase (CS), NAD-malic enzyme (NAD-ME) and NADP-isocitrate dehydrogenase (NADP-ICDH) activities and increase in redox ratios of malate and OAA (Zhang et al., 2010; Hebbelmann et al., 2012; Padmasree and Raghavendra, 1999c; Yoshida et al., 2007). Further, an increase in pyruvate and malate levels parallel to AOX catalyzed respiration under high light in presence of SHAM indicated the role of these metabolites in dissipating excess chloroplastic reducing equivalents through AOX pathway (Dinakar et al., 2010a). Most of these experiments also revealed the importance of AOX in preventing ROS formation which is generated on exposure to light due to over-excitation/over-reduction of chloroplastic electron transport carriers (Giraud et al., 2008; Dinakar et al., 2010b; Xu et al., 2011; Zhang et al., 2011; Strodtkötter et al., 2009).

In the present study, we used *aox1a* mutant of *A. thaliana* to gain further insight into the physiological role of AOX under photoinhibitory conditions. Here we monitored the following parameters which are essential for efficient photosynthesis and cellular redox homeostasis under HL stress: (i) heat dissipation from over-energized chloroplasts (ii) changes in redox balance by direct measurement of NAD(P) and NAD(P)H pools and ratios, and (iii) possible alternate sinks for utilization of excess chloroplastic reducing equivalents.

4.2 Results

4.2.1 Confirmation of T-DNA insertion in *aox1a* mutant

T-DNA insertion within the AOX1A gene (SALK_084897 T-DNA insertion line) was verified by a genomic PCR with T-DNA-specific primers. A homozygous T-DNA insertion line was identified from the next generation by a genomic PCR, RT-PCR and northern blot analysis (Strodtkötter et al., 2009). The same homozygous line was used in the present study. However, *aox1a* mutant line was further confirmed through RT-PCR analysis using *AOX1A* gene specific primers, which showed an amplification of 165 bp PCR product from WT, but not in case of *aox1a* mutant **(Fig. 4.1)**.

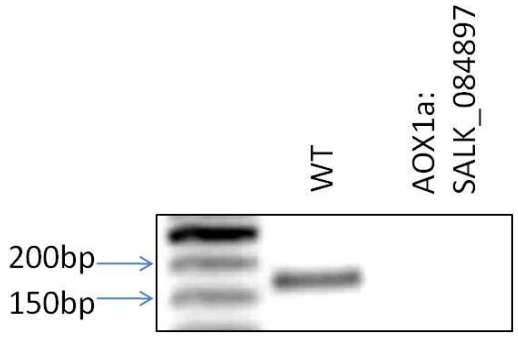

Fig.4.1. Characterization of T-DNA insertion line for AOX1a (SALK_084897) using reverse transcriptase PCR analysis. A 165 bp PCR product was amplified from the WT cDNA, but not from *aox1a* cDNA.

4.2.2 Determination of photoinhibitory light intensity and effect of AOX1a deficiency on O_2 uptake and O_2 evolution

To examine the role of AOX under HL stress, different groups used different light intensities in *A. thaliana* like 320-450 µmol photons $m^{-2}s^{-1}$ (Yoshida et al., 2008; Yoshida and Noguchi, 2009; Rosso et al., 2009), 800-1000 µmol photons $m^{-2}s^{-1}$ (Zhang et al., 2010; Florez-Sarasa et al., 2011; Gandin et al., 2012) and 1800 µmol photons $m^{-2}s^{-1}$ (Talla et al., 2011). In order to avoid too much light that can cause permanent damage to the photosynthetic machinery and ascertain the photoinhibitory light intensity, we pre-illuminated the leaf discs to a range of light intensities starting from 50 µmol photons

$m^{-2}s^{-1}$ (growth light, GL, which is given to plants used in the present study) to 700 µmol photons $m^{-2}s^{-1}$ (HL, maximum light emitted by the LEDs of the leaf disc oxygen electrode chamber) and monitored the rates of respiratory O_2 uptake and photosynthetic O_2 evolution.

At GL, the rates of respiratory O_2 uptake in WT and *aox1a* were similar with 2.40 ± 0.11 and 2.37 ± 0.13 µmol O_2 m^{-2} s^{-1}, respectively. After pre-illumination, the respiratory O_2 uptake increased at all light intensities in both WT and *aox1a* as compared to GL. However, the increase in O_2 uptake at 250 µmol photons $m^{-2}s^{-1}$ was more pronounced in *aox1a* than WT **(Fig. 4.2A)**.

Similar to respiration, rates of photosynthesis were maximal (5.67 ± 0.13 and 5.07 ± 0.09 µmol O_2 m^{-2} s^{-1}) at 250 µmol photons $m^{-2}s^{-1}$, but minimal (2.12 ± 0.12 and 1.16 ± 0.02 µmol O_2 m^{-2} s^{-1}) at 700 µmol photons $m^{-2}s^{-1}$ in both, WT and *aox1a*, respectively. On the other hand, the rates of O_2 evolution were significantly decreased at 500 µmol photons $m^{-2}s^{-1}$ when compared to 250 µmol photons $m^{-2}s^{-1}$ light intensity, but with no significant difference between WT and *aox1a* **(Fig. 4.2B)**. Thus, these results suggest that 700 µmol photons $m^{-2}s^{-1}$ can be applied as the photoinhibitory light to reveal the importance of AOX1a in sustaining photosynthesis.

4.2.3 Effect of AOX1a deficiency on chlorophyll fluorescence and P700 parameters under HL stress

To evaluate further the role of AOX1a in keeping up photochemical reactions and providing photoprotection against HL, we measured the maximum quantum yield of PSII (Fv/Fm) after initial saturation pulse (SP). Both WT and *aox1a* showed no significant difference in Fv/Fm under GL which was > 0.8. In contrast, under HL, Fv/Fm decreased from 0.82 ± 0.003 to 0.62 ± 0.03 in WT and from 0.82 ± 0.004 to 0.51 ± 0.02 in *aox1a*, respectively **(Fig. 4.3A)**.

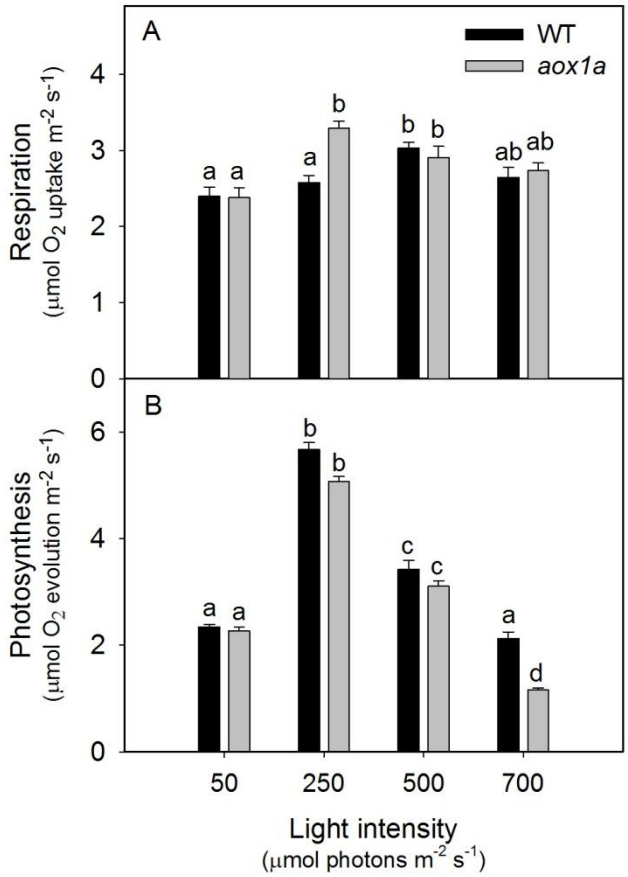

Fig. 4.2. The rates of (A) respiratory O_2 uptake and (B) photosynthetic O_2 evolution in leaf discs of WT and *aox1a* after pre-illuminating (6 h) at different light intensities: 50, 250, 500 and 700 µmol photons m^{-2} s^{-1} at 25 °C. After pre-illumination, leaf discs were in dark for 10-15 during electrode calibration before measuring the respiration rates. Respiration was measured for 5 min followed by photosynthesis measured for 10 min as $NaHCO_3$-dependent (ca. 5% v/v) O_2 evolution at light intensities given during pre-illumination. Different lowercase alphabetical letters indicate statistically significant difference ($P < 0.05$).

After measurement of Fv/Fm, actinic light (AL) was switched off for 40 s to allow the complete reoxidation of PSII reaction centres. Further, we recorded quantum yield [Y(II)], photochemical quenching (qP), non-photochemical quenching (NPQ), electron transport rate of PSII [ETR(II)], quantum yield of PSI [Y(I)] and reduced state of P700 (P700 red.) with every SP given up to 260 s at regular intervals of 20 s. Under GL, a very similar pattern of Y(II), qP, NPQ, ETR(II), Y(I) and P700 red. was observed between WT and *aox1a* **(Fig. 4.3B-E and 4.4A,B)**. On exposure to HL, a drastic decrease in both Y(II) and qP was observed in both WT and *aox1a*. However, this decrease was more pronounced in *aox1a* **(Fig. 4.3B,C)**. Under HL, NPQ was higher in WT when compared to *aox1a* **(Fig. 4.3D)**. Further, under HL, ETR(II) was more inhibited in case of *aox1a* compared with WT **(Fig. 4.3E)**. On the other hand, Y(I) was less affected compared to Y(II) and decreased similarly in both WT and *aox1a*, while P700 reduction was more evident in *aox1a* **(Fig. 4.4A,B)**. Thus, these results indicate the role of AOX1a in keeping up the photosynthetic quantum yield, particularly of PSII.

4.2.4 Effects of AOX1a deficiency on redox ratio under HL stress

The changes in the cellular redox status on exposure to HL were monitored by direct quantification of NAD^+, NADH, $NADP^+$ and NADPH. Under GL, the total cellular levels of NAD^+ and NADH were similar in both WT and *aox1a* **(Fig. 4.5A,B)**. But, when exposed to HL, NAD^+ levels increased in WT from 256.66 ± 3.22 nmoles g^{-1} FW at GL to 277.44 ± 7.37 nmoles g^{-1} FW at HL and decreased in *aox1a* from 253.88 ± 4.69 nmoles g^{-1} FW at GL to 236.77 ± 9.34 nmoles g^{-1} FW at HL **(Fig. 4.5A)**. On the other hand, NADH levels were increased in both genotypes, namely in WT from 36.50 ± 1.54 nmoles g^{-1} FW at GL to 41.44 ± 2.05 nmoles g^{-1} FW and in *aox1a* from 37.25 ± 1.76 nmoles g^{-1} FW at GL to 42.87 ± 1.71 nmoles g^{-1} FW at HL **(Fig. 4.5B)**. However, the ratio of NADH to the total cellular NAD^+ + NADH pool increased significantly from

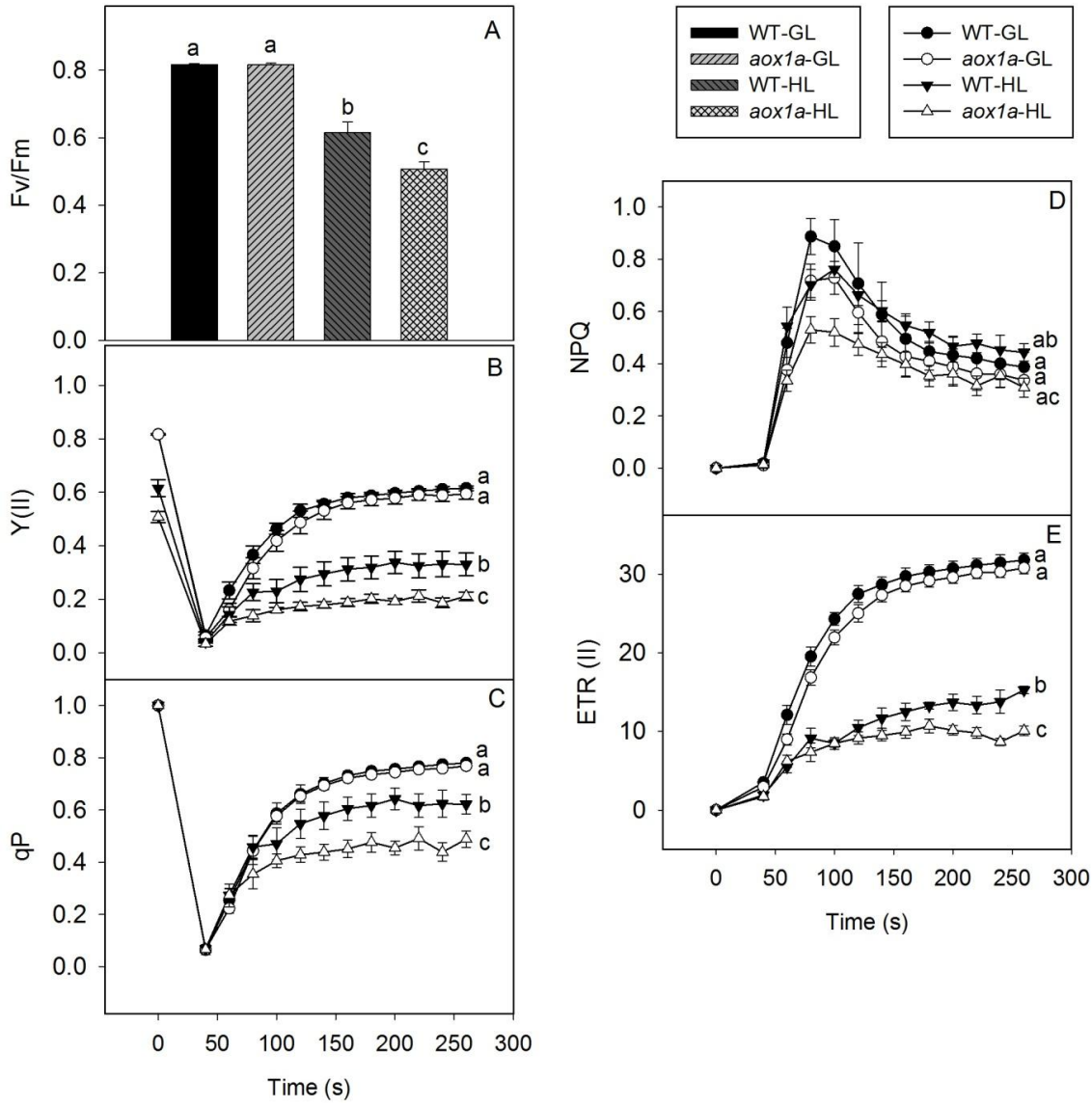

Fig.4.3. Characteristics of chlorophyll fluorescence parameters in WT and *aox1a* after pre-illumination (6 h) in GL (50 µmol photons m^{-2} s^{-1}) and HL (700 µmol photons m^{-2} s^{-1}) at 25 °C: (A) maximum quantum yield of PSII (Fv/Fm); (B) relative quantum yield of PSII [Y(II)]; (C) photochemical quenching (qP); (D) non-photochemical quenching (NPQ); (E) electron transport rate of PSII [ETR(II)]. Details for measurement of chlorophyll fluorescence parameters were as described in materials and methods. Different lowercase alphabetical letters indicate statistically significant difference ($P < 0.05$).

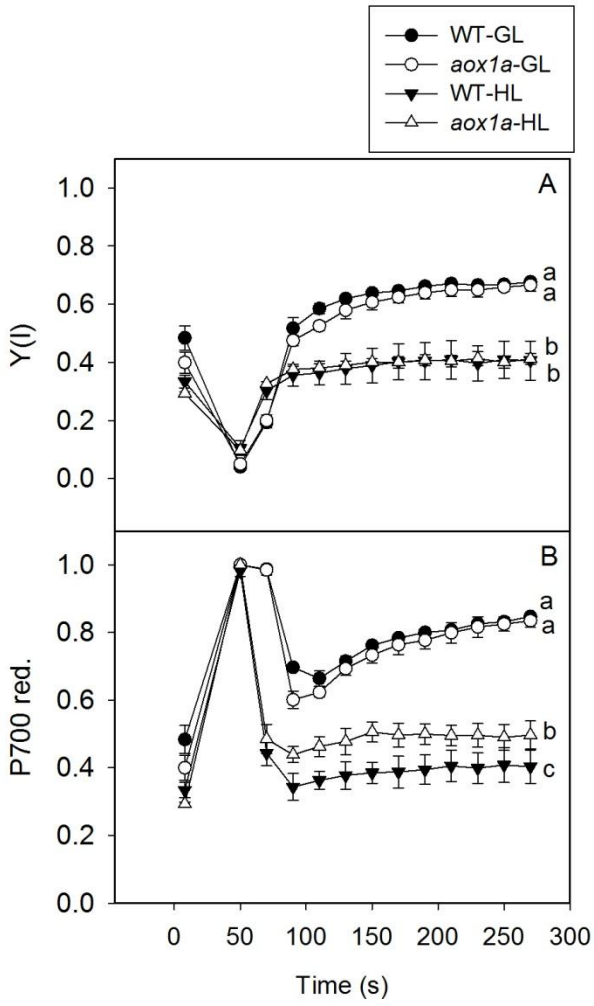

Fig.4.4. Characteristics of P700 parameters in WT and *aox1a* after pre-illumination (6 h) in GL (50 µmol photons m^{-2} s^{-1}) and HL (700 µmol photons m^{-2} s^{-1}) 25 °C: (A) quantum yield of PSI [Y(I)]; (B) reduced P700 (P700 red). Details for measurement of P700 parameters were as described in materials and methods. Different lowercase alphabetical letters indicate statistically significant difference ($P < 0.05$).

0.129 ± 0.006 at GL to 0.156 ± 0.007 at HL in *aox1a* when compared to WT where the increase in ratio was marginal from 0.125 ± 0.005 to 0.130 ± 0.008 **(Fig. 4.5C)**.

Under GL, the total cellular levels of $NADP^+$ and NADPH did not change significantly between WT and *aox1a* **(Fig. 4.5D,E)**. But upon exposure to HL, $NADP^+$ levels decreased while NADPH levels increased in both WT and *aox1a*. The levels of $NADP^+$ decreased in WT from 434 ± 5.29 at GL to 391.66 ± 4.36 nmoles g^{-1} FW at HL and in *aox1a* from 414.16 ± 10.33 nmoles g^{-1} FW at GL to 367 ± 1.77 nmoles g^{-1} FW at HL **(Fig. 4.5D)**. The levels of NADPH increased in WT from 270.18 ± 2.02 nmoles g^{-1} FW at GL to 278.92 ± 2.19 nmoles g^{-1} FW at HL and in *aox1a* from 255.95 ± 4.05 nmoles g^{-1} FW at GL to 282.62 ± 2.61 nmoles g^{-1} FW at HL **(Fig. 4.5E)**. Furthermore, the redox ratio of NADPH to the total cellular $NADP^+$ + NADPH pools increased significantly in *aox1a* from 0.379 ± 0.009 at GL to 0.447 ± 0.010 at HL when compared to WT which increased from 0.383 ± 0.004 at GL to 0.415 ± 0.002 at HL **(Fig. 4.5F)**. These results suggest the importance of AOX1a in dissipating the excess reducing equivalents under HL.

4.2.5 Effect of AOX1a deficiency on intracellular ROS production and malondialdehyde content under HL stress

The changes in ROS levels were monitored as dichlorofluorescein (DCF) fluorescence in mesophyll cells of leaf discs. Under GL, DCF fluorescence was marginally high in *aox1a* when compared to WT **(Fig. 4.6A,B)**. On illumination of leaf discs with HL, DCF fluorescence increased significantly in *aox1a* when compared to WT **(Fig. 4.6C,D)**. Further, malondialdehyde (MDA) which is considered as an indicator of stress induced cell damage increased significantly at HL by 24% in *aox1a* when compared to WT which showed an increase of MDA by 12% **(Fig. 4.7)**. These results indicate the role of AOX1a in preventing intracellular ROS generation under HL and thereby membrane damage.

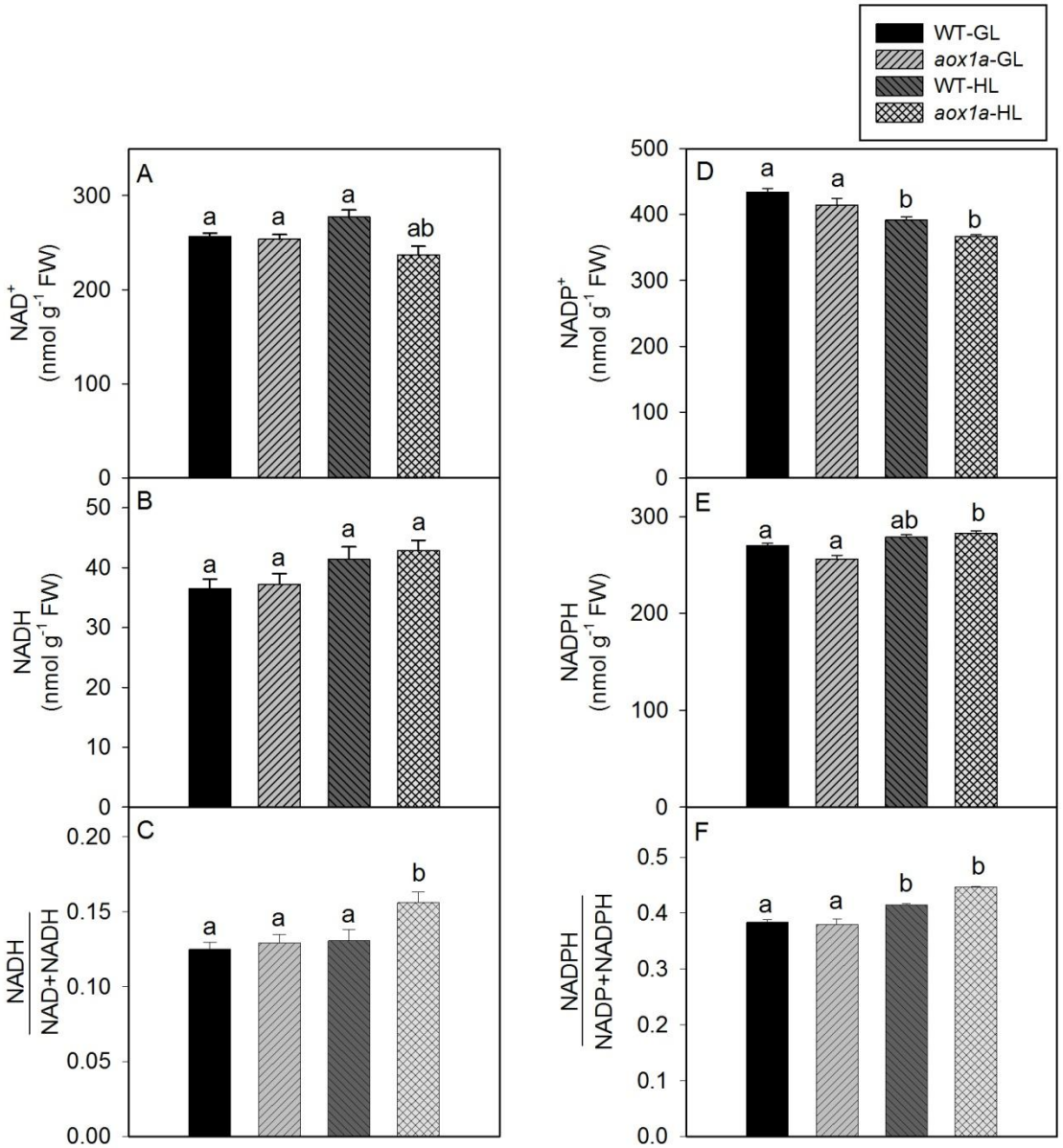

Fig.4.5. Changes in total cellular levels of oxidized and reduced forms of pyridine nucleotides and their redox ratios in leaf discs of WT and *aox1a* after pre-illumination (6 h) in GL (50 µmol photons m^{-2} s^{-1}) and HL (700 µmol photons m^{-2} s^{-1}) at 25 °C: (A) NAD^+; (B) NADH; (C) $NADH/NAD^+$ + NADH ratio; (D) $NADP^+$; (E) NADPH and (F) $NADPH/NADP^+$ +NADPH ratio. Pyridine nucleotide contents were calculated with their corresponding standards. Different lowercase alphabetical letters indicate statistically significant difference ($P < 0.05$).

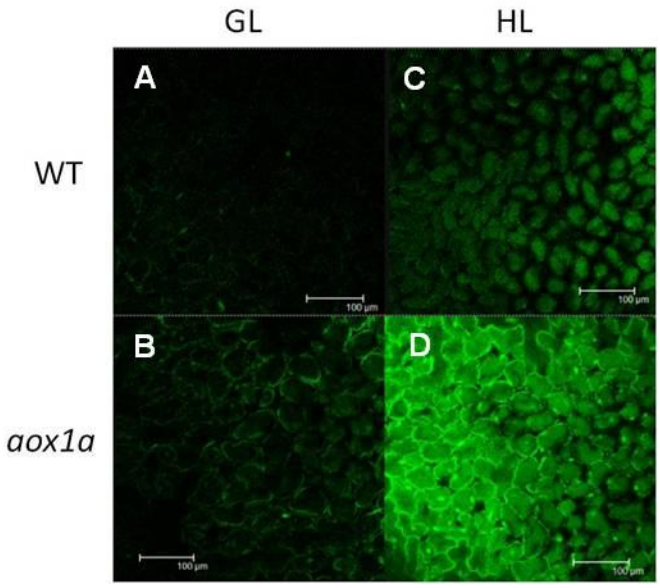

Fig.4.6. Measurement of ROS formation after pre-illuminating leaf discs of WT and *aox1a* in GL (A,B) and under HL (C,D) for 6 h at 25 °C. Leaf discs of WT and *aox1a* were immediately infiltrated with fluorescent probe (25 µM H_2DCF-DA) after pre-illumination in GL or HL and DCF fluorescence was measured under confocal laser scanning microscopy at 488 nm (excitation) and 525 nm (emission) wavelengths as described in materials and methods.

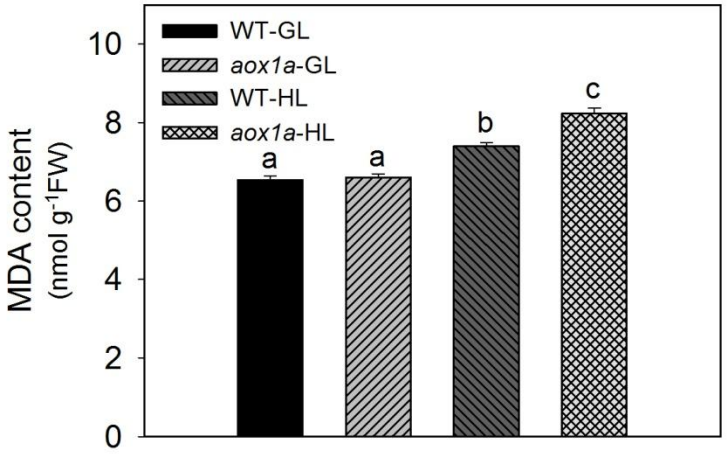

Fig.4.7. Lipid peroxidation measured as MDA levels in leaf discs of WT and *aox1a* pre-illuminated (6 h) in GL (50 µmol photons m^{-2} s^{-1}) and HL (700 µmol photons m^{-2} s^{-1}) 25 °C. Further details were as described in materials and methods. Different lowercase alphabetical letters indicate statistically significant difference ($P < 0.05$).

4.2.6 Changes in expression of genes encoding antioxidant, malate-OAA shuttle, respiratory and photorespiratory enzymes under HL stress

The relative changes in the transcript levels of genes related to (i) antioxidant enzymes: cytosolic superoxide dismutase (*CSD1*), peroxisomal/chloroplastic catalase (*CAT1*), peroxisomal catalase (*CAT2*), stromal ascorbate peroxidase (s*APX*), thylakoid ascorbate peroxidase (*tAPX*) and cytosolic ascorbate peroxidase (*cAPX*); (ii) malate-OAA shuttle: NADP-dependent chloroplastic malate dehydrogenase (*ChlMDH*), NAD-dependent mitochondrial malate dehydrogenase (*MMDH1*) and NADP-dependent isocitrate dehydrogenase (*ICDH*); (iii) respiratory metabolism: mitochondrial cytochrome c oxidase (*COX15*), mitochondrial alternative oxidase (*AOX1a*), cytosolic phosphofructokinase (*PFK4*), cytosolic UDP-glucose pyrophosphorylase (*UGP1*) and cytosolic glucose-6-phosphate dehydrogenase (*G6PD6*); (iv) photorespiratory metabolism: mitochondrial glycine decarboxylase (*GDCH*) and chloroplastic/peroxisomal glycolate oxidase (*GOX1*), were examined in GL versus HL **(Fig. 4.8)**.

Under GL, expression of all the genes examined in the *aox1a* was either similar to WT or increased marginally compared to WT except for *cAPX* and *GOX1* **(Fig. 4.8A-D)**. Under HL, among the antioxidant genes examined, the expression of *CSD1*, *CAT1* and *sAPX* in *aox1a* increased significantly up to ~16.7 fold when compared to WT, which showed an increase up to ~12.5 fold **(Fig. 4.8A)**. On the other hand, *tAPX* remained unchanged while *CAT2* (~ 4.5 fold) and *cAPX* (~ 1.5 fold) were increased to similar extent in both WT and *aox1a* under HL stress **(Fig. 4.8A)**.

Under HL, the expression of genes *MMDH1* and *ICDH* related to malate-OAA shuttle was significantly increased up to ~18.9 fold in *aox1a* as compared to WT, which showed an increase up to ~10.2 fold. On the other hand, *ChlMDH* was equally increased in both WT and *aox1a* **(Fig. 4.8B)**.

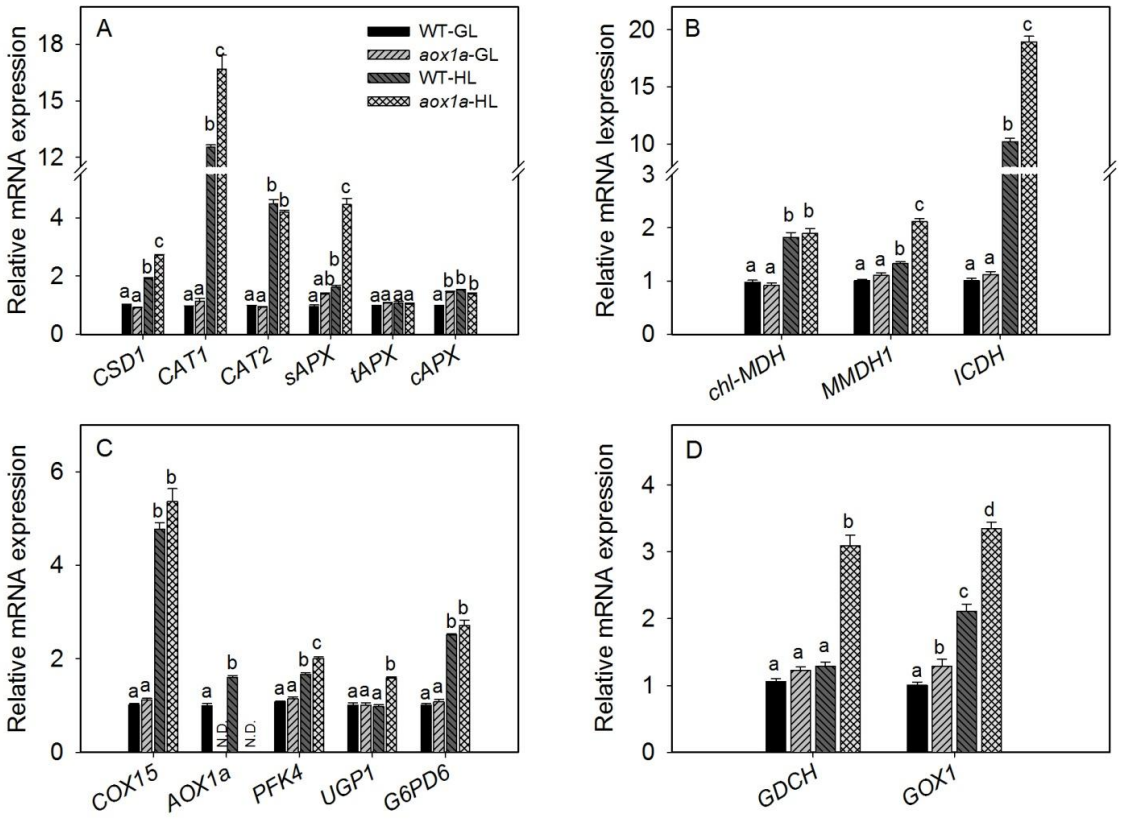

Fig.4.8. Gene expression profiles under GL (50 µmol photons m^{-2} s^{-1}) and HL (700 µmol photons m^{-2} s^{-1}) in the leaf discs of WT and *aox1a* related to (A) antioxidant enzymes (*CSD1*, *CAT1*, *CAT2*, *sAPX*, *tAPX* and *cAPX*); (B) malate-OAA shuttle enzymes (*ChlMDH*, *MMDH1*, and *NADP-ICDH*); (C) respiratory enzymes (*COX15*, *AOX1a*, *PFK4*, *G6PD6* and *UGP1*) where N.D. denotes not detected; (D) photorespiratory enzymes (*GDCH* and *GOX1*). The transcript abundance was quantified by $\Delta\Delta C_T$ method by using *UBQ5* as a reference gene. Further details were as described in materials and methods. Different lowercase alphabetical letters indicate statistically significant difference ($P < 0.05$).

The expression of genes such as *PFK4*, *UGP1*, *GDCH*, and *GOX1* related to respiratory and photorespiratory metabolism was increased significantly in *aox1a* up to ~3.34 fold as compared to WT which showed an increase up to ~2.11 fold **(Fig. 4.8C,D)**. The transcripts of *AOX1A* increased significantly in WT under GL or HL while no expression was apparent in *aox1a* as expected. Both *COX15* and *G6PD6* were marginally increased in *aox1a* when compared to WT under HL **(Fig. 4.8C)**.

4.3 Discussion

In the present study, we investigated the role of AOX pathway, particularly AOX1a in sustaining photosynthesis by maintaining cellular redox homeostasis under HL stress. All physiological and biochemical parameters were compared between WT (control) and *aox1a*. The results obtained from present study further corroborated the physiological importance of AOX pathway in optimizing photosynthesis against photoinhibitory light as discussed below.

4.3.1 Essentiality of AOX1a in maintaining redox status of photosynthetic electron transport chain and sustaining photosynthetic carbon assimilation under HL

Under GL conditions, there was no difference between WT and *aox1a* in phenotype as well as respiratory O_2 uptake, photosynthetic O_2 evolution, chlorophyll fluorescence and P700 parameters **(Figs. 4.2, 4.3 and 4.4)**. These observations are in agreement with earlier findings. Moreover, there was similarity in other parameters such as leaf area, rosette size and number of leaves between WT and *aox1a* (Zhang et al., 2010; Strodtkötter et al., 2009; Gandin et al., 2012). Taken together, the above information suggests that deficiency in AOX1a does not affect either the leaf morphology or developmental growth or the essential basic metabolism like photosynthesis and respiration as long as plants are maintained under non-limiting growth conditions. But, the role of AOX in all these processes was exemplified whenever the plants are exposed to various abiotic stresses such as HL, cold, drought etc. (Dinakar at al., 2010a; Giraud et

al., 2008; Watanabe et al., 2008; Armstrong et al., 2008). Furthermore, the importance of AOX in photosynthetic metabolism under all light intensities was evident when the AOX pathway was inhibited by SHAM (Dinakar at al., 2010a; Padmasree and Raghavendra 1999a; Yoshida et al., 2006) or in the *aox1a* mutant exposed to oxidative stress conditions caused by inhibition of the cytochrome pathway with AA (Zhang et al., 2010; Strodtkötter et al., 2009).

In the present study, the remarkable increase in respiratory O_2 uptake in leaf discs of WT after exposure to increasing light intensities (250, 500 and 700 µmol photons m^{-2} s^{-1}) perhaps could be due to the phenomenon of light enhanced dark respiration, where photorespiratory intermediates and organic acids which accumulated in presence of light are oxidized by mitochondria in the subsequent dark period **(Fig. 4.2A)**. But, we observed persistence of either similar respiratory O_2 uptake rates in both *aox1a* and WT or even more than WT in *aox1a* under all given light intensities. These results suggest that in the absence of AOX1a, the COX pathway should be responsible to maintain cellular respiration. Nevertheless, it is also possible that other isoforms of AOX are expressed to maintain cellular respiration in cooperation with COX pathway (Strodtkötter et al., 2009). These studies demonstrated that the knockout mutants for AOX1a enhanced the transcript level of AOX1d upon treatment with AA in the light. However, irrespective of the maintenance of cellular respiration, the $NaHCO_3$-dependent photosynthetic O_2 evolution rates which indicate the efficiency of photosynthetic carbon assimilation did not change significantly between WT and *aox1a* at 50, 250 and 500 µmol photons m^{-2} s^{-1}. But, the rates of photosynthetic O_2 evolution decreased significantly at 700 µmol photons m^{-2} s^{-1} in *aox1a* as compared to WT emphasizing the importance of AOX1a in sustaining photosynthetic carbon assimilation at high light intensities **(Fig. 4.2B)**. Therefore, to compare the effects of HL on all other parameters examined in the present study, we pre-illuminated the leaf discs at 700 µmol photons m^{-2} s^{-1}.

The changes observed in chlorophyll fluorescence and P700 parameters indicate the role of AOX1a in the regulation of PSII and PSI under HL. On exposure to HL, the significant decrease in Fv/Fm and Y(II) in *aox1a* compared to WT reveal that AOX1a helps to sustain higher quantum yield of PSII by keeping up high ratio of open PSII reaction centres as evident by higher level of qP (puddle model) in WT **(Fig. 4.3A,B,C)**. Further qL, a parameter that indicate the openness of PSII reaction centres according to Lake Model (Kramer et al., 2004) also showed a similar pattern as qP (data not shown). On the other hand, HL caused over reduction of P700 in *aox1a* compared to WT **(Fig. 4.4B)**. In this situation over-reduction of P700 may in turn lead to over reduction of PQ pool and subsequently Q_A as PSI reaction centres cannot take further electrons from PSII as evidenced by decrease in ETR(II) in *aox1a* compared to WT **(Fig. 4.3E)**. The over-reduction of the PQ pool in *aox1a* compared to WT under short-term HL treatment was shown in a previous study through direct measurement of PQ pool by HPLC analysis (Yoshida et al., 2010, 2011a). These results suggest that AOX1a plays a significant role in maintaining the redox status of the photosynthetic electron transport chain under HL by preventing over-reduction of photosynthetic electron transport carriers. Further, NPQ was inhibited in *aox1a* in contrast to WT after HL treatment indicating the possible role of AOX1a in thermal dissipation **(Fig. 4.3D)**. In contrast, AOX1 over expressing lines of tobacco showed that AOX act as an active sink for excess NAD(P)H generated in chloroplasts, thus allowing the ATP synthesis and NPQ generation by maintaining the electron flow between PSI and PSII, and redox state of pETC (Dahal et al., 2015).

4.3.2 AOX1a sustains photosynthesis under HL by oxidizing excess chloroplastic reducing equivalents and preventing cellular ROS generation

Under HL, the reducing equivalents (NADPH) generated in excess of the requirement of the Calvin cycle and other reductive anabolic processes by photosynthetic electron transport are exported indirectly in the form of malate from chloroplasts to other

organelles including mitochondria through operation of malate-OAA shuttle, where they are released as NADH during oxidation of malate to OAA and used in different metabolic pathways (Dinakar et al., 2010a; Noguchi and Yoshida 2008; Zhang et al., 2010). In the earlier studies, the importance of the AOX pathway in dissipating the reducing equivalents that entered the mitochondrial electron transport chain through malate-OAA shuttle was evaluated by monitoring the changes in the activity of following cytosolic and mitochondrial enzymes, namely NADP-MDH, NAD-MDH, CS, NAD-ME and NADP-ICDH in *aox1a*, as also in *pgr5* deficient in cyclic electron transport (Zhang et al., 2010; Xu et al., 2011; Yoshida et al., 2007). Three significant observations made in the present study complement the role of AOX1a in dissipating the excess reducing equivalents accumulated in chloroplasts under HL to maintain the photosynthetic electron transport carriers in the oxidized state: (i) increase in cellular redox ratios of pyridine nucleotides NADH and NADPH corresponding to their total oxidized and reduced pools; (ii) up-regulation in transcript levels of *MMDH1* and *ICDH* and (iii) correlation between the increase in NADH and NADPH levels and the up-regulation of transcript levels of *MMDH1* and *ICDH* in aox1a when compared to WT under HL **(Figs. 4.5B,C,E,F and 4.8B)**. We suggest that the WT is more successful in sustaining photosynthesis under HL than aox1a perhaps by keeping up the recycling rates of NAD^+ and $NADP^+$, respectively, at higher levels **(Fig. 4.5A,D)**. Further, the rise in the cellular redox ratios of both NADH and NADPH observed in the present study might add to the positive impact on the activation of AOX protein and thereby AOX pathway capacity possibly by acting through the disulfide/sulfhydryl system (Arnholdt-Schmitt et al., 2006). Further, the role of AOX in re-oxidizing the UQ pool and at the same time of the PQ pool for keeping up efficient photosynthetic performance was demonstrated during short-term treatments with HL (Yoshida et al., 2011a).

ROS generated under biotic or abiotic stress conditions are scavenged by non-enzymatic (ascorbate, glutathione, tocopherol, flavonoids, alkaloids and carotenoids) or

enzymatic (superoxide dismutase, ascorbate peroxidase, glutathione peroxidase and catalase) mechanisms (Apel and Hirt, 2004). In the present study, transcript levels of genes related to enzymatic antioxidant systems such as *CSD1*, *CAT1* and *sAPX* were increased significantly correlating to the higher ROS level under HL in *aox1a* **(Figs. 4.6 and 4.8A)**. These results indicate that in absence of AOX1a, antioxidant systems work more efficiently to minimize the ROS generated from photosynthetic electron transport carriers as well as mitochondrial electron transport carriers (**Fig. 4.8A**; Amirsadeghi et al., 2006). The importance of AOX in ROS alleviation has been shown before under various stresses such as light, drought and AA treatment. The results from these studies indicated that ROS accumulation was low in AOX over-expression lines and high in low-expression or mutant lines compared to WT plants (Giraud et al., 2008; Strodtkötter et al., 2009; Maxwell et al., 1999).

4.3.3 Inefficiency of photorespiration to function as an alternative sink for dissipation of reducing power in *aox1a*

Studies using metabolic inhibitors or transgenic/reverse genetic approaches indicated that any interference in electron transport through the following components of mitochondrial respiratory chain: complex I, COX pathway, AOX pathway, oxidative phosphorylation or TCA cycle caused a significant decrease in CO_2 assimilation (Bartoli et al., 2005; Dinakar et al., 2010a; Padmasree and Raghavendra 1999a; Yoshida et al., 2011b; Florez-Sarasa et al., 2011; Yoshida et al., 2006; Krömer et al., 1993; Juszczuk et al., 2007; Nunes-Nesi et al., 2010). The importance of both COX and AOX pathways in protecting the photosynthetic machinery from photoinhibition under HL was revealed in mesophyll protoplasts of pea and Rumex K-1 leaves (Dinakar et al., 2010b; Zhang et al., 2010). Further, HL caused a shift in AOX protein from its oxidized inactive to reduced active form (Noguchi et al., 2005). In the present study, the *AOX1a* transcript level was significantly increased in WT under HL. On other hand, after HL treatment an increase in

COX15 in both WT and *aox1a* suggest that the COX pathway attempt to keep the pace of photosynthesis along with AOX pathway **(Fig. 4.8C)**.

UGP1 synthesizes UDP-glucose from glucose-1-phosphate. UDP-glucose is the precursor in cell wall biosynthesis and its overexpression in tobacco enhanced the plant growth (Coleman et al., 2006). PFK plays an important role in converting the hexose-phosphate pool into a triose-phosphate pool that in turn provides precursors for the synthesis of glycerol and membrane lipids. Thus, up-regulation in transcript level of *UGP1* and *PFK4* in *aox1a* caused by HL may account for synthesis of cell wall or cellular membranes to compensate for the membrane damage (indicated by MDA content) caused by ROS **(Figs. 4.6,4.7 and 4.8C)**.

Photorespiration is known as alternate sink for excess reducing equivalents and energy in order to regenerate free acceptor molecules such as ADP, Fd_{ox} and $NADP^+$ via glycine oxidation, ammonium reassimilation, glycolate detoxification and hydroxypyruvate reduction (Voss et al., 2013). Thus increased *GOX1* and *GDCH* gene expression in *aox1a* indicate that photorespiration might serve as an alternate sink for excess reducing equivalents under HL compensating the role of AOX1a **(Fig. 4.8D)**.

Taken together, these results suggest that under HL, *aox1a* plants attempt to decrease the ROS level by increasing the transcript level of antioxidant genes. Respiration, malate-OAA shuttle and photorespiration mutually interact to maintain cellular redox homeostasis. In spite of these metabolic interactions, they could not fully compensate the role of AOX1a, when it was completely lacking in the knockout line, and therefore *aox1a* plants showed inefficient redox dissipation and low photosynthetic performance under HL.

***

Chapter 5

Importance of AOX1a in optimizing photosynthesis during restriction of electron transport through cytochrome oxidase pathway in *Arabidopsis thaliana*

5.1 Introduction

Several studies have demonstrated that any interference in the COX or AOX pathway (using mutants or chemicals) caused a significant decrease in photosynthetic O_2 evolution in mesophyll protoplasts or leaf tissue (Padmasree and Raghavendra, 1999a; Yoshida et al., 2006; Strodtkötter et al., 2009; Dinakar et al., 2010a,b; Zhang et al., 2012). However, during stress conditions (drought, high light, high CO_2 and temperature) the engagement of the AOX pathway was found to be much higher compared with the COX pathway. It dissipates excess energy in the form of heat and thereby prevents the over-reduction of the UQ pool, which in turn mitigates the ROS generation (Vassileva et al., 2009; Dinakar et al., 2010b; Yoshida et al., 2011a; Gandin et al., 2012; Gandin et al., 2014b; Zhang et al., 2014). The role of AOX is also recognized in alleviation of reactive nitrogen species, particularly of NO levels in mitochondria, which are induced by reducing equivalents (Gupta et al., 2012; Cvetkovska et al., 2014; Igamberdiev et al., 2014).

The chloroplastic NADP-MDH uses excess NADPH generated via the photosynthetic electron transport chain to convert OAA to malate, regenerating the electron acceptor $NADP^+$ (Scheibe, 2004). This malate is subsequently translocated to the cytosol via the malate-OAA shuttle, where the interconversion of malate to OAA takes place by cytosolic NAD-MDH activity (Hara et al., 2006). This mechanism allows chloroplastic reducing equivalents to be indirectly transferred to the cytosol and other sub-cellular compartments, for instance mitochondria, to avoid (i) imbalances in the generation and utilization of reducing equivalents by photochemical reactions and the Calvin cycle and (ii) depletion of chloroplast energy carriers which would lead to

oxidative stress. A concomitant rise in AOX protein and its respiratory capacity in parallel to an increase in the activity of various enzymes (NADP-MDH, NAD-MDH, NAD-ME, NADP-ICDH) involved in the transport of these reducing equivalents suggests a role of AOX in modulating the cellular redox state to sustain the photosynthesis under HL conditions (Fernie et al., 2004; Scheibe et al., 2005; Yoshida et al., 2007, 2008; Xu et al., 2011). The rise in cellular levels of pyruvate under HL conditions further emphasized the role of AOX in dissipating excess chloroplastic reducing equivalents (Dinakar et al., 2010b). Thus, the function of AOX is tightly coupled with photosynthesis, as it has a direct impact on the supply and demand of ATP, NAD(P)H and carbon intermediates (Vanlerberghe, 2013). The co-expression of AOX with other non-phosphorylating genes of the mitochondrial electron transport chain such as *NDB2*, *UCP1* and *UCP2* is well known under HL treatment to prevent an over-reduction of the (PQ) and UQ pools (Yoshida et al., 2008; Yoshida et al., 2011a).

Apart from mitochondrial respiration, plants possess several other defense strategies such as photorespiration and antioxidative systems to cope with stress conditions. Interestingly, these metabolic pathways were found to be modulated by any constraint in AOX (Strodtkötter et al., 2009; Voss et al., 2013). Ascorbate (Asc) is an antioxidant molecule that is abundantly present in all sub-cellular compartments of plant tissues and occur at as high as 20 mM in chloroplasts (Smirnoff and Wheeler, 2000). It plays an important role in the detoxification of H_2O_2 during stress conditions. Furthermore, *AOX1A* overexpression lines showed higher rates of Asc production when compared with WT in *Arabidopsis* leaves (Bartoli et al., 2006). Various mitochondrial retrograde regulation (MRR) signals are shown to stimulate the expression of *AOX1A* (Rhoads and Subbaiah, 2007; Suzuki et al., 2012). In rice, *AOX1A* and *AOX1B* were expressed during abiotic stress conditions through MRR signaling mediated by O_2^- radicals (Li et al., 2013b). The deficiency of AOX1A during the restriction of the COX pathway caused a significant reduction in photosynthesis, increase in ion leakage and

ROS generation which ultimately led to wilting and necrosis of the plant in spite of the increase in photorespiration (Strodtkötter et al., 2009; Voss et al., 2013).

In the present study, we employed both chemical and reverse genetic approaches together to examine (i) the physiological importance of AOX1A in modulating the redox state of chloroplastic electron transport carriers and non-photochemical quenching to sustain photosynthesis, and (ii) the impact of AOX1A in regulating the malate valve and the antioxidative systems to maintain the cellular redox state and ROS for optimal photosynthetic performance when the COX pathway is restricted at Complex III.

5.2 Results

5.2.1 Effect of AA on total respiratory O_2 uptake and photosynthetic O_2 evolution in wild-type plants and AOX1A T-DNA mutants (*aox1a*)

The rates of total respiratory O_2 uptake and bicarbonate-dependent photosynthetic O_2 evolution, the latter an indicator of photosynthetic carbon assimilation (Calvin cycle activity), were monitored in leaf discs of WT and *aox1a* mutants in the presence of AA, a metabolic inhibitor of complex III, to examine the significance of the AOX pathway in optimizing photosynthesis. The inhibition of electron transport through the COX pathway simulates a metabolic state of oxidative stress. In the controls, the rates of respiratory O_2 uptake and photosynthetic O_2 evolution varied marginally between WT and *aox1a* mutants. However, the rates of respiratory O_2 uptake and photosynthetic O_2 evolution varied significantly between WT and *aox1a* plants when the leaf discs were exposed to increasing concentrations of AA **(Fig. 5.1A, B)**. When the concentration of AA was increased from zero to 40 µM, WT leaf discs showed 54% inhibition in rates of respiratory O_2 uptake and 60% inhibition in rates of photosynthetic O_2 evolution when compared with their controls without AA. In contrast to WT, in the presence of 40 µM AA, *aox1a* mutants showed 84% inhibition in rates of respiratory O_2 uptake and 81%

inhibition in rates of photosynthetic O_2 evolution. Thus, these results suggest that disturbances in the mitochondrial electron transport through the COX pathway compromised the photosynthetic carbon assimilation of chloroplasts more seriously in *aox1a* than in WT. As AA is also known to inhibit cyclic electron transport, a low concentration of AA (20 µM) was used in further experiments. At this concentration, AA caused marginal decreases in rates of respiration and photosynthesis in WT, while the rates of respiration and photosynthesis were drastically reduced in *aox1a* mutants **(Fig. 5.1A, B)**.

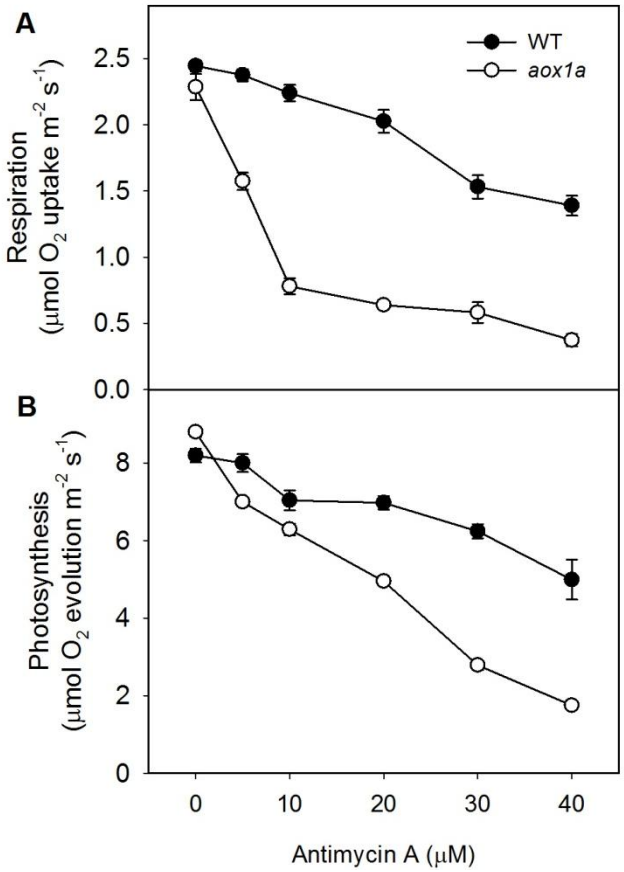

Fig. 5.1. The rates of respiratory O_2 uptake (A) and photosynthetic O_2 evolution (B) in leaf discs of WT and *aox1a* mutants after pre-illumination (6 h) at PPFD of 50 µmoles m^{-2} s^{-1} at 25°C in the absence and presence of AA. After pre-illumination, leaf discs were incubated in the dark for 10-15 min during electrode calibration. Subsequently, respiration was measured in the dark for 5 min followed by photosynthesis measured in the light for 10 min at 250 µmoles m^{-2} s^{-1} as $NaHCO_3$-dependent (ca. 5% v/v) O_2 evolution.

These results suggest that 20 µM AA can be applied for the restriction of the COX pathway to reveal the importance of AOX1A in optimizing photosynthetic carbon assimilation.

5.2.2 Effect of AOX1A deficiency on chlorophyll fluorescence and P700 parameters in the presence of AA

The changes occurring in chloroplastic reaction centres and the electron transport chain were monitored to examine the importance of AOX1A in keeping up photochemical reactions and thermal dissipation, which play significant roles in photoprotection and meeting the energy demands of the photosynthetic carbon reduction cycle during oxidative stress due to the restriction of electron transport through the COX pathway. The maximum quantum yield of PSII (F_v/F_m) which indicates the maximum efficiency of PSII was measured after applying the initial saturation pulse (SP). In the absence of AA, both WT and *aox1a* knock-out plants showed no significant differences in their F_v/F_m ratio. After AA treatment, the F_v/F_m ratio decreased in both genotypes but to a larger extent in *aox1a* mutants than in WT **(Fig. 5.2A)**. These results suggest the importance of the AOX pathway in maintaining PSII efficiency at their maximum levels. After measurement of the F_v/F_m ratio, the AL was switched off (40 s) to allow the reaction centers of PSII to attain their oxidized state. Subsequently, various parameters related to chlorophyll fluorescence and P700 were recorded with every SP given up to 260 s at regular intervals of 20 s. In the absence of AA, a similar pattern of Y(II), ETR(II), qP, NPQ, Y(I), Y(ND), Y(NA) and $P700_{red}$ was observed for WT and *aox1a* plants **(Fig. 5.2B-E and 5.3A-D)**. However, after AA treatment Y(II), ETR(II) and qP were significantly decreased in *aox1a* compared with WT **(Fig. 5.2B-D)**.

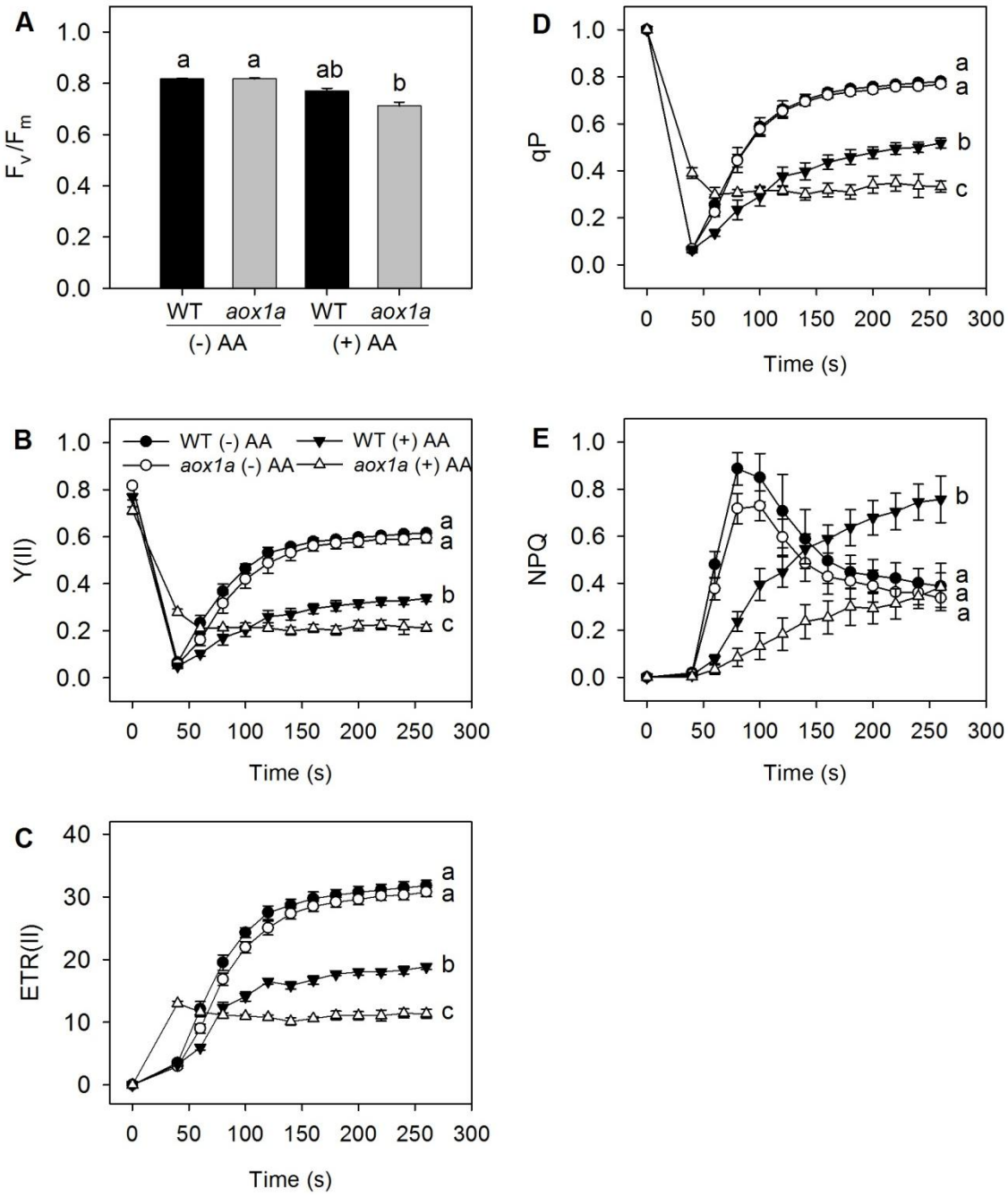

Fig. 5.2. Characteristics of chlorophyll fluorescence parameters in WT and *aox1a* from control (Tween-20) and treated (20 µM AA in Tween-20) leaf discs pre-illuminated (6 h) at a PPFD of 50 µmoles m^{-2} s^{-1} at 25 °C: (A) maximum quantum yield of PSII (F_v/F_m), (B) relative quantum yield of PSII [Y(II)], (C) electron transport rate of photosystem II (ETR II), (D) photochemical quenching (qP), (E) non-photochemical quenching (NPQ). Other details for measurement of chlorophyll fluorescence parameters were as described in materials and methods. Different lowercase alphabetical letters indicate statistically significant differences ($P < 0.05$).

On the other hand, NPQ, an indicator of thermal dissipation was increased in WT but remained unchanged in *aox1a* mutants **(Fig. 5.2E)**. Similarly, Y(I) and the reduction state of P700 decreased drastically in *aox1a* compared with WT upon AA treatment **(Fig. 5.3A, B)**. Y(ND) increased in both genotypes but to a larger extent in *aox1a* mutants. However, such increase in Y(NA) was not observed in both WT and *aox1a* plants, irrespective of AA treatment **(Fig. 5.3C, D)**. These results indicate that AOX1A plays a crucial role in maintaining the electron flow between PSII to PSI, consequently ΔpH and thereby NPQ to dissipate excess energy in form of heat.

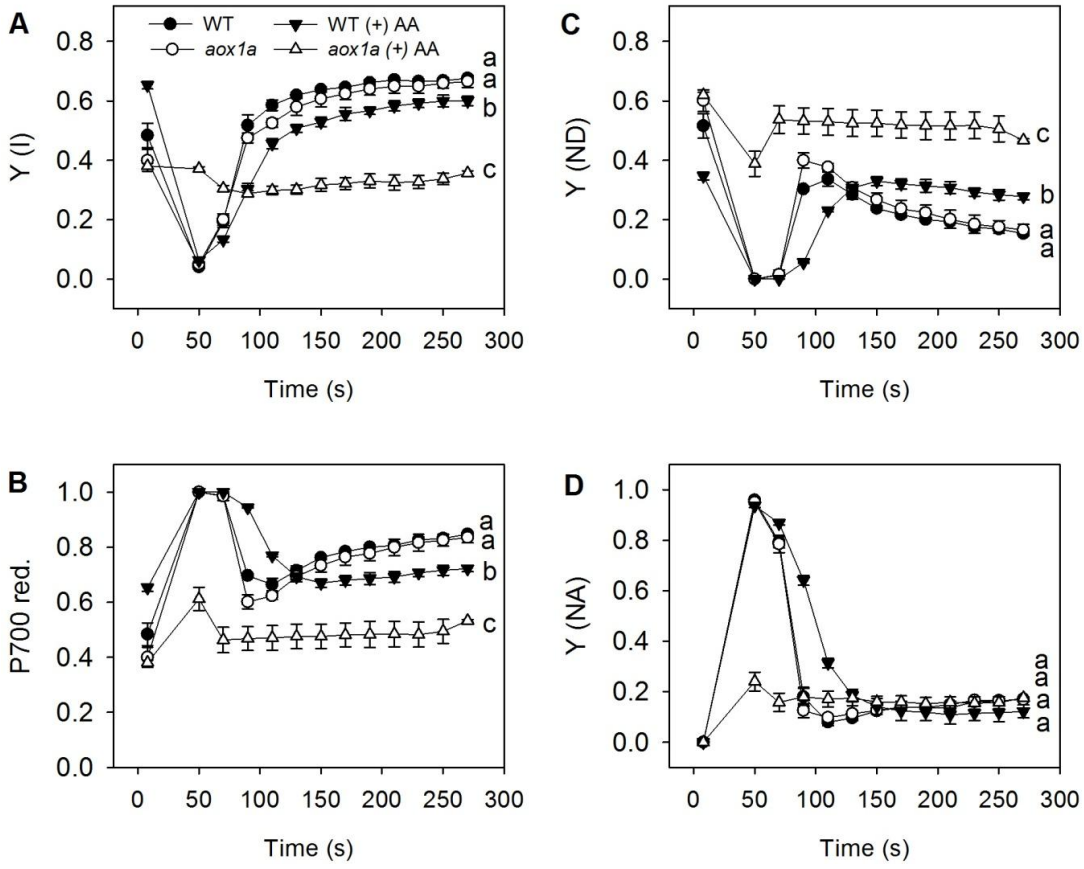

Fig. 5.3. Characteristics of P700 parameters in WT and *aox1a* mutants from control (Tween-20) and treated (20 µM AA in Tween-20) leaf discs pre-illuminated (6 h) at a PPFD of 50 µmoles m^{-2} s^{-1} at 25 °C: (A) quantum yield of PSI [Y(I)], (B) reduced P700 ($P700_{red}$), (C) limitation at the acceptor side of PSI [Y(NA)], (D) limitation at the donor side of PSI [Y(ND)]. Other details for measurement of P700 parameters were as described in materials and methods. Different lowercase alphabetical letters indicate statistically significant differences ($P < 0.05$).

5.2.3 Effect of AOX1A deficiency on cellular redox couples in the presence of AA

The role of the AOX pathway in regulating cellular redox homeostasis to optimize photosynthesis during oxidative stress was determined by monitoring changes in total cellular oxidized and reduced pools of redox couples related to NAD(H), NADP(H) and Asc **(Figs. 5.4 and 5.5)**. In control samples, the levels of $NAD(P)^+$, NAD(P)H and the ratio of NAD(P)H to the total cellular pools of $NAD(P)^+$ plus NAD(P)H were similar in both WT and *aox1a* mutants **(Fig. 5.4)**. Upon AA treatment, the increase in the ratio of NADH to the total cellular NAD^+ plus NADH pool was significant in *aox1a* mutants when compared with WT plants **(Fig. 5.4C)**. In contrast, the redox ratio of NADPH to the total cellular $NADP^+$ plus NADPH pools increased significantly in both genotypes **(Fig. 5.4F)**.

In control samples, the cellular levels of Asc and its oxidized form dehydroascorbate (DHA) did not vary between WT and *aox1a*, while the redox ratios (Asc/DHA) were modulated marginally **(Fig. 5.5)**. Upon AA treatment, the Asc levels increased in WT but decreased in *aox1a* plants compared with their respective controls **(Fig. 5.5A)**. By contrast, the levels of DHA increased in both genotypes compared with their respective controls **(Fig. 5.5B)**. Also, Asc/DHA ratio decreased significantly in both genotypes in the presence, but not in the absence of AA **(Fig. 5.5C)**.

These results suggest that the deficiency of AOX1A did not alter the cellular redox state under control conditions. However, upon restriction of the COX pathway, the cellular redox homeostasis was disturbed in both WT and *aox1a* genotypes. The imbalance in the cellular redox state was more prominent in *aox1a* compared with WT indicating the important role of AOX1A in regulating cellular redox homeostasis and thereby photosynthetic performance.

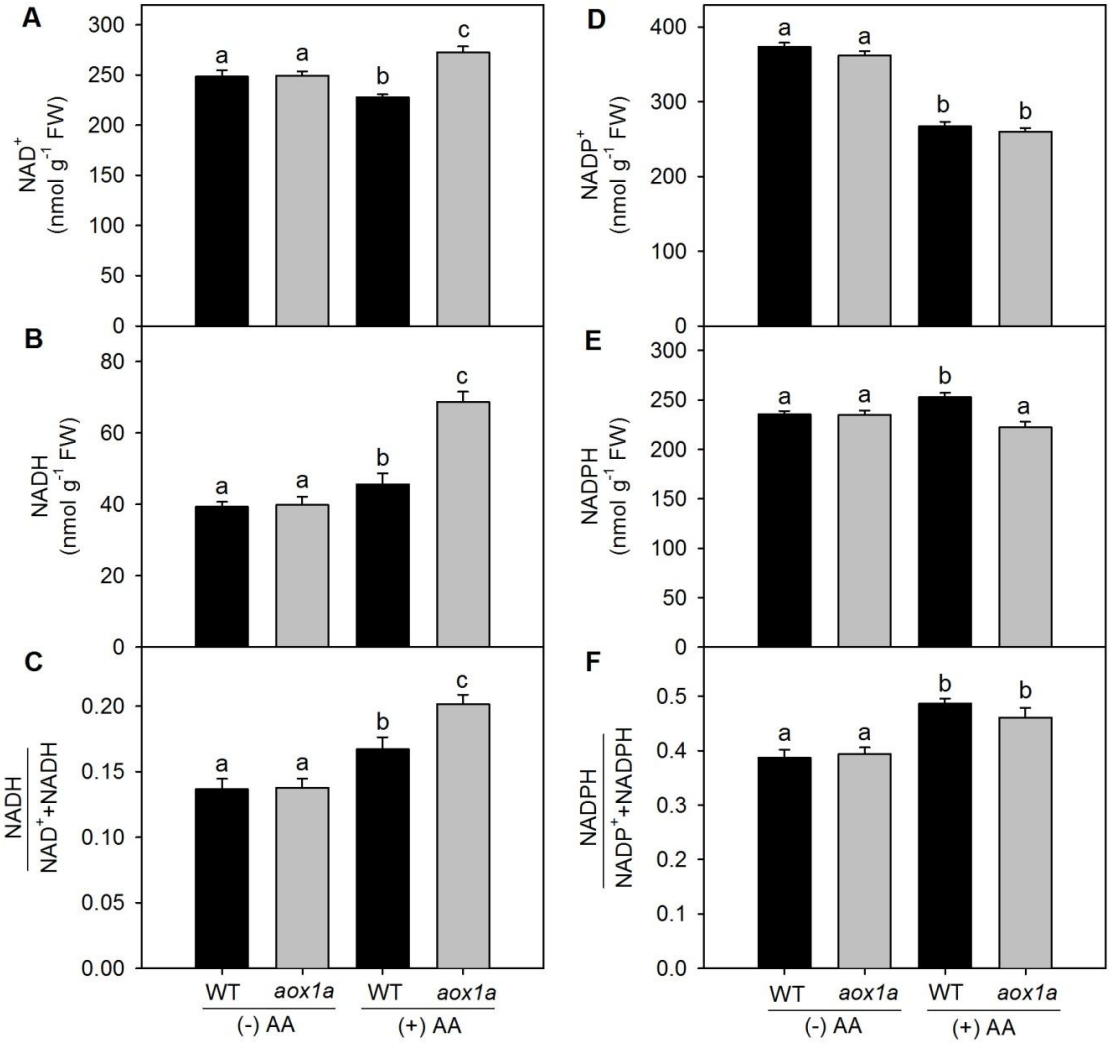

Fig. 5.4. Changes in total cellular oxidized and reduced pools of redox couples related to NAD(H) and NADP(H) and their redox ratio in WT and *aox1a* mutants from control (Tween-20) and treated (20 µM AA in Tween-20) leaf discs pre-illuminated (6 h) at a PPFD of 50 µmoles m^{-2} s^{-1} at 25°C: (A) NAD^+, (B) NADH, (C) NADH/NAD^++NADH ratio, (D) $NADP^+$, (E) NADPH and (F) NADPH/$NADP^+$+NADPH ratio. Pyridine nucleotide contents were calculated with their corresponding standards. Other details for measurement of NAD(P) and NAD(P)H were as described in materials and methods. Different lowercase alphabetical letters indicate statistically significant differences ($P < 0.05$).

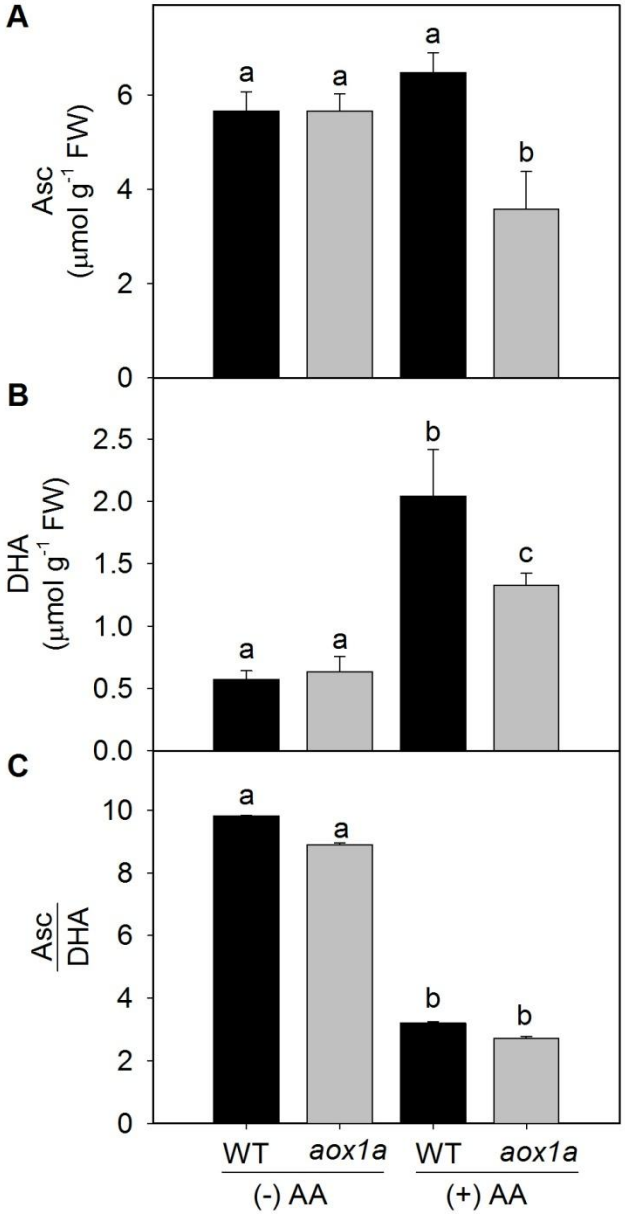

Fig.5.5. Changes in total cellular oxidized and reduced pools of Asc redox couple in WT and *aox1a* mutants from control (Tween-20) and treated (20 µM AA in Tween-20) leaf discs pre-illuminated (6 h) at a PPFD of 50 µmoles m^{-2} s^{-1} at 25 °C: (A) Asc, (B) DHA and (C) Asc/DHA ratio. Other details for measurement of Asc were as described in materials and methods. Different lowercase alphabetical letters indicate statistically significant differences ($P < 0.05$).

5.2.4 Effect of AOX1A deficiency on adenylate status in the presence of AA

The role AOX1a in modulating the energy status was studied by measurement of total adenylate content in the presence or absence of AA. Under control conditions, ATP was approximately 1.5 fold higher in *aox1a* than WT. By contrast, upon AA treatment, a significant decrease in ATP levels was seen in *aox1a* when compared with WT **(Fig. 5.6A)**. However, ADP levels remained similar in both plants under all conditions **(Fig. 5.6B)**. Consequently, *aox1a* showed a lower ATP/ADP ratio compared with WT **(Fig. 5.6C)**.

5.2.5 Effect of AOX1A deficiency on intracellular ROS accumulation and membrane damage in the presence of AA

The role of AOX1A in alleviating cellular ROS and minimizing membrane damage as well as the optimization of photosynthetic performance of leaves during oxidative stress was evaluated by monitoring changes in cellular ROS levels as DCF fluorescence as well as H_2O_2 and MDA content **(Figs. 5.7 and 5.8)**. Furthermore, changes in chloroplastic ROS were differentiated from other cellular ROS by monitoring the pseudo orange/yellow color formed due to superimposition of chlorophyll autofluorescence and DCF fluorescence. In control leaf discs, DCF fluorescence and orange/yellow fluorescence was marginally higher in *aox1a* mutants compared with WT **(Fig. 5.7A)**. In contrast, after AA treatment, DCF as well as orange/yellow fluorescence increased significantly in *aox1a* mutants **(Fig. 5.7B)**. Besides, both genotypes showed an increase in H_2O_2 levels and the MDA content in the presence of AA **(Fig. 5.8)**. The increase in H_2O_2 was more pronounced in *aox1a* than in WT compared with their respective controls **(Fig. 5.8A)**. These results suggest that the deficiency of AOX1A caused an accumulation of total cellular as well as chloroplastic ROS.

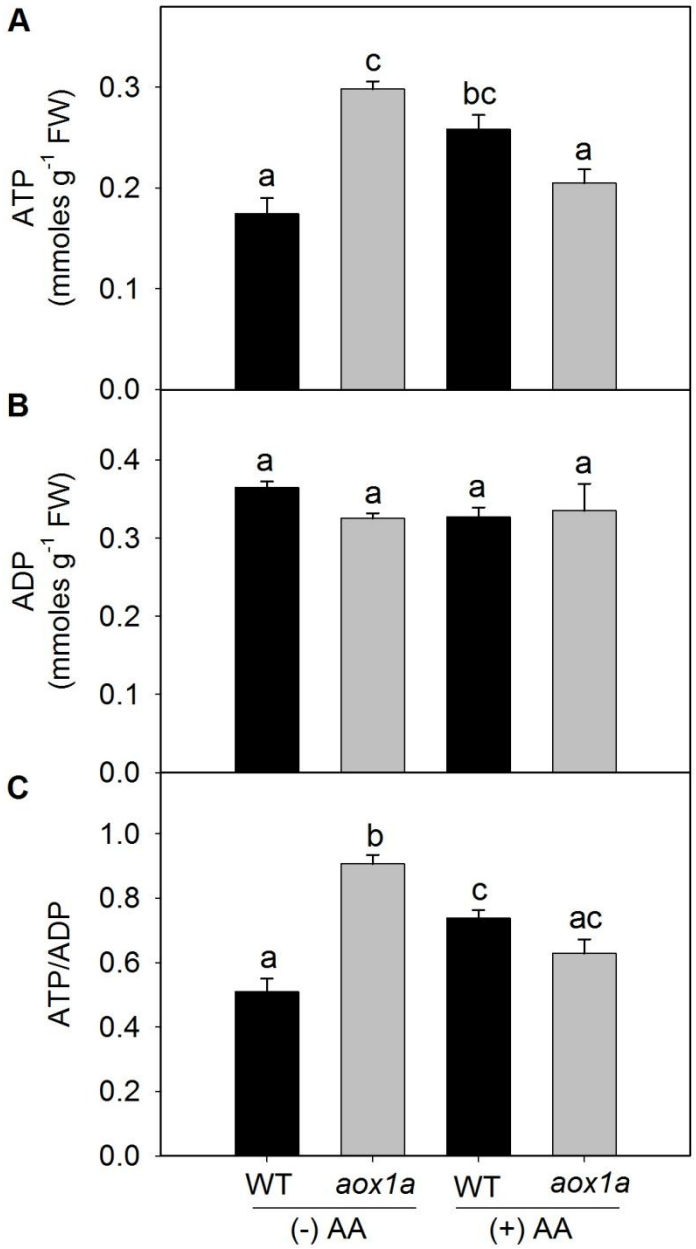

Fig.5.6. Changes in total adenylate content in WT and *aox1a* mutants from control (Tween-20) and treated (20 µM AA in Tween-20) leaf discs pre-illuminated (6 h) at a PPFD of 50 µmoles m^{-2} s^{-1} at 25 °C: (A) ATP, (B) ADP and (C) ATP/ADP ratio. Other details for measurement of adenylate content were as described in materials and methods. Different lowercase alphabetical letters indicate statistically significant differences ($P < 0.05$).

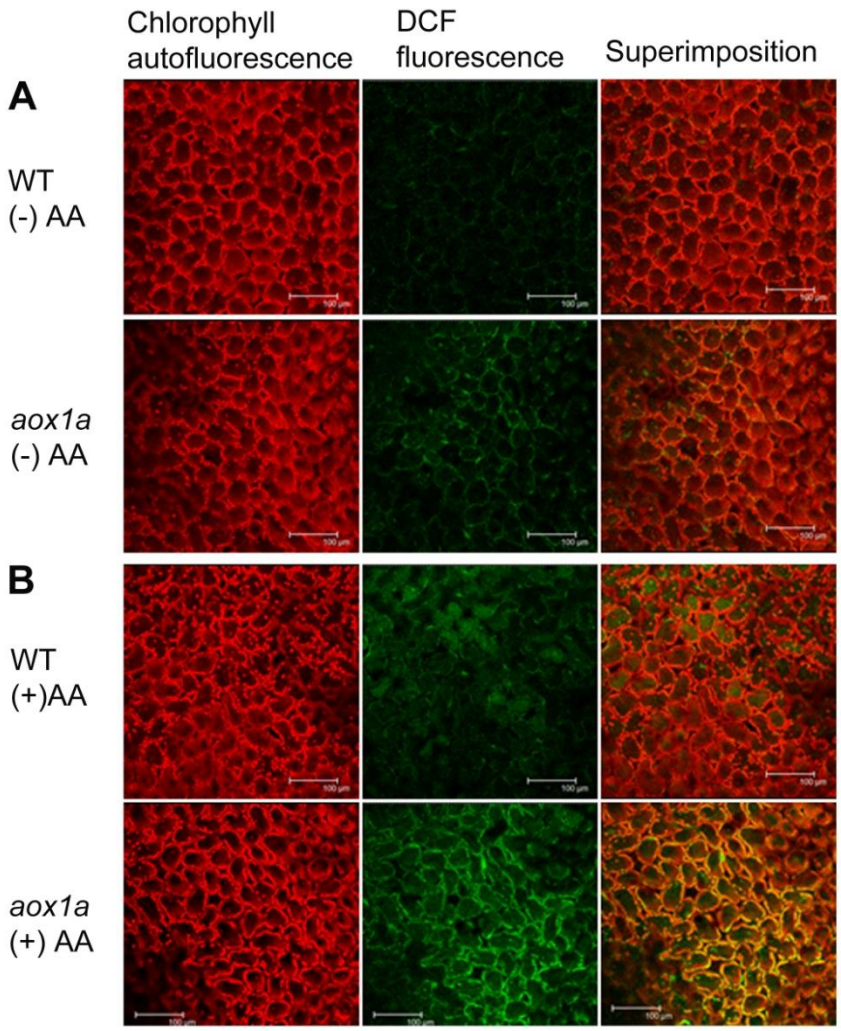

Fig. 5.7. Measurement of ROS formation in WT and *aox1a* from (A) control (Tween-20) and (B) treated (20 µM AA in Tween-20) leaf discs pre-illuminated (6 h) at a PPFD of 50 µmoles m^{-2} s^{-1} at 25°C using confocal laser scanning microscopy. Chlorophyll autofluorescence is shown in red, DCF fluorescence represents cellular ROS, is shown in green color and superimposed images representing chloroplastic ROS in pseudo orange/yellow. All scale bar=100 µm.

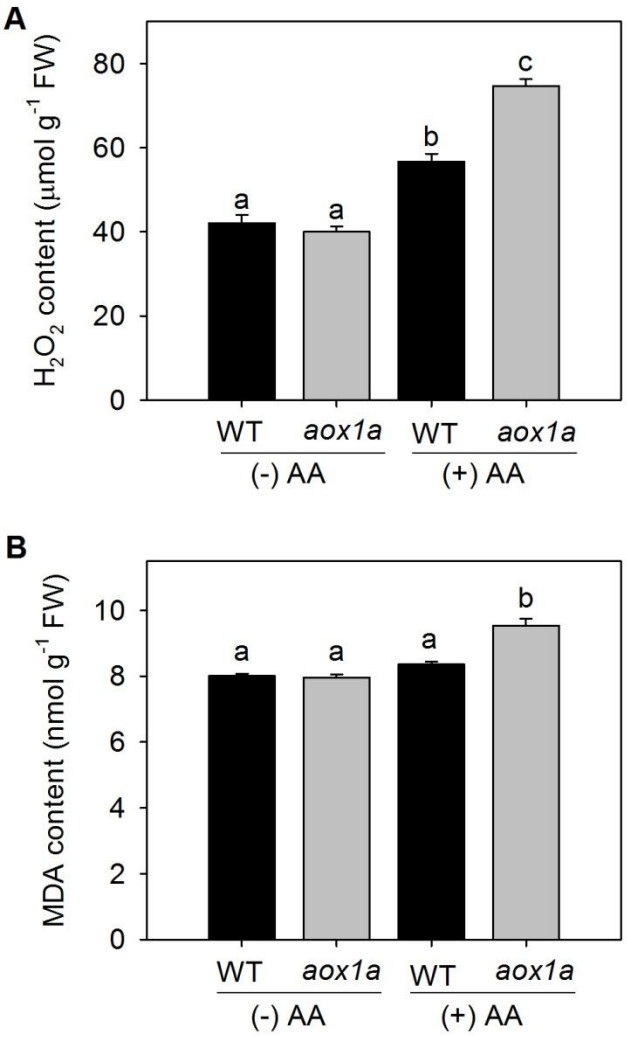

Fig. 5.8. Quantification of H_2O_2 formation (A) and lipid peroxidation as MDA content (B) in WT and *aox1a* from control (Tween-20) and treated (20 µM AA in Tween-20) leaf discs pre-illuminated (6 h) at a PPFD of 50 µmoles m^{-2} s^{-1} at 25°C. Further details were as described in materials and methods. Different lowercase alphabetical letters indicate statistically significant differences ($P < 0.05$).

5.2.6 Effect of AOX1A deficiency on gene expression of antioxidants, the malate-OAA shuttle and respiratory enzymes in the presence of AA

The role of AOX1A in regulating the malate-OAA shuttle and the antioxidative system during oxidative stress was monitored by evaluating changes in transcript levels of genes related to (i) respiratory metabolism: *PFK4* - phosphofructokinase, *AOX1A* - alternative oxidase, *COX15* - cytochrome oxidase; (ii) malate-OAA shuttle: *chlMDH* - NADP-dependent chloroplastic malate dehydrogenase, *MMDH1* - NAD-dependent mitochondrial malate dehydrogenase, *ICDH* NADP-dependent chloroplastic/peroxisomal isocitrate dehydrogenase and (iii) antioxidative enzymes: *CSD1* - cytosolic superoxide dismutase, *CAT1* - peroxisomal/chloroplastic catalase and *sAPX* - stromal ascorbate peroxidase **(Fig. 5.9)**. The expression of *AOX1A* was notably increased in WT (18-fold) in the presence of AA, whereas no transcript could be detected in *aox1a* plants as expected for this knock-out mutant **(Fig. 5.9A)**. In the absence of AA, the expression of all genes examined in *aox1a* knock-out mutants was mostly similar to WT except sAPX, which is increased in *aox1a* compared with WT. Upon AA treatment, the expression of the glycolytic enzyme *PFK4* decreased in both genotypes compared with controls without AA. In contrast, the expression of *COX15* increased in WT, while it remained unchanged in *aox1a* **(Fig. 5.9A)**. Similar to *PFK4*, in the presence of AA, the expression of *chlMDH*, *MMDH1* and *ICDH* genes related to the malate-OAA shuttle decreased in both genotypes **(Fig. 5.9B)**. However, the decrease in the expression of *MMDH1* and *ICDH* were more pronounced in *aox1a* than in WT. By contrast, in the presence of AA, the expression of the antioxidative genes *CSD1*, *CAT1* and *sAPX* increased in WT. In contrast, these genes showed differential expression in *aox1a*. Transcript levels of *CSD1* increased while *sAPX* decreased in leaf discs treated with AA, whereas *CAT1* expression was unchanged **(Fig. 5.9C)**. These results suggest that during COX pathway inhibition, the deficiency of AOX1A not only perturbs respiratory

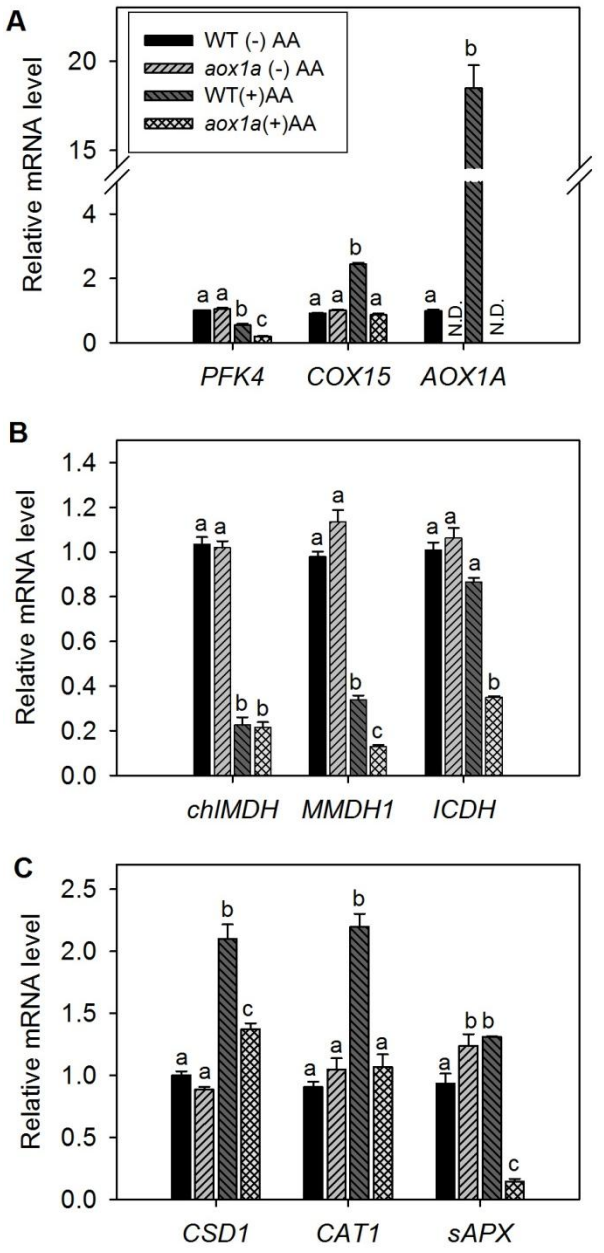

Fig. 5.9. Gene expression profiles in WT and *aox1a* from control (Tween-20) and treated (20 µM AA in Tween-20) leaf discs pre-illuminated (6 h) at a PPFD of 50 µmoles m^{-2} s^{-1} at 25°C: (A) Respiratory enzymes (*PFK4*, *COX15* and *AOX1A*), (B) Malate-OAA shuttle enzymes (*MMDH1*, *chlMDH* and *ICDH*) and (C) Antioxidative enzymes (*CSD1*, *CAT1* and *sAPX*). N.D. denotes expression of gene was not detected (A). Transcript abundance was quantified by the $\Delta\Delta C_T$ method using *UBQ5* as a reference gene. Further details were as described in materials and methods. Different lowercase alphabetical letters indicate statistically significant differences ($P < 0.05$).

metabolism, but also modulates the antioxidative system to balance ROS generation and detoxification.

Overall, the results of the present study revealed the impact of deficiency of AOX1A on mitochondrial respiration and chloroplastic photosynthesis when electron transport through the COX pathway is restricted, which is schematically represented in **Fig. 5.10**.

5.3 Discussion

The dependence of chloroplastic photosynthesis on mitochondrial respiration is well documented (Raghavendra et al., 1994; Krömer, 1995; Padmasree et al., 2002; Fernie et al., 2004; Raghavendra and Padmasree 2003; Noguchi and Yoshida 2008; Vanlerberghe, 2013). Different components of mitochondrial respiration, including Krebs cycle, electron transport, oxidative phosphorylation and UCP were found to be important to sustain photosynthetic performance during normal growth or under various biotic/abiotic stress conditions (Krömer et al., 1993; Padmasree 1999a; Sweetlove et al., 2006; Dinakar et al., 2010b; Yoshida et al., 2011a; Araújo et al., 2012; Araújo et al., 2014; Gandin et al., 2014a). The relative importance and contribution of the COX and AOX pathways in benefitting different components of photosynthesis such as carbon assimilation, photochemical reactions, photosynthetic induction and light activation of Calvin cycle enzymes was revealed in several model plants using specific metabolic inhibitors as well as transgenic/reverse genetic approaches (Padmasree and Raghavendra, 1999a,b; Padmasree and Raghavendra, 2001; Yoshida et al., 2006; Dinakar et al., 2010a; Zhang et al., 2011; Zhang et al., 2014). Further, the significant role of the AOX1A isoform over AOX1D in coordinating the COX pathway to optimize photosynthesis was established in our previous studies (Strodtkötter et al., 2009). In the present study, we investigated the physiological role of AOX1A in regulating cellular redox homeostasis and ROS

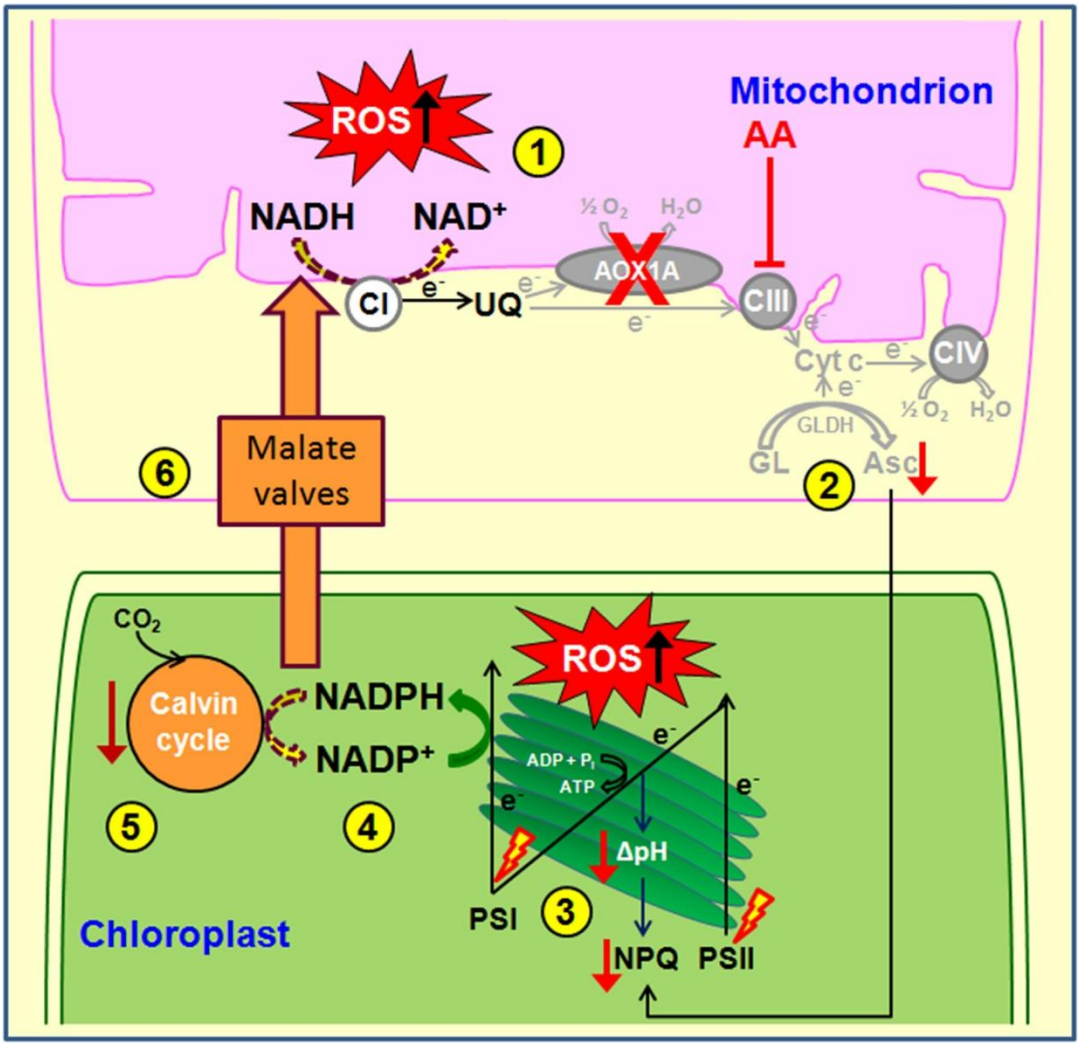

Fig. 5.10. A simple scheme illustrating the impact of AOX1A deficiency on mitochondrial respiration and chloroplastic photosynthesis, when electron transport through the COX pathway is restricted at complex III using AA in leaf discs of *Arabidopsis* under growth light conditions: (1) over-reduction of mETC and ROS accumulation due to restricted COX and AOX pathways; (2) decrease in Ascorbate biosynthesis; (3) low thylakoid energization; (4) acceptor limitation at PSI; (5) decrease in photosynthetic carbon assimilation; (6) lack of electron sink in mitochondria leads to impairment of photosynthesis. The broken lined arrows indicate a reduction in utilization of reducing equivalents. AA – antimycin A; AOX1A – alternative oxidase 1a; Asc – ascorbate; CI – complex I; CIII– complex III; CIV–complex IV; mETC – mitochondrial electron transport chain; GL – $_{L}$-galactono-1,4-lactone; GLDH – $_{L}$-galactono-1,4-lactone dehydrogenase; NPQ – non-photochemical quenching; PSI – Photosystem I; PSII – photosystem II; ROS – reactive oxygen species; UQ – ubiquinone.

generation to benefit different components of photosynthesis when the electron transport through the COX pathway of the mETC is restricted at complex III.

5.3.1 Essentiality of AOX1A for optimal photosynthetic performance and chloroplastic heat dissipation

The use of *aox1a* mutants along with AA treatment allowed us to analyse the state of COX pathway restriction in the background of an impaired AOX pathway, whereas the treatment of WT with AA resulted only in COX pathway restriction. The restriction of the electron transport through complex III was ascertained by monitoring the decrease in rates of respiratory O_2 uptake with increasing concentrations of AA **(Fig. 5.1A)**. The interference of the mETC through complex III caused a drastic reduction in both photosynthetic carbon assimilation and photochemical reactions in *aox1a* mutants compared with WT **(Figs. 5.1B, 5.2 and 5.3)**. The studies of Strodtkötter et al. (2009) showed the induction of AOX1D to compromise the function of AOX1A in T-DNA insertion mutants of *aox1a*. However, in spite of the expression of AOX1D, *aox1a* mutants could neither maintain respiration nor their photosynthetic performance as WT plants when electron transport through the COX pathway is inhibited.

AA is well known to bind to the Q_i site of the cyt_{bc1} complex in mETC (Xia et al., 1997). However, its effect on cyclic electron flow around PSI (CEF-PSI) was also reported (Endo et al., 1998; Munekage et al., 2004). Such interference of AA on CEF-PSI might be small or negligible in the present study for the following reasons: (i) the concentration of AA required to inhibit CEF-PSI is 10-100 times higher than that required to inhibit the COX pathway (Taira et al., 2013); (ii) the effects of AA on respiration and photosynthesis were found to be biphasic in the present study. For instance, the treatment of WT leaf discs with concentrations ≤ 20 μM AA, caused only < 18% decrease in rates of both respiration and photosynthesis, while a treatment with ≥ 20 μM AA caused a drastic decrease up to ≤ 70% in their rates **(Fig. 5.1A, B)**; (iii) the

total cellular levels of ATP as well as the ATP/ADP ratio were higher in *aox1a* plants (with and without AA treatment) compared with WT (without AA) in both protoplasts and leaf discs (**Fig. 5.6** and Strodtkötter et al., 2009); and (iv) the effects of AA on most of the parameters examined in the present study were always less pronounced in WT than in *aox1a* plants **(Figs. 5.1-5.9)**. Unlike the protoplasts or cyanobacteria (Yeremenko et al., 2005) where AA is easily permeable through plasma/cell membranes, leaf discs are less permeable to AA. Hence, effective concentrations of AA that ultimately reach chloroplasts at the cellular level are expected to be much less than 20 µM. Moreover, the effect of 20 µM AA observed in respiratory and photosynthetic rates of *aox1a* leaf discs in the present study corroborated well with the effects examined on mesophyll protoplasts of *aox1a* mutants (Fig. 5.1A, B; Strodtkötter et al., 2009). Thus, AA was used at 20 µM in all further studies to exemplify the physiological role of AOX1A in optimizing photosynthesis.

Linear electron flow and CEF-PSI are coupled to proton pumping across the thylakoid membrane resulting in the acidification of the thylakoid lumen, thereby generating a proton gradient (ΔpH). This ΔpH is utilized for ATP synthesis and NPQ induction (Shikanai, 2007, 2014). The impact of the proton gradient on NPQ induction was evident through an *Arabidopsis pgr5* (proton gradient regulation) mutant (defective in CEF), which showed a lower NPQ at high irradiance (Yoshida et al., 2011b). Although the role of AOX1A in modulating NPQ was not shown in their study, several other studies have demonstrated that the lack of AOX caused a significant decrease in quantum yield of PSII, ETR and NPQ under HL conditions (Zhang et al., 2010; Zhang et al., 2012). Further, *aox1a pgr5* double mutants showed a significant decrease in CEF-PSI compared with *pgr5* indicating the synergetic function of AOX1A and CEF-PSI (Yoshida et al., 2011b). In *Arabidopsis*, the targeting of *AOX1A* and *AOX2* into chloroplasts using its own transpepetide resulted in induction of NPQ and also suggested that these isoforms have the ability to substitute the function of PTOX, which mediates the electron flow

from PQ to O_2 and thus, prevent the over reduction of PQ during excess light (Mc Donald et al., 2011; Fu et al., 2012). In the present study, although the activity of PTOX was not measured directly, a significant decrease in ETR(II) and NPQ in *aox1a* mutants compared with WT plants suggest that PTOX could not compensate for the lack of AOX1A. Further, an increase in Y(ND) in *aox1a* mutants indicates the down-regulation of PSII due to donor-side limitation of PSI, as evident by a decrease in ETR(II), Y(II) and qP **(Fig. 5.2B-D and 5.3C)**. Taken together, these results demonstrate that AOX1A plays a crucial role in maintaining the balanced electron flow between PSI and PSII, thereby ΔpH and NPQ induction, which protect photosynthesis from photoinhibition when electron flow through the COX pathway was restricted.

5.3.2 AOX1A maintains the redox balance between photochemical reactions and the Calvin cycle by regulating the malate valve to dissipate excess chloroplastic reducing equivalents

During active photosynthesis, photochemical reactions generate reducing equivalents at much higher magnitudes than their demands in the Calvin cycle. Under such conditions, excess reducing equivalents are transported to peroxisomes or mitochondria via the cytosol through the malate valve which allows the exchange of malate for OAA across the chloroplast membrane via specific transporters (Noguchi and Yoshida, 2008; Weber and Linka, 2011). The mitochondrial electron transport chain oxidizes these reducing equivalents by external/internal NAD(P)H dehydrogenases and AOX (Rasmusson et al., 2004; Noguchi and Yoshida, 2008). The activity of the enzymes NADP-MDH, NAD-MDH, citrate synthase (CS), NADP-ICDH and NAD-ME, which are known to actively coordinate the malate-OAA shuttle were significantly increased in *aox1a* knock-out plants compared with WT under HL conditions in order to prevent an over-reduction of chloroplastic electron transport carriers (Zhang et al., 2010; Xu et al., 2011). Further, the *aox1a* mutants exhibited an increase in NAD(P)H levels and redox ratios of their

corresponding redox couples under HL conditions when compared with WT plants. This indicates the significance of AOX1A in oxidizing excess reducing equivalents **(Chapter 4)**. Similarly, *aox1a* plants showed an excess NADH level compared with WT when the COX pathway is restricted **(Fig. 5.4B)**. By contrast, NADPH levels did not further increase in *aox1a* mutants compared with WT plants as expected **(Fig. 5.4E)**. This is because, as *aox1a* is more prone to oxidative damage caused by AA compared with WT, which is evident by increase in H_2O_2 and MDA content **(Fig. 5.8)**, it might exhibit metabolic adjustments to oxidize/utilize excess NADPH in the following reactions: (i) generation of O_2^- by NADPH oxidase (Sagi and Fluhr, 2006; Andronis et al., 2014), (ii) photorespiration, as evident by an increase in the glycine decarboxylase P- protein in *aox1a* plants after treatment with AA (Strodtkötter et al., 2009; Voss et al., 2013) and (iii) ascorbate-glutathione cycle or glutathione cycle to scavenge H_2O_2 by ascorbate peroxidase or glutathione peroxidase (Foyer and Noctor, 2011; Gill et al., 2013). However, a pronounced increase in the ratio of the NADH redox couple as well as the decrease in transcript levels of *MMDH1* and *ICDH* in *aox1a* mutants implicated the importance of AOX1A in relieving excess reductive pressure on chloroplastic redox carriers by regulating the malate valve particularly when the COX pathway is compromised **(Figs. 5.4C and 5.9B)**.

5.3.3 Significance of AOX1A in regulating cellular ROS and antioxidative system

The AOX pathway plays a significant role in the dissipation of chloroplastic reducing equivalents through the malate valve and prevents the over-reduction of mETC carriers. Such a role was hypothesized earlier by using SHAM, an inhibitor of the AOX pathway, and was further confirmed in the present study by using *aox1a* mutants (Padmasree and Raghavendra, 1999c; Yoshida et al., 2006; **Figs. 5.4 and 5.8B**). Therefore, the likelihood of electron leakage from mETC is expected to be higher in AA treated *aox1a* mutants (Møller, 2001; Strodtkötter et al., 2009; Yoshida et al., 2011a). When single electrons

react with molecular oxygen, ROS (OH^-, O_2^- and H_2O_2) are generated which can influence the expression of the genes related to antioxidative strategies by modifying transcription factors through retrograde regulatory mechanisms (Apel and Hirt, 2004; Choudhury et al., 2013; Li et al., 2013b). These include biosynthesis of carotenoids and flavonoids, the xanthophyll cycle, water-water cycle, NPQ, photorespiration and ROS scavenging enzymes (Niyogi, 2000; Murchie and Niyogi, 2011). If cellular ROS generation exceeds the scavenging capacity of the above-mentioned defense strategies, it leads to oxidative stress and ROS can damage various cellular structures including DNA, proteins, lipids or cell walls (Foyer and Noctor, 2005; Gill and Tuteja, 2010; del Río, 2015). During salt stress, the activity and transcript levels of antioxidative enzymes were shown to be significantly increased to scavenge excess ROS (Wang et al., 2010). In agreement with this, in the present study, AA treatment induced the expression of antioxidant genes in WT plants, and hence ROS accumulation was less which is not the case in *aox1a* mutants **(Figs. 5.7B, 5.8A and 5.9C)**. In *aox1a* mutant, AA treatment resulted in an accumulation of total cellular ROS including chloroplastic ROS, as indicated by localization of DCF fluorescence in those areas which contain high chlorophyll autofluorescence **(Fig. 5.7B)**. Furthermore, the increase in membrane damage under these conditions was evident from the increase in MDA content **(Fig. 5.8B)**. The expression of antioxidative genes was much lower in AA treated *aox1a* mutants that could be due to the partial impairment of antioxidative systems. This may explain AOX1A signaling in the induction of antioxidative enzymes or synergistic expression of AOX1A and antioxidative genes **(Fig. 5.9A)**.

The cellular redox state also plays an important role in mediating the signaling linked to developmental processes or environmental changes (Foyer and Noctor, 2005; Suzuki et al., 2012). NAD^+, $NADP^+$, glutathione and Asc, the key players of the Ascorbate-glutathione cycle, interact strongly with ROS to maintain cellular redox homeostasis (Noctor, 2006). Among ROS, H_2O_2 is more stable compared with O_2^- and

$^1O_2$. Asc, the most abundant antioxidant in plant cells, is oxidized by H_2O_2 to monodehydroascorbate in the presence of ascorbate peroxidase and is efficiently recycled back by the action of monodehydroascorbate reductase or dehydroascorbate reductase (Smirnoff, 2000). Thus, Asc plays an important role in the detoxification of ROS under various stress conditions. In the present study, the pronounced decrease in Asc and s*APX* levels along with reduction in respiratory O_2 uptake or photosynthetic O_2 evolution in *aox1a* mutants upon treatment with AA as opposed to WT plants indicate the relative importance of AOX1A over the COX pathway in regulating the antioxidative system to optimize photosynthesis **(Figs. 5.1A,B, 5.5A and 5.9C**; Yabuta et al., 2007; Dinakar et al., 2010a). Furthermore, the increase in Asc levels parallels to an increase in the *COX15* in WT, but not in *aox1a* plants suggesting a role of the AOX pathway in regulating Asc biosynthesis (**Figs. 5.5A and 5.9A**; Bartoli et al., 2000). Moreover, Asc is a cofactor of violaxanthin de-epoxidase that activates the zeaxanthin-dependent qE (energy-dependent quenching) and thus induces NPQ (Tóth et al., 2013). In the present study, after restriction of complex III, a decrease in NPQ in *aox1a* mutants could also be due to low Asc levels **(Figs. 5.2E and 5.5A)**. The importance of ROS, antioxidative metabolites and antioxidative enzymes in mediating beneficial interactions between mitochondrial respiration and chloroplastic photosynthesis was shown in *Pisum sativum* (Dinakar et al., 2010a).

Thus, the present study suggests the physiological importance of AOX1A in performing mitochondrial and extra mitochondrial functions to optimize chloroplastic photosynthesis when electron transport through the COX pathway is restricted **(Fig. 5.10)**. In mitochondria, AOX1A plays a role: (1) in the maintenance of the mETC redox homeostasis; (2) preventing accumulation of reducing equivalents and thereby ROS generation and (3) regulation of Asc biosynthesis. On the other hand, AOX1A performs the following functions outside the mitochondria: (1) sustenance of photosynthetic carbon assimilation; (2) induction of NPQ; (3) operation of Mal-OAA shuttle to dissipate excess

chloroplastic reducing equivalents and recycle redox carriers; (4) maintenance of redox homeostasis by preventing the over-reduction of chloroplastic ETC carriers and ROS generation and (5) coordinate with antioxidative systems to maintain the cellular ROS at optimal levels.

***

Chapter 6

Importance of AOX pathway in alleviating oxidative stress using *Saccharomyces cerevisiae* as a model organism

6.1 Introduction

Earlier literature and **Chapters 4** and **5** demonstrated that on exposure to abiotic stress, the AOX deficient plants showed an increase in intracellular ROS and decrease in photosynthetic performance compared to wild-type plants (Giraud et al., 2008; Strodtkötter et al., 2009; Watanabe et al., 2010). On the other hand, AOX overexpression lines showed enhanced photosynthetic efficiency with lower levels of cellular ROS when compared with wild-type during abiotic stress conditions (Umbach et al., 2005; Abu-Romman et al., 2012; Mhadhbi et al., 2013). In Arabidopsis, overexpression of AOX1a alleviated the Al induced programmed cell death (PCD) by decreasing the ROS production due to efficient mitochondrial electron flux and subsequently, caspase-3-like activation (Liu et al., 2014). Also, the role of AOX has been extensively studied in lower organisms since last two decades. Kumar and Söll (1992) reported for the first time heterologous expression of *A. thaliana* AOX into hemA deficient strains of *Escherichia coli*, which acquired resistance to cyanide and exhibited aerobic respiration. Later, several other studies also demonstrated the expression of AOX in many fungal and bacterial species which resulted in successful operation of cyanide-insensitive respiration (Chaudhuri and Hill, 1996; Affourtit et al., 1999; Kirimura et al., 1999; Magnani et al., 2007; Martins et al., 2011; Honda et al., 2012; Papagianni and Avramidis, 2012). The role of AOX is also revealed in survival of pathogenic fungi such as *Aspergillus fumigatus* and *Histoplasma capsulatum* inside the host under stress conditions (Tudella et al., 2003; Johnson et al., 2003). Similar to plants, the AOX mutant of pathogenic yeast *Cryptococcus neoformans* showed susceptibility to oxidative stress (Akhter et al., 2003). Furthermore, expression of AOX from *Hansenula anomala* in *S. cerevisiae* resulted in

up-regulation of several proteins related to major metabolic pathways such as Krebs cycle and amino acid biosynthesis suggesting the physiological role of AOX in mitoproteome plasticity (Mathy et al., 2006).

Yeast cells have become one of the most preferred experimental models to study the PCD and aging under oxidative stress, owing to special characteristics such as short life cycle and easy genetic manipulation along with presence of core cellular processes similar to eukaryotes (Carmona-Gutierrez et al., 2010). In most of the aerobic cells, respiration is the major source for generation of superoxide radical (O_2^-) as electrons leak out from the mitochondrial electron transport chain at Complex I and Complex III. Further, dismutation of O_2^- by superoxide dismutase (SOD) generates H_2O_2, a quite stable toxic product which creates oxidative environment inside the cell (Turrens, 1997). To detoxify the cellular H_2O_2, mitochondria have evolved an efficient antioxidant defence system such as catalase and peroxiredoxins, which include glutathione peroxidase/glutathione reductase and thioredoxin peroxidase/thioredoxin reductase (Kowaltowski et al., 2009). In spite of the existence of such strong antioxidant defence system, several pet mutants (impaired in mitochondrial electron transport chain) of *S. cerevisiae* showed accumulation of H_2O_2. But, the addition of exogenous cytochrome c to isolated mitoplasts significantly decreased H_2O_2 levels (Barros et al., 2003). In *Candida albicans* and *Aspergillus niger*, AOX was also induced along with cytochrome c under oxidizing conditions (Brown and Tuffery, 2010; Papagianni and Avramidis, 2012). Thus, AOX pathway is known to play an important role in the alleviation of ROS and thereby oxidative stress independently or in association with COX pathway and/or antioxidant defence system. Furthermore, a direct or indirect role of AOX has also been demonstrated in maintaining redox homeostasis in higher plants in response to several abiotic stresses (Vanlerberghe et al., 2009; Zhang et al., 2010; Zhang et al., 2014). However, such type of significance of AOX in lower organisms is yet to be elucidated.

In *Arabidopsis*, AOX1a is induced under various oxidative stresses and developmental stages (Saisho et al., 1997, 2001; Clifton et al., 2006; Giraud et al., 2008; Strodtkötter et al., 2009). In the present study, AtAOX1a was heterologously expressed in *S. cerevisiae* (a eukaryotic model system devoid of AOX) to characterize its role in alleviating oxidative stress across the kingdom. To create the oxidative environment inside the cells, *S. cerevisiae* were incubated with different concentrations of H_2O_2 and t-BOOH. The functional expression of AtAOX1a and its characterization have been studied by monitoring the changes in respiration, growth, viability, ROS and redox state under oxidizing conditions.

6.2 Results

6.2.1 Expression of AtAOX1a in *E. coli* and mass analysis

The expression of AtAOX1a protein induced in the presence of 0.1 mM IPTG in *E. coli* was visualized on SDS-PAGE as ~36 kDa band as it includes AtAOX1a sequence encoding mature protein (32.34 kDa) and pET28a(+) vector sequence (3.83 kDa) **[Fig. 6.1]**. The four major peptide fragments obtained during MALDI-TOF-TOF analysis of trypsin digested 36 kDa protein showed the following sequence in Biotools: WPTDLFFQR (1209.81 Da), DVNHFASDIHYQGR (1658.04 Da), GNIENVPAPAIAIDYWR (1898.27 Da) and ELDKGNIENVPAPAIAIDYWR (2383.58 Da) **[Fig. 6.2A-E]**. As these sequences showed 100% matching with *Arabidopsis* AOX1a protein sequence **(Fig. 6.2F)**, the purified protein was injected to rabbit and the polyclonal antibody was obtained.

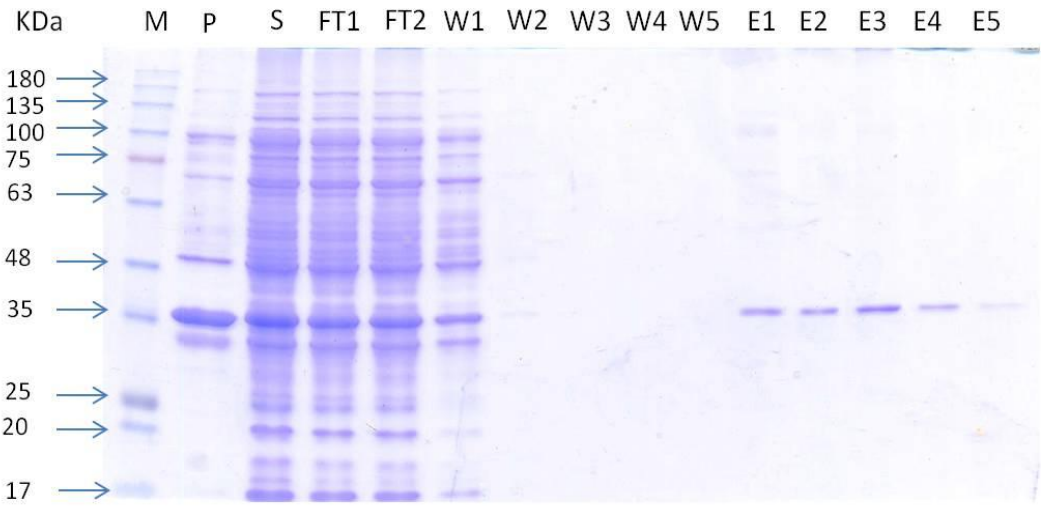

Fig. 6.1 Purification profile of polyhistidine tagged pET28a-AtAOX1a recombinant protein. (A) 12.5% SDS-PAGE depicting a ~36 kDa AtAOX1a protein in different fractions of purification protocol. Abbreviations used are as follows: M- marker, P- pellet (insoluble protein), S- supernatant (soluble protein), FT- flow through (supernatant passed through Ni-NTA column), W- washing fractions, E- elute (purified protein).

A

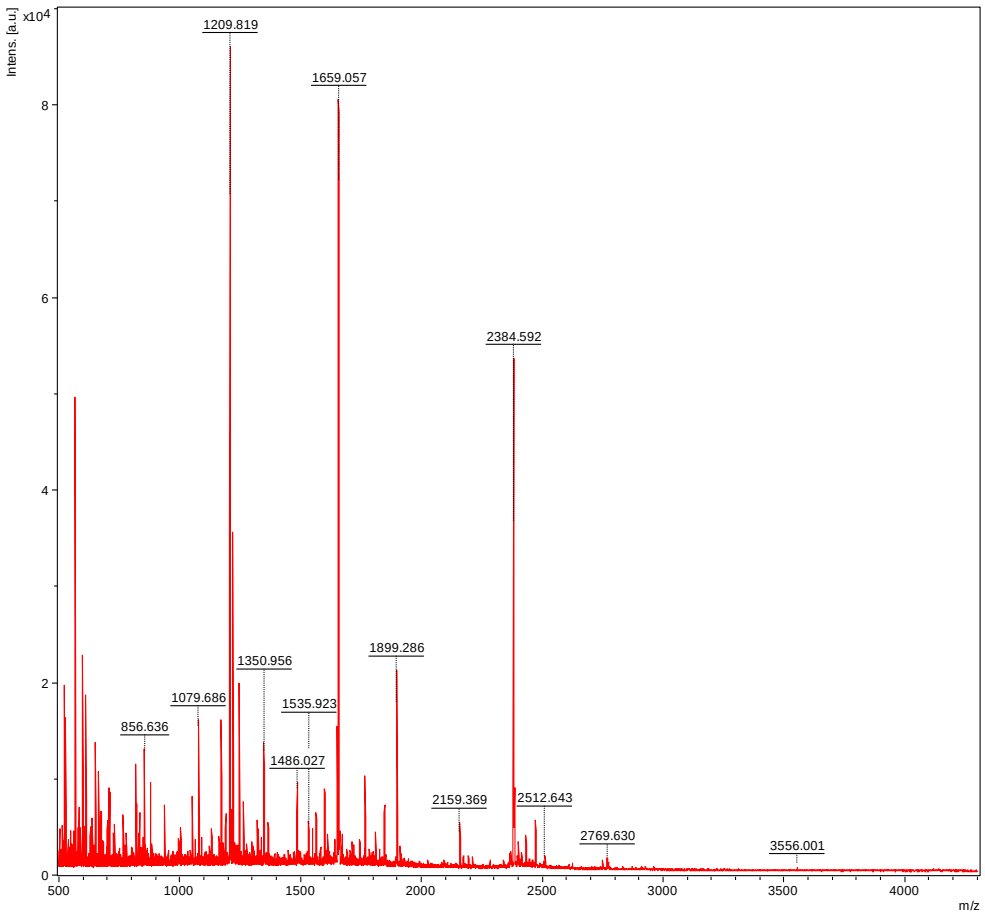

B

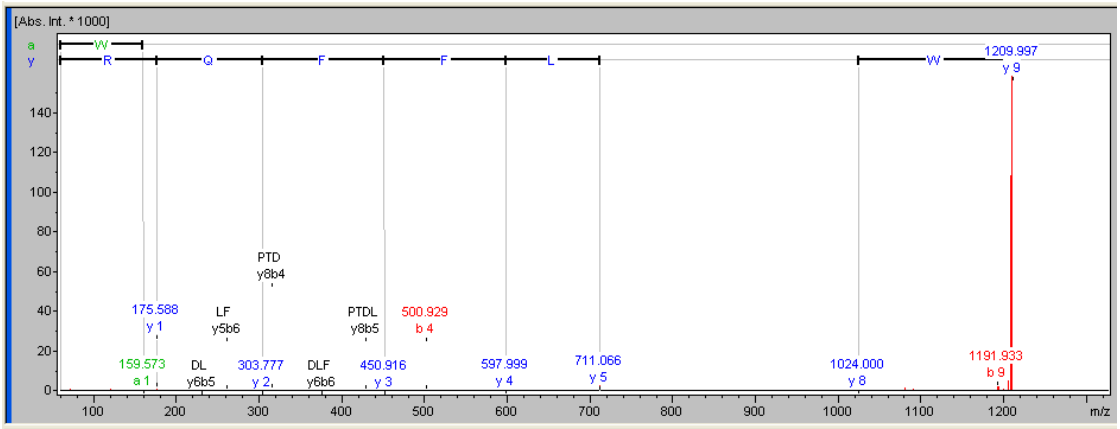

Protein View | Match Errors | MSMS fragments | MSMS Analysis

Sequence: WPTDLFFQR (Peptide Mods:)

Masses: Monoisotopic / Average

MH+(mono): 1209.605 MH+(avg): 1210.362 Calculate: Masses

MS/MS Tol: 2.000 Threshold: 0.000

Peaks: 34 Above Threshold: 34 Assigned: 10 Not Assigned: 24

	W	P	T	D	L	F	F	Q	R	Trp	Pro	Thr	Asp	Leu	Phe	Phe	Gln	Arg
Ion	1	2	3	4	5	6	7	8	9	1	2	3	4	5	6	7	8	9
a	W	P	T	D	L	F	F	Q	R	159.092	256.144	357.192	472.219	585.303	732.372	879.440	1007.499	1163.600
b	W	P	T	D	L	F	F	Q	R	187.087	284.139	385.187	500.214	613.298	760.366	907.435	1035.493	1191.595
y	W	P	T	D	L	F	F	Q	R	175.119	303.178	450.246	597.314	710.398	825.425	926.473	1023.526	1209.605
	9	8	7	6	5	4	3	2	1	Arg	Gln	Phe	Phe	Leu	Asp	Thr	Pro	Trp

C

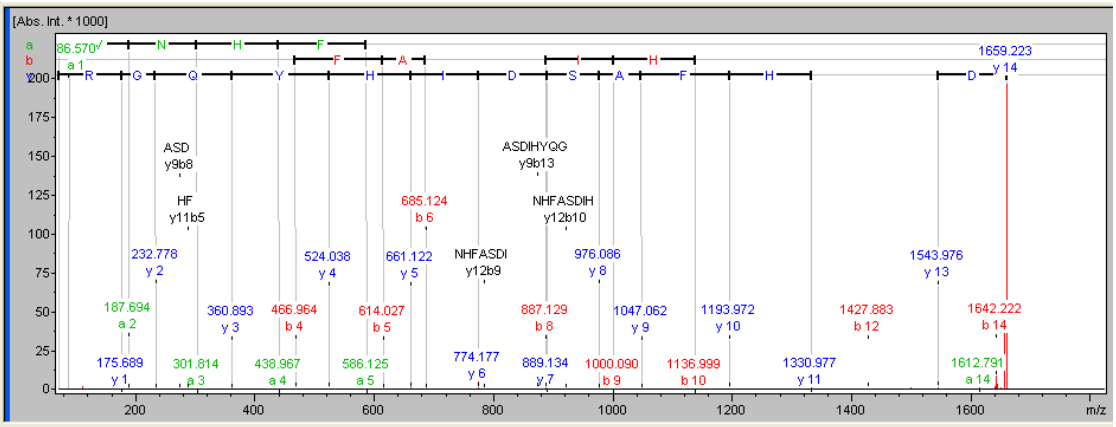

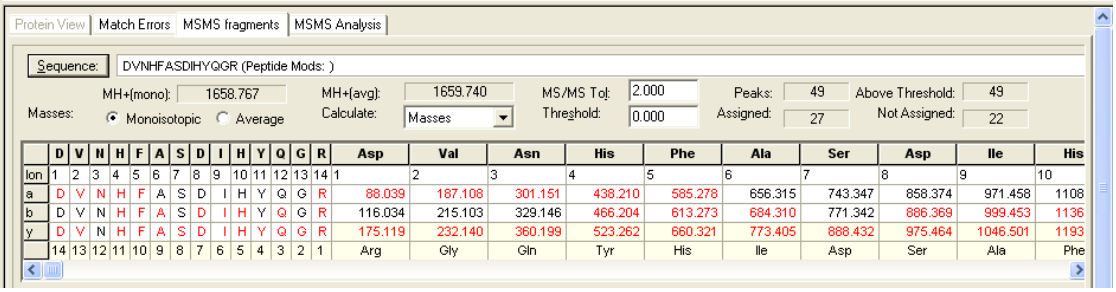

	D	V	N	H	F	A	S	D	I	H	Y	Q	G	R	Asp	Val	Asn	His	Phe	Ala	Ser	Asp	Ile	His
Ion	1	2	3	4	5	6	7	8	9	10	11	12	13	14	1	2	3	4	5	6	7	8	9	10
a	D	V	N	H	F	A	S	D	I	H	Y	Q	G	R	88.039	187.108	301.151	438.210	585.278	656.315	743.347	858.374	971.458	1108
b	D	V	N	H	F	A	S	D	I	H	Y	Q	G	R	116.034	215.103	329.146	466.204	613.273	684.310	771.342	886.369	999.453	1136
y	D	V	N	H	F	A	S	D	I	H	Y	Q	G	R	175.119	232.140	360.199	523.262	660.321	773.405	888.432	975.464	1046.501	1193
	14	13	12	11	10	9	8	7	6	5	4	3	2	1	Arg	Gly	Gln	Tyr	His	Ile	Asp	Ser	Ala	Phe

D

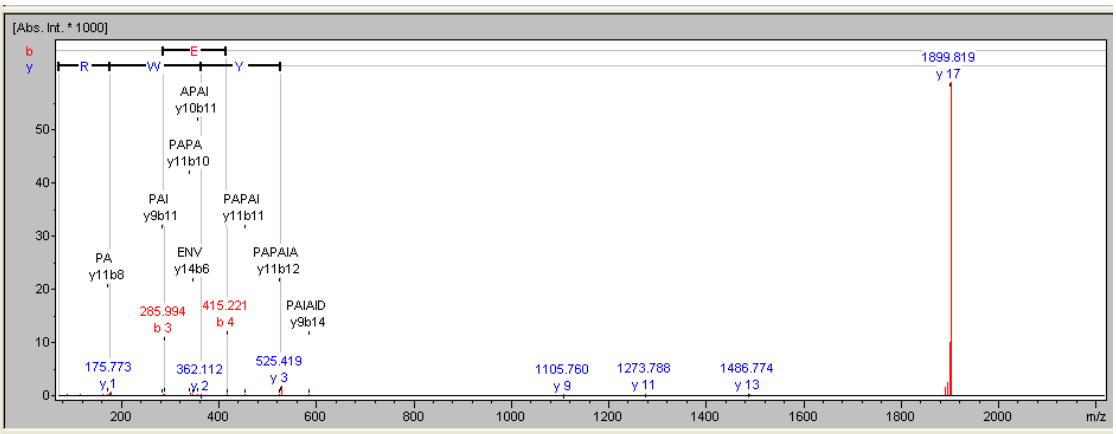

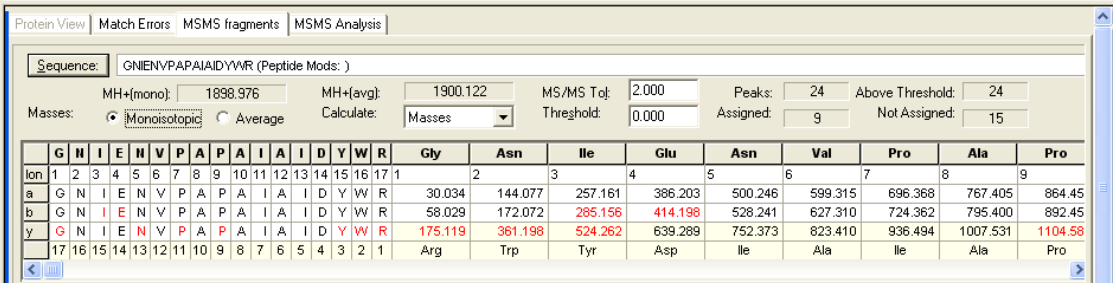

	G	N	I	E	N	V	P	A	P	A	I	A	I	D	Y	W	R	Gly	Asn	Ile	Glu	Asn	Val	Pro	Ala	Pro
Ion	1	2	3	4	5	6	7	8	9	10	11	12	13	14	15	16	17	1	2	3	4	5	6	7	8	9
a	G	N	I	E	N	V	P	A	P	A	I	A	I	D	Y	W	R	30.034	144.077	257.161	386.203	500.246	599.315	696.368	767.405	864.45
b	G	N	I	E	N	V	P	A	P	A	I	A	I	D	Y	W	R	58.029	172.072	285.156	414.198	528.241	627.310	724.362	795.400	892.45
y	G	N	I	E	N	V	P	A	P	A	I	A	I	D	Y	W	R	175.119	361.198	524.262	639.289	752.373	823.410	936.494	1007.531	1104.58
	17	16	15	14	13	12	11	10	9	8	7	6	5	4	3	2	1	Arg	Trp	Tyr	Asp	Ile	Ala	Ile	Ala	Pro

E

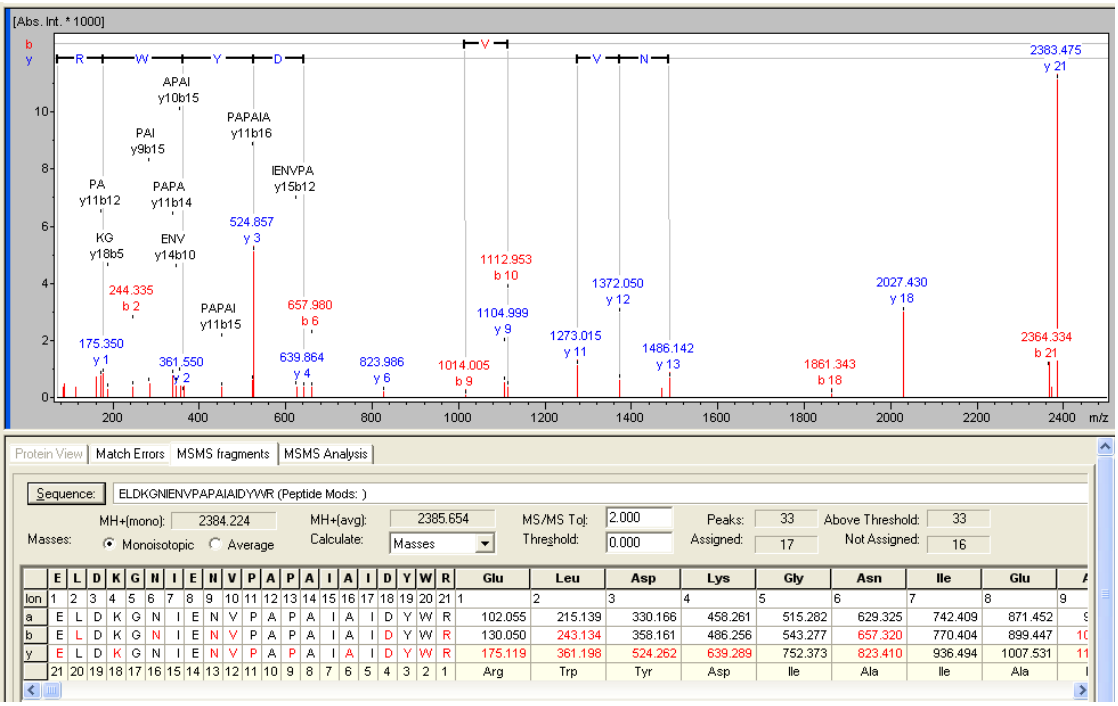

	E	L	D	K	G	N	I	E	N	V	P	A	P	A	I	A	I	D	Y	W	R	Glu	Leu	Asp	Lys	Gly	Asn	Ile	Glu	
Ion	1	2	3	4	5	6	7	8	9	10	11	12	13	14	15	16	17	18	19	20	21	1	2	3	4	5	6	7	8	9
a	E	L	D	K	G	N	I	E	N	V	P	A	P	A	I	A	I	D	Y	W	R	102.055	215.139	330.166	458.261	515.282	629.325	742.409	871.452	
b	E	L	D	K	G	N	I	E	N	V	P	A	P	A	I	A	I	D	Y	W	R	130.050	243.134	358.161	486.256	543.277	657.320	770.404	899.447	
y	E	L	D	K	G	N	I	E	N	V	P	A	P	A	I	A	I	D	Y	W	R	175.119	361.198	524.262	639.289	752.373	823.410	936.494	1007.531	
	21	20	19	18	17	16	15	14	13	12	11	10	9	8	7	6	5	4	3	2	1	Arg	Trp	Tyr	Asp	Ile	Ala	Ile	Ala	

F

1 MDTRAPTIGG MRFASTITLG EKTPMKEEDA NQKKTENEST GGDAAGGNNK
51 GDKGIASYWG VEPNKITKED GSEWKWNCFR PWETYKADIT IDLKKHHVPT
101 TFLDRIAYWT VKSLR**WPTDL** **FFQR**RYGCRA MMLETVAAVP GMVGGMLLHC
151 KSLRRFEQSG GWIKALLEEA ENERMHLMTF MEVAKPKWYE RALVITVQGV
201 FFNAYFLGYL ISPKFAHRMV GYLEEEAIHS YTEFLK**ELDK** **GNIENVPAPA**
251 **IAIDYWR**LPA DATLRDVVMV VRADEAHHR**D** **VNHFASDIHY** **QGR**ELKEAPA
301 PIGYH

Fig. 6.2 MALDI-TOF-TOF mass spectrum of tryptic digested purified AtAOX1a protein between 500-5,000 m/z. (A) The prominent peaks corresponding to 1209.819, 1659.057, 1899.286 and 2384.592 Da were subjected to MS-MS analysis. Lift spectrum and Biotools display of four major peaks: (B) 1209.819 Da, (C) 1659.057 Da, (D) 1899.286 Da and (E) 2384.592 Da. (F) The sequences obtained from these peptides showed 100% matching to internal sequences (indicated in BOLD) of *A. thaliana* AOX1a (AT3G22370) retrieved from NCBI database.

6.2.2 Functional characterization of AtAOX1a in *S. cerevisiae*

The protein expression of AtAOX1a induced in the presence of 2% galactose in *S. cerevisiae* AOX1a transformants (pYES2AtAOX1a) were confirmed through western blot analysis using AOX1a antibody **(Fig. 6.3A)**. The size of recombinant AtAOX1a protein was ~44 kDa which include signal sequence (7.65 kDa), AtAOX1a sequence encoding mature protein (32.34 kDa) and pYES2 sequence (4.37 kDa). Throughout the present study, pYES2 was used as a control. To ascertain the function of AtAOX1a, cyanide sensitive and cyanide insensitive respiration were monitored in pYES2 and pYES2AtAOX1a using 1 mM KCN and 2 mM SHAM, respectively. In the absence of KCN/SHAM the respiratory rates of pYES2AtAOX1a (8.6 ±0.11 nmol O_2 s^{-1}) were similar to pYES2 (8.45 ±0.09 nmol O_2 s^{-1}). But, in the presence of KCN, pYES2 showed a pronounced decrease in respiratory rates when compared with pYES2AtAOX1a. In contrast, addition of SHAM significantly decreased the respiratory rates of pYES2AtAOX1a but not of pYES2 **(Fig. 6.3B)**.

Similar to respiratory O_2 uptake, the exponential growth pattern (OD_{600} = 2.1) of both pYES2 and pYES2AtAOX1a were found to be similar upto 6 h under control conditions (without KCN). But, treatment with KCN remarkably decreased their exponential growth **(Fig 6.3C)**. However, the decrease in exponential growth of pYES was more significant when compared with pYES2AtAOX1a. Further, in the presence of KCN, growth recovery was found to be higher in pYES2AtAOX1a than pYES2 **(Fig. 6.3D)**. Taken together, these results indicate that AtAOX1a was successfully expressed and functional in *S. cerevisiae*.

6.2.3 Changes in cellular ROS during oxidative stress

The role of AtAOX1a in minimizing the ROS generation was determined by treatment with KCN as well as mimicking oxidative stress in *S. cerevisiae* using H_2O_2 and t-BOOH.

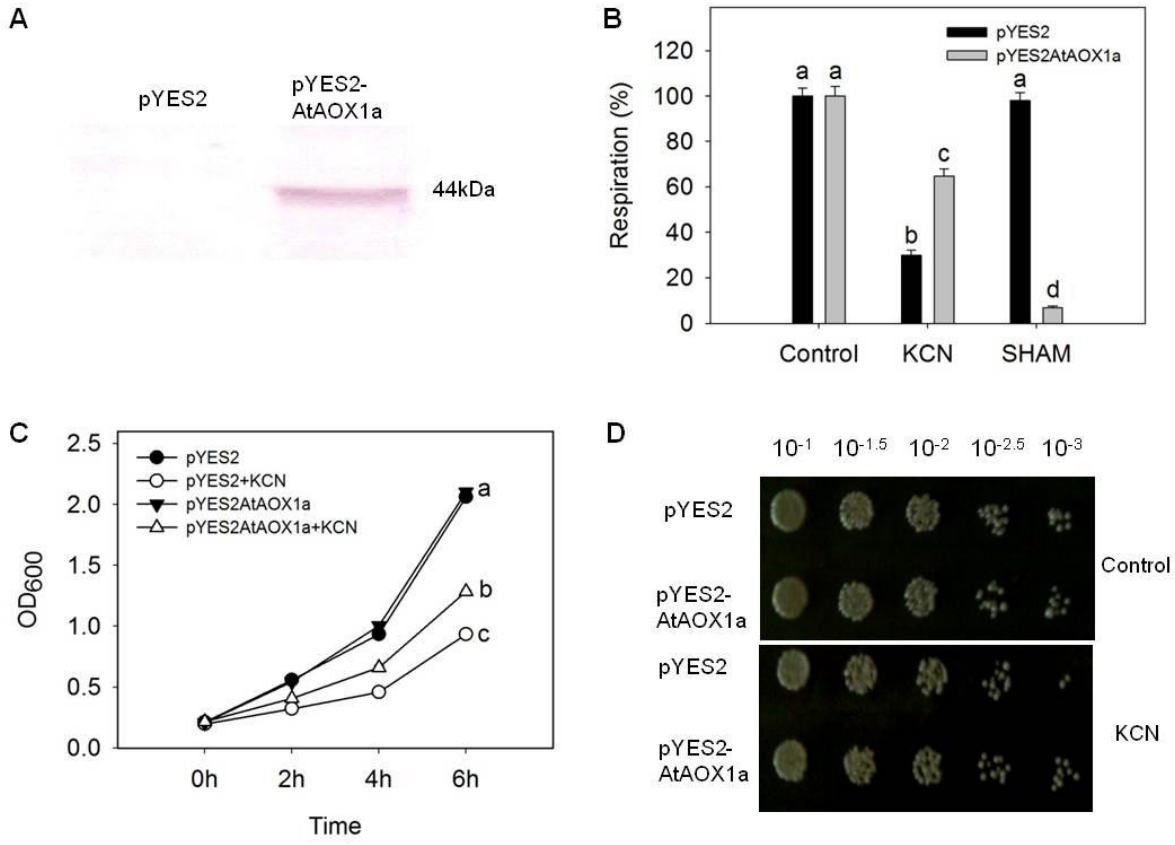

Fig. 6.3 Functional expression of AtAOX1a in *S. cerevisiae*. (A) Western blot showing the AtAOX1a protein (44 kDa) expression in pYES2AtAOX1a (left side) but not in PYES2 (right side), (B) Rates of oxygen uptake by pYES2 and pYES2AtAOX1a in the absence or presence of KCN (1mM) and SHAM (2mM), (C) Growth curve of pYES2 and pYES2AtAOX1a in absence or presence of KCN (1mM), (D) Growth recovery after KCN (1 mM) treatment for 4h.. Different lowercase alphabetical letters indicate statistically significant difference ($P < 0.05$).

But, upon treatment with KCN, H_2O_2 or t-BOOH, the fluorescence increased steadily in pYES2. In contrast, pYES2AtAOX1a restricted the increase in fluorescence on treatment with either KCN or oxidants (H_2O_2 and t-BOOH) indicating the importance of AOX1a in preventing and/or regulating the ROS generation **(Fig. 6.4)**.

6.2.4 Changes in cell survival rate and growth recovery during oxidative stress

The significance of AOX1a in sustaining the cell viability was assessed by monitoring the rates of cell survival in the presence of H_2O_2 and t-BOOH. Among these oxidants, H_2O_2 was found to be more lethal than t-BOOH. However, upon treatment with these oxidants, the survival rates of pYES2 decreased drastically when compared with pYES2AtAOX1a **(Fig. 6.5A)**.

Also return to growth assay clearly indicated enhanced colony number in pYES2AtAOX1a than in pYES2 under all oxidizing conditions. However, a clear visible difference was observed only at $1\times10^{-2.5}$ and 1×10^{-3} dilutions **(Fig. 6.5B)**. It appears that AOX1a plays a critical role in decreasing the rates of cell death and improving their growth recovery under oxidizing conditions.

6.2.5 Differential antioxidant gene expression profile during oxidative stress

The ROS scavenging efficiency of pYES2 and pYES2AtAOX1a was measured by monitoring changes in transcript levels of antioxidant genes viz., *Superoxide dismutase 1* (*SOD1*), *Superoxide dismutase 2* (*SOD2*), *Glutathione peroxidase 2* (*GPX2*) and *Thioredoxin peroxidase 2* (*TSA2*) during oxidative stress **(Fig. 6.6)**. Under control conditions, the expression of these antioxidant genes was approximately similar in both pYES2 and pYES2AtAOX1a. Upon treatment with H_2O_2 or t-BOOH, the expression of *SOD1* (> 8-fold), *SOD2* (> 6-fold), *GPX2* (> 52-fold) and *TSA2* (> 157-fold) increased significantly by several fold in both pYES2 and pYES2AtAOX1a **(Fig. 6.6A-D)**.

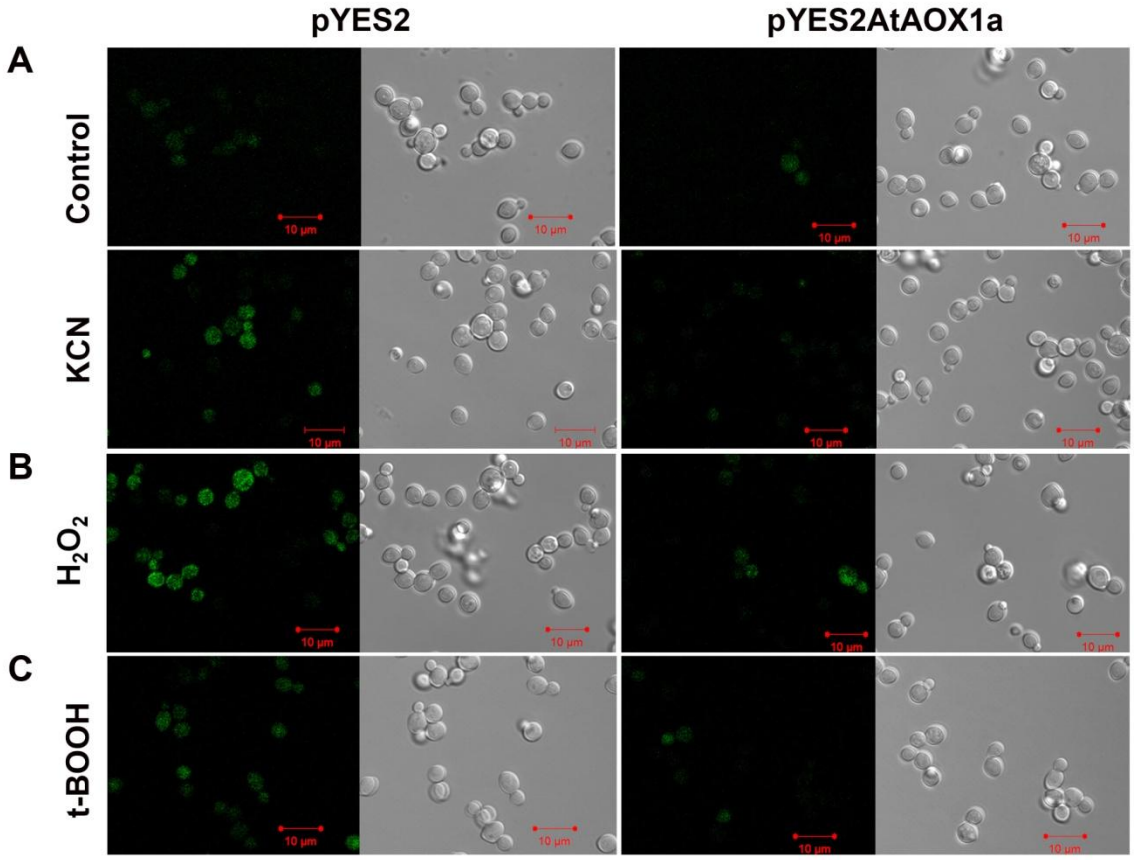

Fig. 6.4 The intracellular ROS were monitored under confocal fluorescence microscope in terms of DCF fluorescence produced by the action of esterases on H_2DCFDA at 488 nm (excitation) and 525 nm (emission) wavelengths as described in materials and methods. For oxidative stress pYES2 and pYES2AtAOX1a were treated with (A) KCN, (B) H_2O_2 or (C) t-BOOH.

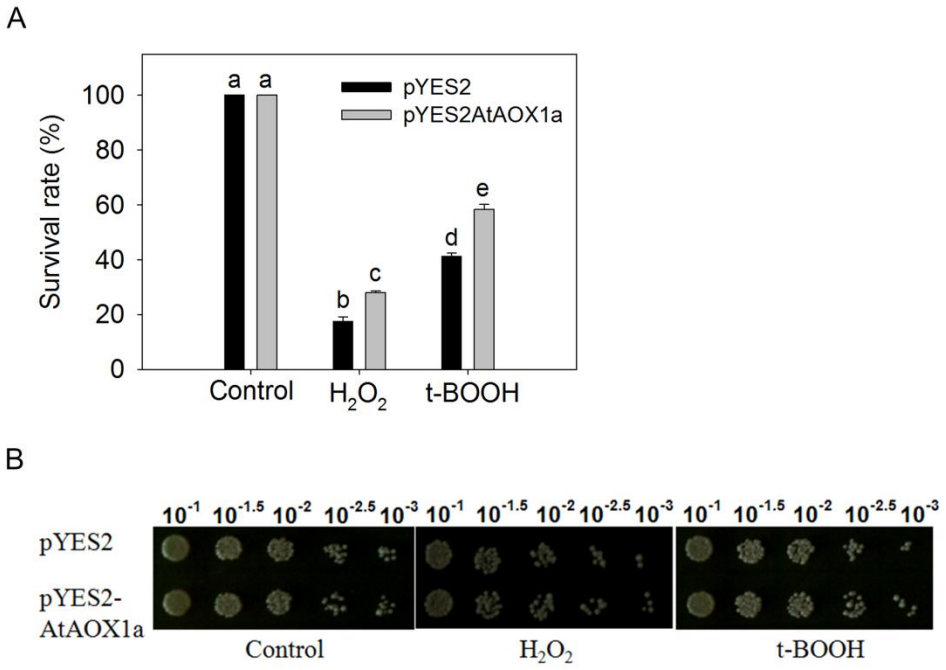

Fig. 6.5 Effect of oxidative stress on cell survival rate of pYES2 and pYES2AtAOX1a in presence of (A) H_2O_2 and (B) t-BOOH. Further, return to growth assay indicates the recovery of cells from oxidative stress in presence of (C) H_2O_2 and (D) t-BOOH. Different lowercase alphabetical letters indicate statistically significant difference ($P < 0.05$).

But, the expression of *GPX2* was down-regulated significantly in pYES2AtAOX1a when compared with pYES2 in presence of both H_2O_2 and t-BOOH **(Fig. 6.6C)**. In contrast, the expression of *TSA2* was down-regulated significantly in pYES2AtAOX1a when treated with t-BOOH, while remained unchanged in the presence of H_2O_2 **(Fig. 6.6D)**.

6.2.6 Changes in cellular redox during oxidative stress

The role of AtAOX1a in maintaining cellular redox balance during oxidative stress was revealed by monitoring the changes in pyridine nucleotide (NAD^+ and NADH) redox couple. In control, the cellular levels of NAD^+, NADH and the redox ratio of NAD^+/NADH were similar in both pYES2 and pYES2AtAOX1a. Upon treatment with H_2O_2, the cellular NAD^+ levels decreased significantly in both pYES2 and pYES2AtAOX1a **(Fig. 6.7A)**. In contrast, the decrease in cellular NADH levels was significant in pYES2AtAOX1a alone **(Fig. 6.7B)**. Consequently, the cellular redox ratio of NAD^+/NADH was maintained at much higher levels in pYES2AtAOX1a when compared with pYES2 in presence of H_2O_2 **(Fig. 6.7C)**.

The responses of NAD^+, NADH and consequently NAD^+/NADH were quite different in t-BOOH treated samples when compared to H_2O_2 treatment. Both NAD^+ and NADH increased significantly while the redox ratio of NAD^+/NADH decreased drastically in pYES2AtAOX1a when compared with pYES2 **(Fig. 6.7)**.

6.3 Discussion

In higher plants, AOX is known to perform several mitochondrial and extra mitochondrial functions, viz: (i) alleviation of ROS, reactive nitrogen species and cell death (Mittler, 2002; Amirsadeghi et al., 2006; Igamberdiev et al., 2014), (ii) preventing over reduction of chloroplastic/mitochondrial electron transport carriers, particularly PQ or UQ (Yoshida et al., 2011a), (iii) maintenance of cellular redox and carbon balance (Sieger et al., 2005), (iv) modulation of cellular energy level (Padmasree and

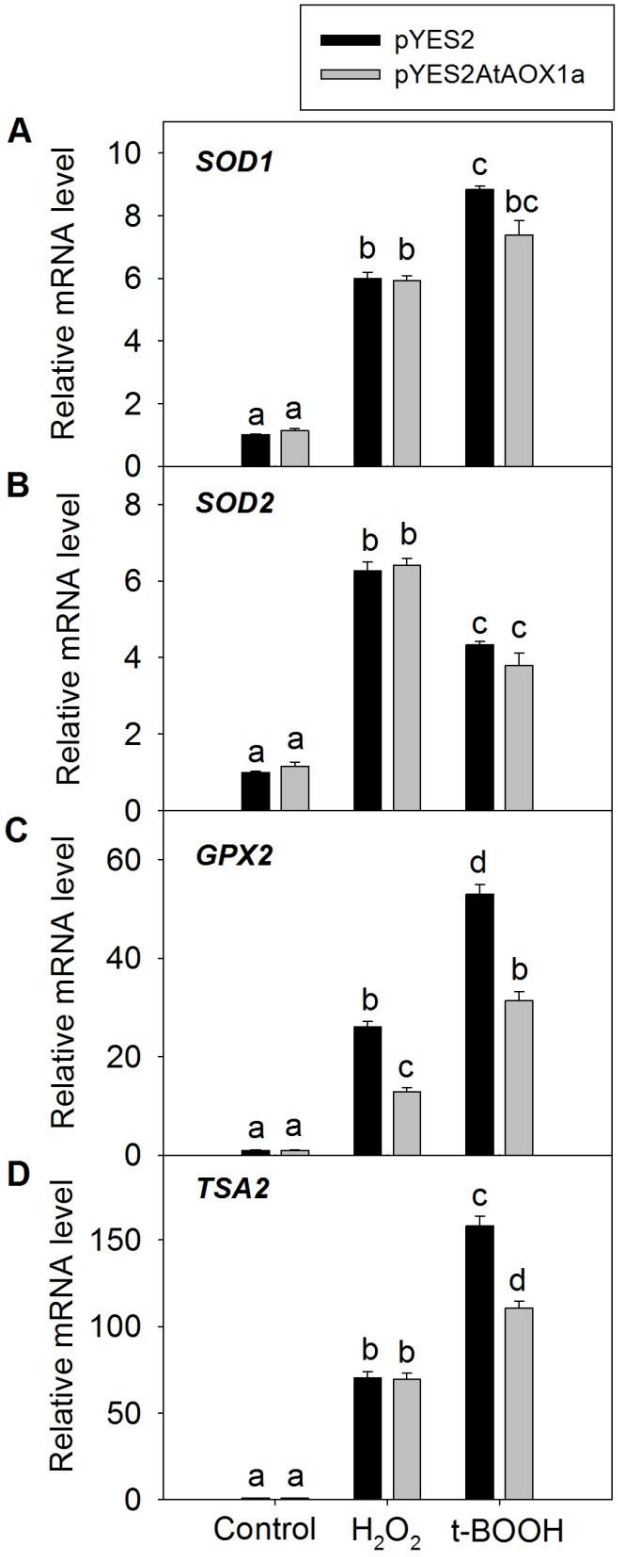

Fig. 6.6 Relative mRNA profile of antioxidant genes (*SOD1*, *SOD2*, *GPX2* and *TSA2*) in pYES2 and pYES2AtAOX1a after exposure to oxidative stress in presence of (A) H_2O_2 and (B) t-BOOH. Different lowercase alphabetical letters indicate statistically significant difference ($P < 0.05$).

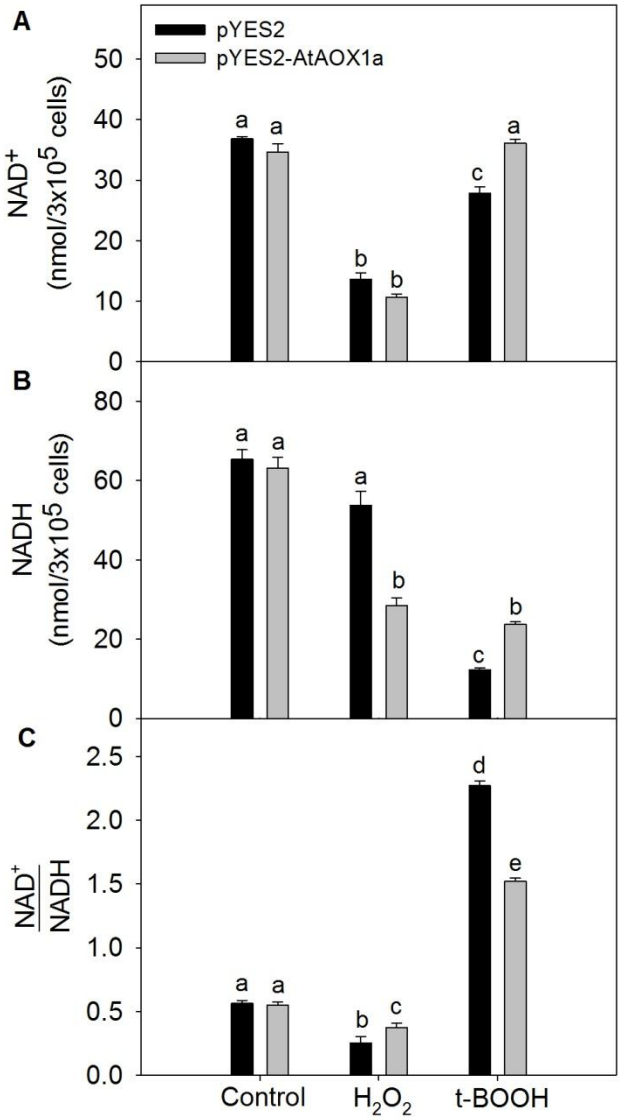

Fig. 6.7 Changes in total cellular pyridine nucleotides (A) NAD^+, (B) NADH and (C) ratio of NAD^+ to NADH in pYES2 and pYES2AtAOX1a during oxidative stress in presence of H_2O_2. Different lowercase alphabetical letters indicate statistically significant difference ($P < 0.05$).

Raghavendra 1999a; Strodtkötter et al., 2009) and (v) optimization of photosynthesis during a wide range of biotic and abiotic stresses (Dinakar et al., 2010b; Vanlerberghe, 2013). The role of AOX in alleviating ROS levels and oxidative stress is not only confined to plants, but is also revealed in several non-photosynthetic organisms including fungi, protists, bacteria and human cells (Matsukawa et al., 2009; Brown and Tuffery, 2010; Honda et al., 2012; Rogov and Zvyagilskaya, 2015). These observations suggest that engineering of AOX into species which are deficient in AOX may help them to cope up against various biotic and abiotic stresses.

S. cerevisiae lacks AOX homolog (Minagawa and Yoshimoto, 1987). Therefore, in the present study, AtAOX1a was expressed in *S. cerevisiae* to validate its physiological function during oxidative stress **(Fig. 6.2A)**. It is well known in plants and fungi that restriction of electron flow through the COX pathway or exposure to oxidative stress leads to induction of AOX at the transcript or protein level and AOX catalysed respiration (Vanlerberghe et al., 2002; Magnani et al., 2007; Dinakar et al., 2010a,b; Abu-Romman et al., 2012). Corroborating with these studies, restriction of the COX pathway by KCN caused reduction in the total respiratory rates of both pYES2 and pYES2AtAOX1a. However, higher respiratory rates retained by pYES2AtAOX1a when compared with pYES2, perhaps attributed to the induction of AOX catalysed respiration. Further, SHAM insensitive respiration in pYES2 indicates the absence of AOX catalysed respiration in *S. cerevisiae*, while SHAM sensitive respiration in pYES2AtAOX1a confirms the functional expression of AtAOX1a in *S. cerevisiae* **(Fig. 6.3B)**. Any increase in the respiratory activity is known to increase the chronological and replicative life span of *S. cerevisiae* (Barros et al., 2004). Also, in the present study, the recovery in the growth curve parallel to a rise in the total respiratory rates of pYES2AtAOX1a compared to pYES2 in presence of KCN reveals the significance of AOX catalyzed respiration in maintenance of S. cerevisiae cell growth **(Fig. 6.3B-D)**.

ROS production is a common phenomenon in cells which occurs during aerobic respiration or in response to several biotic or abiotic stresses. However, if they exceed beyond detoxification capacity of the cell's antioxidant machinery, it leads to oxidative stress (Finkel, 2003; Apel and Hirt, 2004; Asada, 2006). Yeast cells are known to show a range of responses depending on the concentration of cellular ROS. At very low levels of ROS, the cells try to adapt themselves. While at higher levels, cells activate their antioxidant defence system which is mediated by Yap1p and Msn2,4p transcription factors (Perrone et al., 2008). But, at further higher levels, ROS may arrest cell cycle leading to apoptosis (Farrugia and Balzan 2012; Ayer et al., 2014). In the present study, the higher levels of cellular ROS induced by KCN, H_2O_2 or t-BOOH in pYES2 were positively correlated with cell death and negatively correlated with growth recovery. In contrast, the lower levels of ROS, better survival rate and growth recovery recorded under oxidising environment in pYES2AtAOX1a indicate the importance of AOX catalyzed respiration in mitigating the cellular ROS production **(Figs. 6.4 and 6.5)**.

In addition, redox homeostasis is a basic requirement to maintain the cellular metabolism and ROS, particularly, during aging (Wheeler and Grant, 2004; Ayer et al., 2014). Accumulation of NADH levels is known to decrease the Sir2 activity, which is essential for chromatin silencing and extension of life span. Thus, any increase in the redox ratio of NAD^+/NADH extends the chronological as well as replicating life span of yeast cells (Lin et al., 2002 and 2004). In agreement with these findings, pYES2AtAOX1a showed an increase in the NAD^+/NADH ratio when compared with pYES2 upon treatment with H_2O_2 or t-BOOH. These results elucidate the importance of AtAOX1a in maintenance of cellular redox homeostasis to increase the life span as evident by cell survival rate of *S. cerevisiae* **(Figs. 6.5A, B and 6.7C)**.

Further, sulphydryl (–SH) group plays a critical role in proper functioning of several of the enzymes, transcription factors and membrane proteins, which in turn play a significant role in maintaining the cellular redox homeostasis (Wheeler and Grant, 2004).

During oxidative stress, cysteine sulfhydryl residues are oxidized to disulfide bonds, thereby leading to a loss in protein activity. Glutaredoxins and thioredoxins are small heat-stable oxidoreductases which catalyze the reduction of disulfides to thiols using thiolated cysteine residues present in the active sites (Rietsch and Beckwith, 1998; Wheeler and Grant, 2004; Herrero et al., 2008). A few studies reported the role of glutaredoxins and thioredoxins in supplying reducing equivalents to the regulatory sulfhydryl/disulfide system to activate AOX which play a role in preventing over-reduction of mitochondrial electron transport carriers and thereby ROS generation (Purvis, 1997; Gelhaye et al., 2004; Arnholdt-Schmitt et al., 2006). In the present study, several fold increase in the transcript levels of *GPX2* and *TSA2* in pYES2 and their down-regulation in pYES2AtAOX1a in presence of H_2O_2 or t-BOOH suggest the role of AOX1a in regulating the expression of *GPX2* and *TSA2*, which play a role in detoxification of ROS and maintenance of cellular redox balance **(Figs. 6.5, 6.6A, B and 6.7C)**.

The results from the present study suggest that transformation of AtAOX1a introduced the AOX catalysed respiration in *S. cerevisiae*. During oxidative stress, AtAOX1a compromise against GPX2 and TSA2 to maintain cellular redox homeostasis, mitigate ROS generation and thereby better cell survival rate.

***

Chapter 7

Summary and Conclusions

The present study aimed to investigate the physiological impact of AOX, particularly AOX1a isoform during oxidising conditions. To reveal the importance of AOX1a in protecting photosynthesis from oxidative stress caused by HL, the leaf discs of WT and *aox1a* mutant of *A. thaliana* were treated with different light intensities (50, 250, 500 and 700 µmol photons m^{-2} s^{-1}) and found a significant decrease in HCO_3 dependent O_2 evolution (an indicator of Calvin cycle) at 700 µmol photons m^{-2} s^{-1} light intensity **(Figs. 4.1 and 4.2)**. Hence, in further studies HL stress was given by illuminating the leaves at 700 µmol photons m^{-2} s^{-1}. Under growth light (50 µmol photons m^{-2} s^{-1}) conditions, *aox1a* plants did not show any changes in photosynthetic parameters, redox ratio of pyridine nucleotides, or respiratory O_2 uptake when compared to WT. However, upon exposure to HL, parallel to a decrease in O_2 evolution, F_v/F_m ratio, quantum yield of PSII, electron transport rates of PSII, photochemical quenching and non-photochemical quenching were significantly decreased in *aox1a* when compared with WT **(Figs. 4.3 and 4.4)**. Further, the reducing equivalents accumulated with concomitant rise in total cellular ROS and MDA content in *aox1a* as compared to WT **(Figs. 4.5-4.7)**. The transcript levels of several genes related to antioxidative system, malate-OAA shuttle, photorespiratory and respiratory enzymes was higher in *aox1a* compared to WT **(Fig. 4.8)**. Taken together, these results demonstrate that under HL, in spite of a significant increase in transcript levels of several genes mentioned above to maintain cellular redox homeostasis and minimize ROS production, *Arabidopsis* plants deficient in AOX1a were unable to sustain photosynthesis as is the case in WT plants.

Subsequently, we investigated the impact of AOX1a in optimizing the photosynthesis during restriction of COX pathway at complex III. The leaf discs of WT and *aox1a* of *Arabidopsis* were treated with AA under growth light. In absence of AA,

both WT and *aox1a* genotypes did not show any difference in physiological, biochemical or molecular parameters. But, after AA treatment, *aox1a* showed significant reduction in both respiratory O_2 uptake and $NaHCO_3$ dependent O_2 evolution as compared to WT (**Fig. 5.1**). Chlorophyll fluorescence and P700 studies revealed that in contrast to WT genotype, *aox1a* was incapable of maintaining the electron flow in chloroplastic electron transport chain and thereby low NPQ was observed. In contrast to *aox1a* mutant, WT showed an increase in ascorbate level and NPQ induction, which suggest that there is a strong correlation among ascorbate level, NPQ induction and AOX (**Figs. 5.2, 5.3 and 5.5**). Thus, these results further emphasize the role of AOX1a in dissipating the excess heat from chloroplasts. Further, *aox1a* exhibited disturbances in cellular redox state of pyridine nucleotides and consequently increase in ROS, followed by lipid peroxidation as compared to WT (**Figs. 5.4, 5.7 and 5.8**). On the other hand, WT showed significant increase in transcript levels of *CSD1*, *CAT1*, *sAPX*, *COX15* and *AOX1A* in contrast to *aox1a* (**Fig. 5.9**), which suggest that AOX1a deficiency during restriction of COX pathway led to enormous increase in ROS levels that could have damaged the antioxidant defense system at transcript/protein levels. Taken together, these results suggest that AOX1a is essential component of mitochondrial electron transport chain which plays a significant role in chloroplastic heat dissipation and maintenance of cellular redox homeostasis and thereby ROS levels to optimize photosynthesis during restriction of COX pathway at complex III (**Fig. 5.10**).

After observing a substantial significance of AOX1a in optimizing photosynthesis by alleviating the photo-oxidative stress or chemically (AA) induced oxidative stress, it was intriguing to investigate its function across the kingdom (*S. cerevisiae*). Firstly, AtAOX1a was heterologously expressed in *E. coli* expression strain BL21(DE3)pLYsS for generating antibody against AtAOX1a, as no specific antibody was available commercially (**Figs. 6.1 and 6.2**). The *S. cerevisiae* cells with empty vector were named as pYES2, while cells transformed with AtAOX1a were named as pYES2AtAOX1a.

Oxidative environment was created by external supply of H_2O_2 and t-BOOH. In the presence of KCN, the total respiration was decreased twice in pYES2 when compared with pYES2AtAOX1a. On the other hand, in presence of SHAM, a drastic reduction in total respiration in pYES2AtAOX1a as compared to pYES2, which indicate the functional expression of AtAOX1a in the mitochondria of *S. cerevisiae* (**Fig. 6.3**). During oxidizing conditions, pYES2AtAOX1a showed better growth and survivilty accompanied by decrease in ROS levels, when compared with pYES2 (**Figs. 6.4 and 6.5**). Additionally, AtAOX1a modulated the cellular redox homeostasis and antioxidant gene expression (*GPX2* and *TSA2*) during oxidative stress (**Figs. 6.6 and 6.7**). Hence, we conclude that expression of AtAOX1a in *S. cerevisiae* enhanced the respiratory capacity, which in turn mitigated the ROS levels and rescued the cells from oxidative stress.

Conclusions

1. AOX1a facilitates efficient photosynthetic performance under HL in *A. thaliana*.
2. Deficiency in AOX1a leads to accumulation of ROS under HL.
3. AOX1a plays a significant role in maintenance of cellular redox homeostasis.
4. AOX1a deficiency enhanced interactions between alternative sinks: respiration, photorespiration, Mal-OAA shuttle and antioxidative system under HL to dissipate redox.
5. During inhibition of COX pathway, AOX1a plays a crucial role inside the mitochondria for optimization of photosynthesis: (i) maintenance of the mETC redox homeostasis; (ii) preventing accumulation of reducing equivalents and thereby ROS generation and (iii) regulation of Asc biosynthesis.
6. Also, AOX1a performs a wide range of functions outside the mitochondria when electron transport through COX pathway is inhibited which include: (i) sustenance of photosynthetic carbon assimilation; (ii) induction of NPQ; (iii) operation of Mal-OAA shuttle to dissipate excess chloroplastic reducing

equivalents and recycle redox carriers; (iv) maintenance of redox homeostasis by preventing the over-reduction of chloroplastic ETC carriers and ROS generation and (v) coordinate with antioxidative systems to maintain the cellular ROS at optimal levels.

7. The expression of AtAOX1a in *S. cerevisiae* resulted in cyanide resistant respiration.
8. AtAOX1a mitigate ROS generation in *S. cerevisiae* during oxidative stress.
9. AtAOX1a regulates the NAD^+/NADH ratio and extend the life span of *S. cerevisiae* during oxidative stress.
10. AtAOX1a compromised against *GPX2* and *TSA2* during oxidative stress.

***

Future Directions

- **Improving crop plants** Plants are often encountered by a wide range of biotic and abiotic stresses, which cause a great economic loss. Using transgenic approach, *AOX* can be over-expressed in crop plants to increase their tolerance level against several biotic/abiotic stresses as already has been demonstrated in present **(Chapter 4 and 5)** and previous studies in several model plants.
- **Industrial use** Results from present study **(Chapter 6)** and previous study (Papagianni and Avramidis, 2012) suggest that genetic engineering of *AOX* in AOX-deficient fungus or bacterial strains might be beneficial in several aspects (e.g. growth, survival and preservative production like nisin against oxidative stress) at industrial level.
- **Disease remedy** AOX has a unique feature of preventing over-reduction of mETC consequently, ROS accumulation and PCD. Therefore, artificial introduction of AOX pathway in animals including human might be a promising tool in curing many diseases caused by dysfunction of mitochondrial respiratory chain (e.g. Parkinson's, Alzheimer's, Leigh's syndrome etc).

***

Literature cited

Abu-Romman S, Shatnawi M, Hasan M, Qrunfleh I, Omar S, Salem N. 2012. cDNA cloning and expression analysis of a putative alternative oxidase *HsAOX1* from wild barley (*Hordeum spontaneum*). *Genes & Genomics*, **34**: 59-66.

Affourtit C, Albury MS, Krab K, Moore AL. 1999. Functional expression of the plant alternative oxidase affects growth of the yeast *Schizosaccharomyces pombe*. *J Biol Chem*, **274**: 6212-8.

Agrimi G, Brambilla L, Frascotti G, Pisano I, Porro D, Vai M, Palmieri L. 2011. Deletion or overexpression of mitochondrial NAD^+ carriers in *Saccharomyces cerevisiae* alters cellular NAD and ATP contents and affects mitochondrial metabolism and the rate of glycolysis. *Appl Environ Microbiol*, **77**: 2239-46.

Akhter S, McDade HC, Gorlach JM, Heinrich G, Cox GM, Perfect JR. 2003. Role of alternative oxidase gene in pathogenesis of *Cryptococcus neoformans*. *Infect Immun*, **71**: 5794-5802.

Albertsson P-Å. 2001. A quantitative model of the domain structure of the photosynthetic membrane. *Trends Plant Sci*, **6**: 349-354.

Albury MS, Affourtit C, Crichton PG, Moore AL. 2002. Structure of the plant alternative oxidase site-directed mutagenesis provides new information on the active site and membrane topology. *J Biol Chem*, **277**: 1190-1194.

Albury MS, Elliott C, Moore AL. 2010. Ubiquinol-binding site in the alternative oxidase: mutagenesis reveals features important for substrate binding and inhibition. *Biochim Biophys Act*, **1797**: 1933-1939.

Allen JF. 2003. Cyclic, pseudocyclic and noncyclic photophosphorylation: new links in the chain. *Trends Plant Sci*, **8**: 15-19.

Aluru MR, Rodermel SR. 2004. Control of chloroplast redox by the IMMUTANS terminal oxidase. *Physiol Plant*, **120**: 4-11.

Alvarez ME. 2000. Salicylic acid in the machinery of hypersensitive cell death and disease resistance. *Plant Mol Biol*, **44**: 429-42.

Amirsadeghi S, Robson CA, McDonald AE, Vanlerberghe GC. 2006. Changes in plant mitochondrial electron transport alter cellular levels of reactive oxygen species and susceptibility to cell death signaling molecules. *Plant Cell Physiol*, **47**: 1509-19.

Amirsadeghi S, Robson CA, Vanlerberghe GC. 2007. The role of the mitochondrion in plant responses to biotic stress. *Physiol Plant*, **129**: 253-266.

Andronis EA, Moschou PN, Toumi I, Roubelakis-Angelakis KA. 2014. Peroxisomal polyamine oxidase and NADPH-oxidase cross-talk for ROS homeostasis which affects respiration rate in *Arabidopsis thaliana*. *Front Plant Sci,* **5**: 132.

Andronis EA, Roubelakis-Angelakis KA. 2010. Short-term salinity stress in tobacco plants leads to the onset of animal-like PCD hallmarks in planta in contrast to long-term stress. *Planta,* **231**: 437-448.

Apel K, Hirt H. 2004. Reactive oxygen species: metabolism, oxidative stress, and signal transduction. *Annu Rev Plant Biol,* **55**: 373-99.

Araújo WL, Nunes-Nesi A, Fernie AR. 2014. On the role of plant mitochondrial metabolism and its impact on photosynthesis in both optimal and sub-optimal growth conditions. *Photosynth Res,* **119**: 141-156.

Araújo WL, Nunes-Nesi A, Nikoloski Z, Sweetlove LJ, Fernie AR. 2012. Metabolic control and regulation of the tricarboxylic acid cycle in photosynthetic and heterotrophic plant tissues. *Plant Cell Environ,* **35**: 1-21.

Armstrong AF, Badger MR, Day DA, Barthet MM, Smith P, Millar AH, Whelan J, Atkin OK. 2008. Dynamic changes in the mitochondrial electron transport chain underpinning cold acclimation of leaf respiration. *Plant Cell Environ,* **31**: 1156-1169.

Arnholdt-Schmitt B, Costa JH, de Melo DF. 2006. AOX–a functional marker for efficient cell reprogramming under stress? *Trends Plant Sci,* **11**: 281-287.

Asada K. 1999. The water-water cycle in chloroplasts: scavenging of active oxygens and dissipation of excess photons. *Annu Rev Plant Biol,* **50**: 601-639.

Asada K. 2000. The water–water cycle as alternative photon and electron sinks. *Philosophical Transactions of the Royal Society B: Biological Sciences,* **355**: 1419-1431.

Asada K. 2006. Production and scavenging of reactive oxygen species in chloroplasts and their functions. *Plant Physiol,* **141**: 391-6.

Asada K, Kiso K, Yoshikawa K. 1974. Univalent reduction of molecular oxygen by spinach chloroplasts on illumination. *J Biol Chem,* **249**: 2175-2181.

Atkin OK, Macherel D. 2009. The crucial role of plant mitochondria in orchestrating drought tolerance. *Ann Bot,* **103**: 581-597.

Ayer A, Gourlay CW, Dawes IW. 2014. Cellular redox homeostasis, reactive oxygen species and replicative ageing in *Saccharomyces cerevisiae*. *FEMS Yeast Res,* **14**: 60-72.

Bagard M, Le Thiec D, Delacote E, Hasenfratz-Sauder MP, Banvoy J, Gérard J, Dizengremel P, Jolivet Y. 2008. Ozone-induced changes in photosynthesis and photorespiration of hybrid poplar in relation to the developmental stage of the leaves. *Physiol Plant,* **134**: 559-574.

Bailleul B, Berne N, Murik O, Petroutsos D, Prihoda J, Tanaka A, Villanova V, Bligny R, Flori S, Falconet D. 2015. Energetic coupling between plastids and mitochondria drives CO_2 assimilation in diatoms. *Nature,* **524**: 366-369.

Barros MH, Bandy B, Tahara EB, Kowaltowski AJ. 2004. Higher respiratory activity decreases mitochondrial reactive oxygen release and increases life span in *Saccharomyces cerevisiae*. *J Biol Chem,* **279**: 49883-8.

Barros MH, Netto LE, Kowaltowski AJ. 2003. H_2O_2 generation in *Saccharomyces cerevisiae* respiratory pet mutants: effect of cytochrome c. *Free Rad Biol Med,* **35**: 179-188.

Bartoli CG, Gomez F, Gergoff G, Guiamét JJ, Puntarulo S. 2005. Up-regulation of the mitochondrial alternative oxidase pathway enhances photosynthetic electron transport under drought conditions. *J Exp Bot,* **56**: 1269-1276.

Bartoli CG, Pastori GM, Foyer CH. 2000. Ascorbate biosynthesis in mitochondria is linked to the electron transport chain between complexes III and IV. *Plant Physiol,* **123**: 335-344.

Bartoli CG, Yu J, Gómez F, Fernández L, McIntosh L, Foyer CH. 2006. Inter-relationships between light and respiration in the control of ascorbic acid synthesis and accumulation in *Arabidopsis thaliana* leaves. *J Exp Bot,* **57**: 1621-1631.

Bennett MD, Leitch IJ, Price HJ, Johnston JS. 2003. Comparisons with *Caenorhabditis* (~100 Mb) and Drosophila (~175 Mb) using flow cytometry show genome size in *Arabidopsis* to be~157 Mb and thus~25% larger than the *Arabidopsis* genome initiative estimate of~125 Mb. *Ann Bot,* **91**: 547-557.

Berthold DA, Stenmark P. 2003. Membrane-bound diiron carboxylate proteins. *Annu Rev Plant Biol,* **54**: 497-517.

Berthold DA, Voevodskaya N, Stenmark P, Gräslund A, Nordlund P. 2002. EPR Studies of the mitochondrial alternative oxidase: evidence for a diiron carboxylate center. *J Biol Chem,* **277**: 43608-43614.

Betzelberger AM, Yendrek CR, Sun J, Leisner CP, Nelson RL, Ort DR, Ainsworth EA. 2012. Ozone exposure response for US soybean cultivars: linear reductions in photosynthetic potential, biomass, and yield. *Plant Physiol,* **160**: 1827-1839.

Botstein D, Chervitz SA, Cherry JM. 1997. Yeast as a model organism. *Science,* **277**: 1259-1260.

Brown S, Tuffery R. 2010. Induction of alternative oxidase activity in *Candida albicans* by oxidising conditions. *Int J Biol Life Sci,* **6**: 26-30.

Campbell C, Atkinson L, Zaragoza-Castells J, Lundmark M, Atkin O, Hurry V. 2007. Acclimation of photosynthesis and respiration is asynchronous in response to changes in temperature regardless of plant functional group. *New Phytol,* **176**: 375-389.

Carmona-Gutierrez D, Eisenberg T, Buttner S, Meisinger C, Kroemer G, Madeo F. 2010. Apoptosis in yeast: triggers, pathways, subroutines. *Cell Death Differ,* **17**: 763-73.

Carol P, Kuntz M. 2001. A plastid terminal oxidase comes to light: implications for carotenoid biosynthesis and chlororespiration. *Trends Plant Sci,* **6**: 31-36.

Castro-Guerrero NA, Rodríguez-Zavala JS, Marín-Hernández A, Rodríguez-Enríquez S, Moreno-Sánchez R. 2008. Enhanced alternative oxidase and antioxidant enzymes under Cd^{2+} stress in Euglena. *J Bioenerg Biomembr,* **40**: 227-235.

Chai T-T, Simmonds D, Day DA, Colmer TD, Finnegan PM. 2010. Photosynthetic performance and fertility are repressed in *GmAOX2b* antisense soybean. *Plant Physiol,* **152**: 1638-1649.

Chaudhuri M, Hill GC. 1996. Cloning, sequencing, and functional activity of the *Trypanosoma brucei brucei* alternative oxidase. *Mol Biochem Parasitol,* **83**: 125-9.

Chivasa S, Murphy AM, Naylor M, Carr JP. 1997. Salicylic acid interferes with tobacco mosaic virus replication via a novel salicylhydroxamic acid-sensitive mechanism. *Plant Cell,* **9**: 547-557.

Choudhury S, Panda P, Sahoo L, Panda SK. 2013. Reactive oxygen species signaling in plants under abiotic stress. *Plant Signal Behav,* **8**: e23681.

Clifton R, Millar AH, Whelan J. 2006. Alternative oxidases in *Arabidopsis*: a comparative analysis of differential expression in the gene family provides new insights into function of non-phosphorylating bypasses. *Biochim Biophys Acta,* **1757**: 730-41.

Coleman HD, Ellis DD, Gilbert M, Mansfield SD. 2006. Up-regulation of sucrose synthase and UDP-glucose pyrophosphorylase impacts plant growth and metabolism. *Plant Biotech J,* **4**: 87-101.

Considine MJ, Daley DO, Whelan J. 2001. The expression of alternative oxidase and uncoupling protein during fruit ripening in mango. *Plant Physiol,* **126**: 1619-1629.

Costa JH, Jolivet Y, Hasenfratz-Sauder M-P, Orellano EG, Lima MdGS, Dizengremel P, de Melo DF. 2007. Alternative oxidase regulation in roots of *Vigna unguiculata* cultivars differing in drought/salt tolerance. *J Plant Physiol,* **164**: 718-727.

Cuypers A, Plusquin M, Remans T, Jozefczak M, Keunen E, Gielen H, Opdenakker K, Nair AR, Munters E, Artois TJ. 2010. Cadmium stress: an oxidative challenge. *Biometals,* **23**: 927-940.

Cvetkovska M, Dahal K, Alber NA, Jin C, Cheung M, Vanlerberghe GC. 2014. Knockdown of mitochondrial alternative oxidase induces the 'stress state' of signaling molecule pools in *Nicotiana tabacum*, with implications for stomatal function. *New Phytol,* **203**: 449-61.

Cvetkovska M, Vanlerberghe GC. 2012. Coordination of a mitochondrial superoxide burst during the hypersensitive response to bacterial pathogen in *Nicotiana tabacum*. *Plant Cell Environ,* **35**: 1121-36.

Cvetkovska M, Vanlerberghe GC. 2013. Alternative oxidase impacts the plant response to biotic stress by influencing the mitochondrial generation of reactive oxygen species. *Plant Cell Environ,* **36**: 721-732.

Dahal K, Martyn GD, Vanlerberghe GC. 2015. Improved photosynthetic performance during severe drought in *Nicotiana tabacum* overexpressing a nonenergy conserving respiratory electron sink. *New Phytol,* **208**: 382-395.

Dahal K, Wang J, Martyn GD, Rahimy F, Vanlerberghe GC. 2014. Mitochondrial alternative oxidase maintains respiration and preserves photosynthetic capacity during moderate drought in *Nicotiana tabacum*. *Plant Physiol,* **166**: 1560-1574.

Dalal A, Vishwakarma A, Singh NK, Gudla T, Bhattacharyya MK, Padmasree K, Viehhauser A, Dietz KJ, Kirti PB. 2014. Attenuation of hydrogen peroxide-mediated oxidative stress by *Brassica juncea* annexin-3 counteracts thiol-specific antioxidant (TSA1) deficiency in *Saccharomyces cerevisiae*. *FEBS Lett,* **588**: 584-93.

Dassa EP, Dufour E, Goncalves S, Jacobs HT, Rustin P. 2009. The alternative oxidase, a tool for compensating cytochrome c oxidase deficiency in human cells. *Physiol Plant,* **137**: 427-434.

Delledonne M. 2005. NO news is good news for plants. *Curr Opin Plant Biol,* **8**: 390-396.

Del Rio AL. 2015. ROS and RNS in plant physiology: an overview. *J Exp Bot*, **66**: 2827-2837.

Demmig-Adams B, Adams WW. 1996. The role of xanthophyll cycle carotenoids in the protection of photosynthesis. *Trends Plant Sci*, **1**: 21-26.

Demmig-Adams B, Adams WW, Heber U, Neimanis S, Winter K, Krüger A, Czygan F-C, Bilger W, Björkman O. 1990. Inhibition of zeaxanthin formation and of rapid changes in radiationless energy dissipation by dithiothreitol in spinach leaves and chloroplasts. *Plant Physiol,* **92**: 293-301.

Demmig B, Winter K, Krüger A, Czygan F-C. 1987. Photoinhibition and zeaxanthin formation in intact leaves a possible role of the xanthophyll cycle in the dissipation of excess light energy. *Plant Physiol,* **84**: 218-224.

Dinakar C, Abhaypratap V, Yearla SR, Raghavendra AS, Padmasree K. 2010a. Importance of ROS and antioxidant system during the beneficial interactions of mitochondrial metabolism with photosynthetic carbon assimilation. *Planta,* **231**: 461-74.

Dinakar C, Raghavendra AS, Padmasree K. 2010b. Importance of AOX pathway in optimizing photosynthesis under high light stress: role of pyruvate and malate in activating AOX. *Physiol Plant,* **139**: 13-26.

Dizengremel P. 2001. Effects of ozone on the carbon metabolism of forest trees. *Plant Physiol Biochem,* **39**: 729-742.

Dizengremel P, Le Thiec D, Bagard M, Jolivet Y. 2008. Ozone risk assessment for plants: central role of metabolism-dependent changes in reducing power. *Environ Pollut,* **156**: 11-15.

Djajanegara I, Finnegan PM, Mathieu C, McCabe T, Whelan J, Day DA. 2002. Regulation of alternative oxidase gene expression in soybean. *Plant Mol Biol,* **50**: 735-742.

Dutilleul C, Garmier M, Noctor G, Mathieu C, Chétrit P, Foyer CH, De Paepe R. 2003. Leaf mitochondria modulate whole cell redox homeostasis, set antioxidant capacity, and determine stress resistance through altered signaling and diurnal regulation. *Plant Cell,* **15**: 1212-1226.

Ederli L, Morettini R, Borgogni A, Wasternack C, Miersch O, Reale L, Ferranti F, Tosti N, Pasqualini S. 2006. Interaction between nitric oxide and ethylene in the induction of alternative oxidase in ozone-treated tobacco plants. *Plant Physiol,* **142**: 595-608.

El-Khoury R, Dufour E, Rak M, Ramanantsoa N, Grandchamp N, Csaba Z, Duvillié B, Bénit P, Gallego J, Gressens P. 2013. Alternative oxidase expression

in the mouse enables bypassing cytochrome c oxidase blockade and limits mitochondrial ROS overproduction. *PLoS Genet,* **9**: e1003182.

El-Khoury R, Kemppainen KK, Dufour E, Szibor M, Jacobs HT, Rustin P. 2014. Engineering the alternative oxidase gene to better understand and counteract mitochondrial defects: state of the art and perspectives. *Br J Pharmacol,* **171**: 2243-2249.

Endo T, Shikanai T, Sato F, Asada K. 1998. NAD(P)H dehydrogenase-dependent, antimycin A-sensitive electron donation to plastoquinone in tobacco chloroplasts. *Plant Cell Physiol,* **39**: 1226-1231.

Farrugia G, Balzan R. 2012. Oxidative stress and programmed cell death in yeast. *Front Oncol,* **2**: 64.

Feng H, Wang Y, Li H, Wang R, Sun K, Jia L. 2010. Salt stress-induced expression of rice AOX1a is mediated through an accumulation of hydrogen peroxide. *Biologia,* **65**: 868-873.

Fernie AR, Carrari F, Sweetlove LJ. 2004. Respiratory metabolism: glycolysis, the TCA cycle and mitochondrial electron transport. *Curr Opin Plant Biol,* **7**: 254-261.

Figueroa P, Léon G, Elorza A, Holuigue L, Araya A, Jordana X. 2002. The four subunits of mitochondrial respiratory complex II are encoded by multiple nuclear genes and targeted to mitochondria in *Arabidopsis thaliana*. *Plant Mol Biol,* **50**: 725-734.

Finkel T. 2003. Oxidant signals and oxidative stress. *Curr Opin Cell Biol,* **15**: 247-54.

Fiorani F, Umbach AL, Siedow JN. 2005. The alternative oxidase of plant mitochondria is involved in the acclimation of shoot growth at low temperature. A study of *Arabidopsis* AOX1a transgenic plants. *Plant Physiol,* **139**: 1795-1805.

Flexas J, Bota J, Galmes J, Medrano H, Ribas-Carbó M. 2006. Keeping a positive carbon balance under adverse conditions: responses of photosynthesis and respiration to water stress. *Physiol Plant,* **127**: 343-352.

Florez-Sarasa I, Flexas J, Rasmusson AG, Umbach AL, Siedow JN, Ribas-Carbo M. 2011. In vivo cytochrome and alternative pathway respiration in leaves of *Arabidopsis thaliana* plants with altered alternative oxidase under different light conditions. *Plant Cell Environ,* **34**: 1373-1383.

Foyer C, Rowell J, Walker D. 1983. Measurement of the ascorbate content of spinach leaf protoplasts and chloroplasts during illumination. *Planta,* **157**: 239-44.

Foyer CH, Noctor G. 2005. Redox homeostasis and antioxidant signaling: a metabolic interface between stress perception and physiological responses. *Plant Cell,* **17**: 1866-75.

Foyer CH, Noctor G. 2011. Ascorbate and glutathione: the heart of the redox hub. *Plant Physiol,* **155**: 2-18.

Fu A, Liu H, Yu F, Kambakam S, Luan S, Rodermel S. 2012. Alternative oxidases (AOX1a and AOX2) can functionally substitute for plastid terminal oxidase in *Arabidopsis* chloroplasts. *Plant Cell,* **24**: 1579-1595.

Gandin A, Denysyuk M, Cousins AB. 2014a. Disruption of the mitochondrial alternative oxidase (AOX) and uncoupling protein (UCP) alters rates of foliar nitrate and carbon assimilation in *Arabidopsis thaliana*. *J Exp Bot,* **65**: 3133-3142.

Gandin A, Duffes C, Day DA, Cousins AB. 2012. The absence of alternative oxidase AOX1A results in altered response of photosynthetic carbon assimilation to increasing CO_2 in *Arabidopsis thaliana*. *Plant Cell Physiol,* **53**: 1627-37.

Gandin A, Koteyeva NK, Voznesenskaya EV, Edwards GE, Cousins AB. 2014b. The acclimation of photosynthesis and respiration to temperature in the C_3–C_4 intermediate *Salsola divaricata*: induction of high respiratory CO_2 release under low temperature. *Plant Cell Environ,* **37**: 2601-2612.

Garcia-Brugger A, Lamotte O, Vandelle E, Bourque S, Lecourieux D, Poinssot B, Wendehenne D, Pugin A. 2006. Early signaling events induced by elicitors of plant defenses. *Mol Plant-Microbe Interact,* **19**: 711-724.

García I, Rosas T, Bejarano ER, Gotor C, Romero LC. 2013. Transient transcriptional regulation of the CYS-C1 gene and cyanide accumulation upon pathogen infection in the plant immune response. *Plant Physiol,* **162**: 2015-2027.

Garmash EV, Grabelnych OI, Velegzhaninov IO, Borovik OA, Dalke IV, Voinikov VK, Golovko TK. 2015. Light regulation of mitochondrial alternative oxidase pathway during greening of etiolated wheat seedlings. *J Plant Physiol,* **174**: 75-84.

Gelhaye E, Rouhier N, Gérard J, Jolivet Y, Gualberto J, Navrot N, Ohlsson P-I, Wingsle G, Hirasawa M, Knaff DB. 2004. A specific form of thioredoxin h occurs in plant mitochondria and regulates the alternative oxidase. *Proc Natl Acad Sci U S A,* **101**: 14545-14550.

Gill SS, Anjum NA, Hasanuzzaman M, Gill R, Trivedi DK, Ahmad I, Pereira E, Tuteja N. 2013. Glutathione and glutathione reductase: a boon in disguise for plant abiotic stress defense operations. *Plant Physiol Biochem,* **70**: 204-12.

Gill SS, Tuteja N. 2010. Reactive oxygen species and antioxidant machinery in abiotic stress tolerance in crop plants. *Plant Physiol Biochem,* **48**: 909-30.

Gilmore AM, Yamamoto HY. 1991. Zeaxanthin formation and energy-dependent fluorescence quenching in pea chloroplasts under artificially mediated linear and cyclic electron transport. *Plant Physiol,* **96**: 635-643.

Giraud E, Ho LH, Clifton R, Carroll A, Estavillo G, Tan YF, Howell KA, Ivanova A, Pogson BJ, Millar AH, Whelan J. 2008. The absence of alternative oxidase1a in *Arabidopsis* results in acute sensitivity to combined light and drought stress. *Plant Physiol,* **147**: 595-610.

Grabelnych O, Borovik O, Tauson E, Pobezhimova T, Katyshev A, Pavlovskaya N, Koroleva N, Lyubushkina I, Bashmakov VY, Popov V. 2014. Mitochondrial energy-dissipating systems (alternative oxidase, uncoupling proteins, and external NADH dehydrogenase) are involved in development of frost-resistance of winter wheat seedlings. *Biochem (Moscow),* **79**: 506-519.

Grabelnych O, Sumina O, Funderat S, Pobezhimova T, Voinikov V, Kolesnichenko A. 2004. The distribution of electron transport between the main cytochrome and alternative pathways in plant mitochondria during short-term cold stress and cold hardening. *J Thermal Biol,* **29**: 165-175.

Gupta Kapuganti J, Igamberdiev AU, Kaiser WM. 2010. New insights into the mitochondrial nitric oxide production pathways. *Plant Signal Behav,* **5**: 999-1001.

Gupta KJ, Fernie AR, Kaiser WM, van Dongen JT. 2011. On the origins of nitric oxide. *Trends Plant Sci,* **16**: 160-168.

Gupta KJ, Igamberdiev AU, Mur LA. 2012. NO and ROS homeostasis in mitochondria: a central role for alternative oxidase. *New Phytol,* **195**: 1-3.

Gupta KJ, Zabalza A, Van Dongen JT. 2009. Regulation of respiration when the oxygen availability changes. *Physiol Plant,* **137**: 383-391.

Guy RD, Berry JA, Fogel ML, Hoering TC. 1989. Differential fractionation of oxygen isotopes by cyanide-resistant and cyanide-sensitive respiration in plants. *Planta,* **177**: 483-491.

Hanqing F, Kun S, Mingquan L, Hongyu L, Xin L, Yan L, Yifeng W. 2010. The expression, function and regulation of mitochondrial alternative oxidase under biotic stresses. *Mol Plant Pathol,* **11**: 429-440.

Hara S, Motohashi K, Arisaka F, Romano PG, Hosoya-Matsuda N, Kikuchi N, Fusada N, Hisabori T. 2006. Thioredoxin-h1 reduces and reactivates the oxidized cytosolic malate dehydrogenase dimer in higher plants. *J Biol Chem,* **281**: 32065-32071.

Heath RL, Packer L. 1968. Photoperoxidation in isolated chloroplasts. I. Kinetics and stoichiometry of fatty acid peroxidation. *Arch Biochem Biophys*, **125**: 189-98.

Heazlewood JL, Howell KA, Millar AH. 2003. Mitochondrial complex I from *Arabidopsis* and rice: orthologs of mammalian and fungal components coupled with plant-specific subunits. *Biochim Biophys Act*, **1604**: 159-169.

Hebbelmann I, Selinski J, Wehmeyer C, Goss T, Voss I, Mulo P, Kangasjärvi S, Aro E-M, Oelze M-L, Dietz K-J, Nunes-Nesi A, Do PT, Fernie AR, Talla SK, Raghavendra AS, Linke V, Scheibe R. 2012. Multiple strategies to prevent oxidative stress in *Arabidopsis* plants lacking the malate valve enzyme NADP-malate dehydrogenase. *J Exp Bot*, **63**: 1445-1459.

Herrero E, Ros J, Bellí G, Cabiscol E. 2008. Redox control and oxidative stress in yeast cells. *Biochim Biophys Act*, **1780**: 1217-1235.

Hilal M, Zenoff AM, Ponessa G, Moreno H, Massa EM. 1998. Saline stress alters the temporal patterns of xylem differentiation and alternative oxidase expression in developing soybean roots. *Plant Physiol*, **117**: 695-701.

Hill R, Bendall F. 1960. Function of the two cytochrome components in chloroplasts: a working hypothesis. *Nature*, **186**: 136-137.

Ho LH, Giraud E, Lister R, Thirkettle-Watts D, Low J, Clifton R, Howell KA, Carrie C, Donald T, Whelan J. 2007. Characterization of the regulatory and expression context of an alternative oxidase gene provides insights into cyanide-insensitive respiration during growth and development. *Plant Physiol*, **143**: 1519-1533.

Hoefnagel MH, Atkin OK, Wiskich JT. 1998. Interdependence between chloroplasts and mitochondria in the light and the dark. *Biochim Biophys Act*, **1366**: 235-255.

Honda Y, Hattori T, Kirimura K. 2012. Visual expression analysis of the responses of the alternative oxidase gene (*aox1*) to heat shock, oxidative, and osmotic stresses in conidia of citric acid-producing *Aspergillus niger*. *J Biosci Bioeng*, **113**: 338-42.

Igamberdiev AU, Ratcliffe RG, Gupta KJ. 2014. Plant mitochondria: Source and target for nitric oxide. *Mitochondrion*, **19**: 329-33.

Jahns P, Holzwarth AR. 2012. The role of the xanthophyll cycle and of lutein in photoprotection of photosystem II. *Biochim Biophys Act*, **1817**: 182-193.

Jang HH, Lee KO, Chi YH, Jung BG, Park SK, Park JH, Lee JR, Lee SS, Moon JC, Yun JW, Choi YO, Kim WY, Kang JS, Cheong GW, Yun DJ, Rhee SG, Cho MJ, Lee SY. 2004. Two enzymes in one; two yeast peroxiredoxins display

oxidative stress-dependent switching from a peroxidase to a molecular chaperone function. *Cell,* **117**: 625-35.

Joët T, Genty B, Josse E-M, Kuntz M, Cournac L, Peltier G. 2002. Involvement of a plastid terminal oxidase in plastoquinone oxidation as evidenced by expression of the *Arabidopsis thaliana* enzyme in tobacco. *J Biol Chem,* **277**: 31623-31630.

Johnson CH, Prigge JT, Warren AD, McEwen JE. 2003. Characterization of an alternative oxidase activity of *Histoplasma capsulatum*. *Yeast,* **20**: 381-388.

Joliot P, Joliot A. 2002. Cyclic electron transfer in plant leaf. *Proc Natl Acad Sci U S A,* **99**: 10209-10214.

Joseph-Horne T, Babij J, Wood PM, Hollomon D, Sessions RB. 2000. New sequence data enable modelling of the fungal alternative oxidase and explain an absence of regulation by pyruvate. *FEBS Lett,* **481**: 141-146.

Juszczuk IM, Flexas J, Szal B, Dąbrowska Z, Ribas-Carbo M, Rychter AM. 2007. Effect of mitochondrial genome rearrangement on respiratory activity, photosynthesis, photorespiration and energy status of MSC16 cucumber (*Cucumis sativus*) mutant. *Physiol Plant,* **131**: 527-541.

Keunen E, Jozefczak M, Remans T, Vangronsveld J, Cuypers A. 2013. Alternative respiration as a primary defence during cadmium-induced mitochondrial oxidative challenge in *Arabidopsis thaliana*. *Environ Exp Bot,* **91**: 63-73.

Keunen E, Schellingen K, Van Der Straeten D, Remans T, Colpaert J, Vangronsveld J, Cuypers A. 2015. Alternative oxidase1a modulates the oxidative challenge during moderate Cd exposure in *Arabidopsis thaliana* leaves. *J Exp Bot,* **66**: 2967-2977.

Kiba A, Lee K-Y, Ohnishi K, Hikichi Y. 2008. Comparative expression analysis of genes induced during development of bacterial rot and induction of hypersensitive cell death in lettuce. *J Plant Physiol,* **165**: 1757-1773.

Kirimura K, Yoda M, Usami S. 1999. Cloning and expression of the cDNA encoding an alternative oxidase gene from *Aspergillus niger* WU-2223L. *Curr Genet,* **34**: 472-7.

Klughammer C, Schreiber U. 2008. Saturation pulse method for assessment of energy conversion in PSI. *PAM Appl Notes,* **1**: 11-14.

Klodmann J, Sunderhaus S, Nimtz M, Jänsch L, Braun H-P. 2010. Internal architecture of mitochondrial complex I from *Arabidopsis thaliana*. *Plant Cell,* **22**: 797-810.

Koornneef A, Pieterse CM. 2008. Cross talk in defense signaling. *Plant Physiol,* **146**: 839-844.

Koornneef M, Meinke D. 2010. The development of *Arabidopsis* as a model plant. *Plant J,* **61**: 909-921.

Kornfeld A, Horton TW, Yakir D, Searle SY, Griffin KL, Atkin OK, Subke JA, Turnbull MH. 2012. A field-compatible method for measuring alternative respiratory pathway activities in vivo using stable O_2 isotopes. *Plant Cell Environ,* **35**: 1518-1532.

Kowaltowski AJ, de Souza-Pinto NC, Castilho RF, Vercesi AE. 2009. Mitochondria and reactive oxygen species. *Free Radic Biol Med,* **47**: 333-43.

Kramer DM, Evans JR. 2011. The importance of energy balance in improving photosynthetic productivity. *Plant Physiol,* **155**: 70-78.

Kramer DM, Johnson G, Kiirats O, Edwards GE. 2004. New fluorescence parameters for the determination of Q_A redox state and excitation energy fluxes. *Photosynth Res,* **79**: 209-218.

Krause M, Durner J. 2004. Harpin inactivates mitochondria in *Arabidopsis* suspension cells. *Mol Plant-Microbe Interact,* **17**: 131-139.

Kreps JA, Wu Y, Chang H-S, Zhu T, Wang X, Harper JF. 2002. Transcriptome changes for *Arabidopsis* in response to salt, osmotic, and cold stress. *Plant Physiol,* **130**: 2129-2141.

Krieger-Liszkay A, Fufezan C, Trebst A. 2008. Singlet oxygen production in photosystem II and related protection mechanism. *Photosynth Res,* **98**: 551-564.

Krömer S. 1995. Respiration during photosynthesis. *Annu Rev Plant Biol,* **46**: 45-70.

Krömer S, Malmberg G, Gardestrom P. 1993. Mitochondrial Contribution to Photosynthetic Metabolism: A Study with Barley (*Hordeum vulgare* L.) Leaf Protoplasts at Different Light Intensities and CO_2 Concentrations. *Plant Physiol,* **102**: 947-955.

Kumar AM, Soll D. 1992. Arabidopsis alternative oxidase sustains *Escherichia coli* respiration. *Proc Natl Acad Sci U S A,* **89**: 10842-6.

Künstler A, Hafez Y, Király L. 2007. Transient suppression of a catalase and an alternative oxidase gene during virus-induced local lesion formation (hypersensitive response) is independent of the extent of leaf necrotization. *Acta Phytopathol Entomol Hung,* **42**: 185-196.

Lacomme C, Roby D. 1999. Identification of new early markers of the hypersensitive response in *Arabidopsis thaliana*. *FEBS Lett,* **459**: 149-153.

Laemmli UK. 1970. Cleavage of structural proteins during the assembly of the head of bacteriophage T4. *Nature,* **227**: 680-685.

Lambers H. 1982. Cyanide-resistant respiration: a non-phosphorylating electron transport pathway acting as an energy overflow. *Physiol. Plant,* **55**: 478-485.

Laskar S, Bhattacharyya MK, Shankar R, Bhattacharyya S. 2011. *HSP90* controls *SIR2* mediated gene silencing. *PLoS One,* **6**: e23406.

Lawlor DW, Tezara W. 2009. Causes of decreased photosynthetic rate and metabolic capacity in water-deficient leaf cells: a critical evaluation of mechanisms and integration of processes. *Ann Bot,* **103**: 561-579.

Lee W-S, Fu S-F, Verchot-Lubicz J, Carr JP. 2011. Genetic modification of alternative respiration in Nicotiana benthamiana affects basal and salicylic acid-induced resistance to potato virus X. *BMC Plant Biol,* **11**: 41.

Lei T, Feng H, Sun X, Dai Q-L, Zhang F, Liang H-G, Lin H-H. 2010. The alternative pathway in cucumber seedlings under low temperature stress was enhanced by salicylic acid. *Plant Growth Regul,* **60**: 35-42.

León G, Holuigue L, Jordana X. 2007. Mitochondrial complex II is essential for gametophyte development in *Arabidopsis*. *Plant Physiol,* **143**: 1534-1546.

Li C, Liang D, Xu R, Li H, Zhang Y, Qin R, Li L, Wei P, Yang J. 2013a. Overexpression of an alternative oxidase gene, *OsAOX1a*, improves cold tolerance in *Oryza sativa* L. *Genet Mol Res,* **12**: 5424-5432.

Li CR, Liang DD, Li J, Duan YB, Li H, Yang YC, Qin RY, Li L, Wei PC, Yang JB. 2013b. Unravelling mitochondrial retrograde regulation in the abiotic stress induction of rice *alternative oxidase 1* genes. *Plant Cell Environ,* **36**: 775-788.

Li X-P, BjoÈrkman O, Shih C, Grossman AR, Rosenquist M, Jansson S, Niyogi KK. 2000. A pigment-binding protein essential for regulation of photosynthetic light harvesting. *Nature,* **403**: 391-395.

Li Y, Zhu L, Xu B, Yang J, Zhang M. 2012. Identification of down-regulated genes modulated by an alternative oxidase pathway under cold stress conditions in watermelon plants. *Plant Mol Biol Report,* **30**: 214-224.

Li Z, Xing D. 2011. Mechanistic study of mitochondria-dependent programmed cell death induced by aluminium phytotoxicity using fluorescence techniques. *J Exp Bot,* **62**: 331-343.

Lin S-J, Ford E, Haigis M, Liszt G, Guarente L. 2004. Calorie restriction extends yeast life span by lowering the level of NADH. *Genes Dev,* **18**: 12-16.

Lin S-J, Kaeberlein M, Andalis AA, Sturtz LA, Defossez P-A, Culotta VC, Fink GR, Guarente L. 2002. Calorie restriction extends *Saccharomyces cerevisiae* lifespan by increasing respiration. *Nature,* **418**: 344-348.

Liu J, Li Z, Wang Y, Xing D. 2014. Overexpression of alternative oxidase1a alleviates mitochondria-dependent programmed cell death induced by aluminium phytotoxicity in *Arabidopsis*. *J Exp Bot,* **65**: 4465-78.

Livak KJ, Schmittgen TD. 2001. Analysis of relative gene expression data using real-time quantitative PCR and the $2^{-\Delta\Delta CT}$ Method. *Methods,* **25**: 402-8.

Lokstein H, Tian L, Polle JE, DellaPenna D. 2002. Xanthophyll biosynthetic mutants of *Arabidopsis thaliana*: altered nonphotochemical quenching of chlorophyll fluorescence is due to changes in photosystem II antenna size and stability. *Biochim Biophys Act,* **1553**: 309-319.

Magnani T, Soriani FM, Martins VP, Nascimento AM, Tudella VG, Curti C, Uyemura SA. 2007. Cloning and functional expression of the mitochondrial alternative oxidase of *Aspergillus fumigatus* and its induction by oxidative stress. *FEMS Microbiol Lett,* **271**: 230-8.

Makino A, Miyake C, Yokota A. 2002. Physiological functions of the water–water cycle (Mehler reaction) and the cyclic electron flow around PSI in rice leaves. *Plant Cell Physio,* **43**: 1017-1026.

Martí MC, Florez-Sarasa I, Camejo D, Ribas-Carbó M, Lázaro JJ, Sevilla F, Jiménez A. 2011. Response of mitochondrial thioredoxin PsTrxo1, antioxidant enzymes, and respiration to salinity in pea (*Pisum sativum* L.) leaves. *J Exp Bot,* **62**: 3863-3874.

Martins VP, Dinamarco TM, Soriani FM, Tudella VG, Oliveira SC, Goldman GH, Curti C, Uyemura SA. 2011. Involvement of an alternative oxidase in oxidative stress and mycelium-to-yeast differentiation in *Paracoccidioides brasiliensis*. *Eukaryot Cell,* **10**: 237-48.

Mathy G, Navet R, Gerkens P, Leprince P, De Pauw E, Sluse-Goffart CM, Sluse FE, Douette P. 2006. Saccharomyces c erevisiae Mitoproteome Plasticity in Response to Recombinant Alternative Ubiquinol Oxidase. *J Prot Res,* 5: 339-348.

Matsukawa K, Kamata T, Ito K. 2009. Functional expression of plant alternative oxidase decreases antimycin A-induced reactive oxygen species production in human cells. *FEBS Lett,* **583**: 148-152.

Maxwell DP, Wang Y, McIntosh L. 1999. The alternative oxidase lowers mitochondrial reactive oxygen production in plant cells. *Proc Natl Acad Sci U S A,* **96**: 8271-6.

McDonald AE, Ivanov AG, Bode R, Maxwell DP, Rodermel SR, Hüner NP. 2011. Flexibility in photosynthetic electron transport: the physiological role of plastoquinol terminal oxidase (PTOX). *Biochim Biophys Act,* **1807**: 954-967.

McDonald AE, Sieger SM, Vanlerberghe GC. 2002. Methods and approaches to study plant mitochondrial alternative oxidase. *Physiol Plant,* **116**: 135-143.

McDonald AE, Vanlerberghe GC, Staples JF. 2009. Alternative oxidase in animals: unique characteristics and taxonomic distribution. *J Exp Biol,* **212**: 2627-34.

Meeuse BJ. 1975. Thermogenic respiration in aroids. *Annu Rev Plant Physiol,* **26**: 117-126.

Mehler AH. 1951. Studies on reactions of illuminated chloroplasts: I. Mechanism of the reduction of oxygen and other hill reagents. *Arch Biochem Biophys,* **33**: 65-77.

Meinke DW, Cherry JM, Dean C, Rounsley SD, Koornneef M. 1998. *Arabidopsis thaliana*: a model plant for genome analysis. *Science,* **282**: 662-682.

Meyer EH, Taylor NL, Millar AH. 2008. Resolving and identifying protein components of plant mitochondrial respiratory complexes using three dimensions of gel electrophoresis. *J Proteome Res,* **7**: 786-794.

Mhadhbi H, Fotopoulos V, Mylona PV, Jebara M, Aouani ME, Polidoros AN. 2013. Alternative oxidase 1 (*Aox1*) gene expression in roots of *Medicago truncatula* is a genotype-specific component of salt stress tolerance. *J Plant Physiol,* **170**: 111-114.

Millar AH, Eubel H, Jänsch L, Kruft V, Heazlewood JL, Braun H-P. 2004. Mitochondrial cytochrome c oxidase and succinate dehydrogenase complexes contain plant specific subunits. *Plant Mol Biol,* **56**: 77-90.

Millar AH, Whelan J, Soole KL, Day DA. 2011. Organization and regulation of mitochondrial respiration in plants. *Annu Rev Plant Biol,* **62**: 79-104.

Millenaar F, Lambers H. 2003. The alternative oxidase: in vivo regulation and function. *Plant Biol,* **5**: 2-15.

Miller RE, Grant NM, Giles L, Ribas-Carbo M, Berry JA, Watling JR, Robinson SA. 2011. In the heat of the night--alternative pathway respiration drives thermogenesis in *Philodendron bipinnatifidum*. *New Phytol,* **189**: 1013-26.

Minagawa N, Yoshimoto A. 1987. The induction of cyanide-resistant respiration in *Hansenula anomala*. *J Biochem,* **101**: 1141-6.

Mittler R. 2002. Oxidative stress, antioxidants and stress tolerance. *Trends Plant Sci,* **7**: 405-10.

Mittova V, Guy M, Tal M, Volokita M. 2004. Salinity up-regulates the antioxidative system in root mitochondria and peroxisomes of the wild salt-tolerant tomato species Lycopersicon pennellii. *J Exp Bot,* **55**: 1105-1113.

Mittova V, Tal M, Volokita M, Guy M. 2003. Up-regulation of the leaf mitochondrial and peroxisomal antioxidative systems in response to salt-induced oxidative stress in the wild salt-tolerant tomato species *Lycopersicon pennellii*. *Plant Cell Environ,* **26**: 845-856.

Miyake C. 2010. Alternative electron flows (water–water cycle and cyclic electron flow around PSI) in photosynthesis: molecular mechanisms and physiological functions. *Plant Cell Physiol*, **51**: 1951-1963.

Moller IM. 2001. Plant mitochondria and oxidative stress: Electron Transport, NADPH Turnover, and Metabolism of Reactive Oxygen Species. *Annu Rev Plant Physiol Plant Mol Biol,* **52**: 561-591.

Møller IM, Bérczi A, Plas LH, Lambers H. 1988. Measurement of the activity and capacity of the alternative pathway in intact plant tissues: identification of problems and possible solutions. *Physiol Plant,* **72**: 642-649.

Moore AL, Albury MS. 2008. Further insights into the structure of the alternative oxidase: from plants to parasites. *Biochem Soc Trans,* **36**: 1022-1026.

Moore AL, Carré JE, Affourtit C, Albury MS, Crichton PG, Kita K, Heathcote P. 2008. Compelling EPR evidence that the alternative oxidase is a diiron carboxylate protein. *Biochim Biophys Act,* **1777**: 327-330.

Moore AL, Shiba T, Young L, Harada S, Kita K, Ito K. 2013. Unraveling the heater: new insights into the structure of the alternative oxidase. *Annu Rev Plant Biol,* **64**: 637-663.

Moore AL, Siedow JN. 1991. The regulation and nature of the cyanide-resistant alternative oxidase of plant mitochondria. *Biochim Biophys Act,* **1059**: 121-140.

Moore AL, Umbach AL, Siedow JN. 1995. Structure-function relationships of the alternative oxidase of plant mitochondria: a model of the active site. *J Bioenerg Biomembr,* **27**: 367-377.

Müller P, Li X-P, Niyogi KK. 2001. Non-photochemical quenching. A response to excess light energy. *Plant Physiol,* **125**: 1558-1566.

Munekage Y, Hashimoto M, Miyake C, Tomizawa K, Endo T, Tasaka M, Shikanai T. 2004. Cyclic electron flow around photosystem I is essential for photosynthesis. *Nature,* **429**: 579-82.

Munekage Y, Hojo M, Meurer J, Endo T, Tasaka M, Shikanai T. 2002. PGR5 is involved in cyclic electron flow around photosystem I and is essential for photoprotection in *Arabidopsis*. *Cell,* **110**: 361-371.

Munekage YN, Genty B, Peltier G. 2008. Effect of PGR5 impairment on photosynthesis and growth in *Arabidopsis thaliana*. *Plant Cell Physiol,* **49**: 1688-1698.

Murakami Y, Toriyama K. 2008. Enhanced high temperature tolerance in transgenic rice seedlings with elevated levels of alternative oxidase, OsAOX1a. *Plant Biotech,* **25**: 361-364.

Murchie EH, Niyogi KK. 2011. Manipulation of photoprotection to improve plant photosynthesis. *Plant Physiol,* **155**: 86-92.

Murphy M. 2009. How mitochondria produce reactive oxygen species. *Biochem J,* **417**: 1-13.

Nagel OW, Waldron S, Jones HG. 2001. An off-line implementation of the stable isotope technique for measurements of alternative respiratory pathway activities. *Plant Physiol,* **127**: 1279-1286.

Nawrocki WJ, Tourasse NJ, Taly A, Rappaport F, Wollman F-A. 2015. The plastid terminal oxidase: its elusive function points to multiple contributions to plastid physiology. *Annu Rev Plant Biol,* **66**: 49-74.

Neimanis K, Staples JF, Hüner NP, McDonald AE. 2013. Identification, expression, and taxonomic distribution of alternative oxidases in non-angiosperm plants. *Gene,* **526**: 275-286.

Nelson N, Yocum CF. 2006. Structure and function of photosystems I and II. *Annu. Rev. Plant Biol,* **57**: 521-565.

Nishikawa Y, Yamamoto H, Okegawa Y, Wada S, Sato N, Taira Y, Sugimoto K, Makino A, Shikanai T. 2012. PGR5-dependent cyclic electron transport around PSI contributes to the redox homeostasis in chloroplasts rather than CO_2 fixation and biomass production in rice. *Plant Cell Physiol,* **53**: 2117-2126.

Niyogi KK. 2000. Safety valves for photosynthesis. *Curr Opin Plant Biol,* **3**: 455-460.

Noctor G. 2006. Metabolic signalling in defence and stress: the central roles of soluble redox couples. *Plant Cell Environ,* **29**: 409-25.

Noctor G, De Paepe R, Foyer CH. 2007. Mitochondrial redox biology and homeostasis in plants. *Trends Plant Sci,* **12**: 125-134.

Noctor G, Dutilleul C, De Paepe R, Foyer CH. 2004. Use of mitochondrial electron transport mutants to evaluate the effects of redox state on photosynthesis, stress tolerance and the integration of carbon/nitrogen metabolism. *J Exp Bot,* **55**: 49-57.

Noguchi K, Taylor NL, Millar AH, Lambers H, Day DA. 2005. Response of mitochondria to light intensity in the leaves of sun and shade species. *Plant Cell Environ,* **28**: 760-771.

Noguchi K, Yoshida K. 2008. Interaction between photosynthesis and respiration in illuminated leaves. *Mitochondrion,* **8**: 87-99.

Nunes-Nesi A, Fernie AR, Stitt M. 2010. Metabolic and signaling aspects underpinning the regulation of plant carbon nitrogen interactions. *Mol Plant,* **3**: 973-996.

Oakley CA, Hopkinson BM, Schmidt GW. 2014. Mitochondrial terminal alternative oxidase and its enhancement by thermal stress in the coral symbiont *Symbiodinium*. *Coral reefs,* **33**: 543-552.

Ogawa T. 1991. A gene homologous to the subunit-2 gene of NADH dehydrogenase is essential to inorganic carbon transport of *Synechocystis* PCC6803. *Proc Natl Acad Sci,* **88**: 4275-4279.

Oliveira M, Morales L, Souza A, Silva G, Correa S, Santos W, Saraiva K, Teixeira AJ, Melo D, Silva M. 2015. Involvement of AOX and UCP pathways in the post-harvest ripening of papaya fruits. *J Plant Physiol*, doi: 10.1016/j.jplph.2015.10.001.

Ordog SH, Higgins VJ, Vanlerberghe GC. 2002. Mitochondrial alternative oxidase is not a critical component of plant viral resistance but may play a role in the hypersensitive response. *Plant Physiol*, **129**: 1858-1865.

Ort DR, Baker NR. 2002. A photoprotective role for O_2 as an alternative electron sink in photosynthesis? *Curr Opin Plant Biol,* **5**: 193-198.

Padmasree K, Padmavathi L, Raghavendra AS. 2002. Essentiality of mitochondrial oxidative metabolism for photosynthesis: optimization of carbon assimilation and protection against photoinhibition. *Crit Rev Biochem Mol Biol,* **37**: 71-119.

Padmasree K, Raghavendra AS. 1999a. Importance of oxidative electron transport over oxidative phosphorylation in optimizing photosynthesis in mesophyll protoplasts of pea (*Pisum sativum* L.). *Physiol Plant,* **105**: 546-553.

Padmasree K, Raghavendra AS. 1999b. Response of photosynthetic carbon assimilation in mesophyll protoplasts to restriction on mitochondrial oxidative metabolism: metabolites related to the redox status and sucrose biosynthesis. *Photosynth Res,* **62**: 231-239.

Padmasree K, Raghavendra AS. 1999c. Prolongation of photosynthetic induction as a consequence of interference with mitochondrial oxidative metabolism in mesophyll protoplasts of the pea (*Pisum sativum* L.). *Plant Science,* **142**: 29-36.

Padmasree K, Raghavendra AS. 2001. Consequence of restricted mitochondrial oxidative metabolism on photosynthetic carbon assimilation in mesophyll protoplasts: decrease in light activation of four chloroplastic enzymes. *Physiol Plant,* **112**: 582-588.

Pádua M, Aubert S, Casimiro A, Bligny R, Millar AH, Day DA. 1999. Induction of alternative oxidase by excess copper in sycamore cell suspensions. *Plant Physiol Biochem,* **37**: 131-137.

Panda SK, Sahoo L, Katsuhara M, Matsumoto H. 2013. Overexpression of alternative oxidase gene confers aluminum tolerance by altering the respiratory capacity and the response to oxidative stress in tobacco cells. *Mol Biotech,* **54**: 551-563.

Papagianni M, Avramidis N. 2012. Cloning and functional expression of the mitochondrial alternative oxidase gene (*aox1*) of *Aspergillus niger* in *Lactococcus lactis* and its induction by oxidizing conditions. *Enzyme Microb Technol,* **50**: 17-21.

Pasqualini S, Reale L, Calderini O, Pagiotti R, Ederli L. 2012. Involvement of protein kinases and calcium in the NO-signalling cascade for defence-gene induction in ozonated tobacco plants. *J Exp Bot,* **63**: 4485-4496.

Peltier G, Cournac L. 2002. Chlororespiration. *Annu Rev Plant Biol,* **53**: 523-550.

Peng L, Yamamoto H, Shikanai T. 2011. Structure and biogenesis of the chloroplast NAD (P) H dehydrogenase complex. *Biochim Biophys Act,* **1807**: 945-953.

Perotti VE, Moreno AS, Podestá FE. 2014. Physiological aspects of fruit ripening: the mitochondrial connection. *Mitochondrion,* **17**: 1-6.

Perrone GG, Tan S-X, Dawes IW. 2008. Reactive oxygen species and yeast apoptosis. *Biochim Biophys Act,* **1783**: 1354-1368.

Planchet E, Jagadis Gupta K, Sonoda M, Kaiser WM. 2005. Nitric oxide emission from tobacco leaves and cell suspensions: rate limiting factors and evidence for the involvement of mitochondrial electron transport. *Plant J,* **41**: 732-743.

Prado C, Rosa M, Pagano E, Prado F. 2013. Metabolic interconnectivity among alternative respiration, residual respiration, carbohydrates and phenolics in leaves of *Salvinia minima* exposed to Cr (VI). *Environ Exp Bot,* **87**: 32-38.

Purvis AC. 1997. Role of the alternative oxidase in limiting superoxide production by plant mitochondria. *Physiol Plant,* **100**: 165-170.

Queval G, Noctor G. 2007. A plate reader method for the measurement of NAD, NADP, glutathione, and ascorbate in tissue extracts: Application to redox profiling during *Arabidopsis* rosette development. *Anal Biochem,* **363**: 58-69.

Raghavendra AS, Padmasree K, Saradadevi K. 1994. Interdependence of photosynthesis and respiration in plant cells: interactions between chloroplasts and mitochondria. *Plant Sci,* **97**: 1-14.

Raghavendra AS, Padmasree K. 2003. Beneficial interactions of mitochondrial metabolism with photosynthetic carbon assimilation. *Trends Plant Sci,* **8**: 546-53.

Rasmusson AG, Soole KL, Elthon TE. 2004. Alternative NAD(P)H dehydrogenases of plant mitochondria. *Annu Rev Plant Biol,* **55**: 23-39.

Ravet K, Pilon M. 2013. Copper and iron homeostasis in plants: the challenges of oxidative stress. *Antioxid Redox Signal,* **19**: 919-932.

Rhoads DM, Subbaiah CC. 2007. Mitochondrial retrograde regulation in plants. *Mitochondrion,* **7**: 177-194.

Rhoads DM, Umbach AL, Subbaiah CC, Siedow JN. 2006. Mitochondrial reactive oxygen species. Contribution to oxidative stress and interorganellar signaling. *Plant Physiol,* **141**: 357-366.

Rhoads DM, Umbach AL, Sweet CR, Lennon AM, Rauch GS, Siedow JN. 1998. Regulation of the Cyanide-resistant Alternative Oxidase of Plant Mitochondria: Identification of the cysteine residue involved in α-keto acid stimulation and intersubunit disulfide bond formation. *J Biol Chem,* **273**: 30750-30756.

Ribas-Carbo M, Aroca R, Gonzàlez-Meler MA, Irigoyen JJ, Sánchez-Díaz M. 2000. The electron partitioning between the cytochrome and alternative respiratory pathways during chilling recovery in two cultivars of maize differing in chilling sensitivity. *Plant Physiol,* **122**: 199-204.

Rietsch A, Beckwith J. 1998. The genetics of disulfide bond metabolism. *Annu Rev Genet,* **32**: 163-184.

Rizhsky L, Liang H, Mittler R. 2002. The combined effect of drought stress and heat shock on gene expression in tobacco. *Plant Physiol,* **130**: 1143-1151.

Rizhsky L, Liang H, Mittler R. 2003. The water-water cycle is essential for chloroplast protection in the absence of stress. *J Biol Chem,* **278**: 38921-38925.

Rogov A, Sukhanova E, Uralskaya L, Aliverdieva D, Zvyagilskaya R. 2014. Alternative oxidase: Distribution, induction, properties, structure, regulation, and functions. *Biochem (Moscow),* **79**: 1615-1634.

Rogov A, Zvyagilskaya R. 2015. Physiological role of alternative oxidase (from yeasts to plants). *Biochem (Moscow),* **80**: 400-407.

Rosso D, Bode R, Li W, Krol M, Saccon D, Wang S, Schillaci LA, Rodermel SR, Maxwell DP, Hüner NP. 2009. Photosynthetic redox imbalance governs leaf sectoring in the *Arabidopsis thaliana* variegation mutants *immutans*, spotty, *var1*, and *var2*. *Plant Cell,* **21**: 3473-3492.

Ruiz OH, Gonzalez A, Almeida AJ, Tamayo D, Garcia AM, Restrepo A, McEwen JG. 2011. Alternative oxidase mediates pathogen resistance in *Paracoccidioides brasiliensis* infection. *PLoS Negl Trop Dis,* **5**: e1353.

Rustin P, Jacobs HT. 2009. Respiratory chain alternative enzymes as tools to better understand and counteract respiratory chain deficiencies in human cells and animals. *Physiol Plant,* **137**: 362-370.

Sagardoy R, Morales F, López-Millán AF, Abadía A, Abadía J. 2009. Effects of zinc toxicity on sugar beet (*Beta vulgaris* L.) plants grown in hydroponics. *Plant Biol,* **11**: 339-350.

Sagi M, Fluhr R. 2006. Production of reactive oxygen species by plant NADPH oxidases. *Plant Physiol,* **141**: 336-40.

Saisho D, Nakazono M, Tsutsumi N, Hirai A. 2001. ATP synthesis inhibitors as well as respiratory inhibitors increase steady-state level of alternative oxidase mRNA in *Arabidopsis thaliana*. *J Plant Physiol,* **158**: 241-245.

Saisho D, Nambara E, Naito S, Tsutsumi N, Hirai A, Nakazono M. 1997. Characterization of the gene family for alternative oxidase from *Arabidopsis thaliana*. *Plant Mol Biol,* **35**: 585-96.

Saradadevi K, Raghavendra AS. 1992. Dark Respiration Protects Photosynthesis Against Photoinhibition in Mesophyll Protoplasts of Pea (*Pisum sativum*). *Plant Physiol,* **99**: 1232-7.

Scheibe R. 2004. Malate valves to balance cellular energy supply. *Physiol Plant,* **120**: 21-26.

Scheibe R, Backhausen JE, Emmerlich V, Holtgrefe S. 2005. Strategies to maintain redox homeostasis during photosynthesis under changing conditions. *J Exp Bot,* **56**: 1481-1489.

Schiff M, Bénit P, Jacobs HT, Vockley J, Rustin P. 2012. Therapies in inborn errors of oxidative metabolism. *Trends Endocrinol Metab,* **23**: 488-495.

Schmitt ME, Brown TA, Trumpower BL. 1990. A rapid and simple method for preparation of RNA from *Saccharomyces cerevisiae*. *Nucleic Acids Res,* **18**: 3091-3092.

Schonbaum GR, Bonner WD, Storey BT, Bahr JT. 1971. Specific inhibition of the cyanide-insensitive respiratory pathway in plant mitochondria by hydroxamic acids. *Plant Physiol,* **47**: 124-128.

Schwarzländer M, Finkemeier I. 2013. Mitochondrial energy and redox signaling in plants. *Antioxid Redox Signal,* **18**: 2122-2144.

Searle SY, Bitterman DS, Thomas S, Griffin KL, Atkin OK, Turnbull MH. 2011a. Respiratory alternative oxidase responds to both low-and high-temperature stress in *Quercus rubra* leaves along an urban–rural gradient in New York. *Functional Ecology,* **25**: 1007-1017.

Searle SY, Thomas S, Griffin KL, Horton T, Kornfeld A, Yakir D, Hurry V, Turnbull MH. 2011b. Leaf respiration and alternative oxidase in field-grown alpine grasses respond to natural changes in temperature and light. *New Phytol,* **189**: 1027-1039.

Seki M, Narusaka M, Ishida J, Nanjo T, Fujita M, Oono Y, Kamiya A, Nakajima M, Enju A, Sakurai T. 2002. Monitoring the expression profiles of 7000 *Arabidopsis* genes under drought, cold and high-salinity stresses using a full-length cDNA microarray. *Plant J,* **31**: 279-292.

Shen B, Jensen RG, Bohnert HJ. 1997. Increased resistance to oxidative stress in transgenic plants by targeting mannitol biosynthesis to chloroplasts. *Plant Physiol,* **113**: 1177-1183.

Shiba T, Kido Y, Sakamoto K, Inaoka DK, Tsuge C, Tatsumi R, Takahashi G, Balogun EO, Nara T, Aoki T. 2013. Structure of the trypanosome cyanide-insensitive alternative oxidase. *Proc Natl Acad Sci* U S A, **110**: 4580-4585.

Shikanai T. 2007. Cyclic electron transport around photosystem I: genetic approaches. *Annu Rev Plant Biol,* **58**: 199-217.

Shikanai T. 2014. Central role of cyclic electron transport around photosystem I in the regulation of photosynthesis. *Curr Opin Biotechnol,* **26**: 25-30.

Shukla P, Singh S, Dubey P, Singh A, Singh A. 2015. Nitric oxide mediated amelioration of arsenic toxicity which alters the alternative oxidase (*Aox1*) gene expression in Hordeum vulgare L. *Ecotoxicol Environ Saf,* **120**: 59-65.

Siedow JN, Umbach AL, Moore AL. 1995. The active site of the cyanide-resistant oxidase from plant mitochondria contains a binuclear iron center. *FEBS Lett,* **362**: 10-14.

Sieger SM, Kristensen BK, Robson CA, Amirsadeghi S, Eng EW, Abdel-Mesih A, Moller IM, Vanlerberghe GC. 2005. The role of alternative oxidase in modulating carbon use efficiency and growth during macronutrient stress in tobacco cells. *J Exp Bot,* **56**: 1499-515.

Simons BH, Millenaar FF, Mulder L, Van Loon LC, Lambers H. 1999. Enhanced Expression and Activation of the Alternative Oxidase during Infection of *Arabidopsis* with *Pseudomonas syringae* pv tomato. *Plant Physiol,* **120**: 529-538.

Smirnoff N. 2000. Ascorbic acid: metabolism and functions of a multi-facetted molecule. *Curr Opin Plant Biol,* **3**: 229-35.

Smirnoff N, Wheeler GL. 2000. Ascorbic acid in plants: biosynthesis and function. *Crit Rev Biochem Mol Biol,* **35**: 291-314.

Smith CA, Melino VJ, Sweetman C, Soole KL. 2009. Manipulation of alternative oxidase can influence salt tolerance in *Arabidopsis thaliana*. *Physiol Plant,* **137**: 459-472.

Strodtkötter I, Padmasree K, Dinakar C, Speth B, Niazi PS, Wojtera J, Voss I, Do PT, Nunes-Nesi A, Fernie AR, Linke V, Raghavendra AS, Scheibe R. 2009. Induction of the AOX1D isoform of alternative oxidase in *A. thaliana* T-DNA insertion lines lacking isoform AOX1A is insufficient to optimize photosynthesis when treated with antimycin A. *Mol Plant,* **2**: 284-97.

Sugie A, Naydenov N, Mizuno N, Nakamura C, Takumi S. 2006. Overexpression of wheat alternative oxidase gene *Waox1a* alters respiration capacity and response to reactive oxygen species under low temperature in transgenic *Arabidopsis*. *Genes Genetic sys,* **81**: 349-354.

Sun X, Wen T. 2011. Physiological roles of plastid terminal oxidase in plant stress responses. *J Biosci,* **36**: 951-956.

Suzuki N, Koussevitzky S, Mittler R, Miller G. 2012. ROS and redox signalling in the response of plants to abiotic stress. *Plant Cell Environ,* **35**: 259-270.

Sweetlove LJ, Lytovchenko A, Morgan M, Nunes-Nesi A, Taylor NL, Baxter CJ, Eickmeier I, Fernie AR. 2006. Mitochondrial uncoupling protein is required for efficient photosynthesis. *Proc Natl Acad Sci* U S A, **103**: 19587-19592.

Taira Y, Okegawa Y, Sugimoto K, Abe M, Miyoshi H, Shikanai T. 2013. Antimycin A-like molecules inhibit cyclic electron transport around photosystem I in ruptured chloroplasts. *FEBS Open Bio,* **3**: 406-10.

Talla S, Riazunnisa K, Padmavathi L, Sunil B, Rajsheel P, Raghavendra AS. 2011. Ascorbic acid is a key participant during the interactions between chloroplasts and mitochondria to optimize photosynthesis and protect against photoinhibition. *J Biosci,* **36**: 163-173.

Tang H, Zhang D-w, Yuan S, Zhu F, Xu F, Fu F-Q, Wang S-x, Lin H-H. 2014. Plastid signals induce alternative oxidase expression to enhance the cold stress tolerance in *Arabidopsis thaliana*. *Plant Growth Regul,* **74**: 275-283.

Thomma BP, Penninckx IA, Cammue BP, Broekaert WF. 2001. The complexity of disease signaling in *Arabidopsis*. *Curr Opin Immunol,* **13**: 63-68.

Tosti N, Pasqualini S, Borgogni A, Ederli L, Falistocco E, Crispi S, Paolocci F. 2006. Gene expression profiles of O_3-treated *Arabidopsis* plants. *Plant Cell Environ,* **29**: 1686-702.

Tóth SZ, Schansker G, Garab G. 2013. The physiological roles and metabolism of ascorbate in chloroplasts. *Physiol Plant,* **148**: 161-75.

Towbin H, Staehelin T, Gordon J. 1979. Electrophoretic transfer of proteins from polyacrylamide gels to nitrocellulose sheets: procedure and some applications. *Proc Natl Acad Sci* U S A, **76**: 4350-4354.

Triantaphylidès C, Havaux M. 2009. Singlet oxygen in plants: production, detoxification and signaling. *Trends Plant Sci,* **14**: 219-228.

Tripathy BC, Oelmüller R. 2012. Reactive oxygen species generation and signaling in plants. *Plant Signal Behav,* **7**: 1621-1633.

Tudella VG, Curti C, Soriani FM, Santos AC, Uyemura SA. 2004. In situ evidence of an alternative oxidase and an uncoupling protein in the respiratory chain of *Aspergillus fumigatus*. *Int J Biochem Cell Biol,* **36**: 162-172.

Turrens JF. 1997. Superoxide production by the mitochondrial respiratory chain. *Biosci Rep,* **17**: 3-8.

Umbach AL, Fiorani F, Siedow JN. 2005. Characterization of transformed *Arabidopsis* with altered alternative oxidase levels and analysis of effects on reactive oxygen species in tissue. *Plant Physiol,* **139**: 1806-20.

Umbach AL, Lacey EP, Richter SJ. 2009. Temperature-sensitive alternative oxidase protein content and its relationship to floral reflectance in natural *Plantago lanceolata* populations. *New Phytol,* **181**: 662-671.

Umbach AL, Siedow JN. 1993. Covalent and noncovalent dimers of the cyanide-resistant alternative oxidase protein in higher plant mitochondria and their relationship to enzyme activity. *Plant Physiol,* **103**: 845-854.

Van Aken O, Giraud E, Clifton R, Whelan J. 2009. Alternative oxidase: a target and regulator of stress responses. *Physiol Plant,* **137**: 354-361.

Vanlerberghe GC. 2013. Alternative Oxidase: A Mitochondrial Respiratory Pathway to Maintain Metabolic and Signaling Homeostasis during Abiotic and Biotic Stress in Plants. *Int J Mol Sci,* **14**: 6805-47.

Vanlerberghe GC, Cvetkovska M, Wang J. 2009. Is the maintenance of homeostatic mitochondrial signaling during stress a physiological role for alternative oxidase? *Physiol Plant,* **137**: 392-406.

Vanlerberghe GC, Cvetkovska M, Wang J. 2009. Is the maintenance of homeostatic mitochondrial signaling during stress a physiological role for alternative oxidase? *Physiol Plant,* **137**: 392-406.

Vanlerberghe GC, McIntosh L. 1992. Lower growth temperature increases alternative pathway capacity and alternative oxidase protein in tobacco. *Plant Physiol,* **100**: 115-119.

Vanlerberghe GC, McIntosh L. 1997. Alternative oxidase: From Gene to Function. *Annu Rev Plant Physiol Plant Mol Biol,* **48**: 703-734.

Vanlerberghe GC, Robson CA, Yip JY. 2002. Induction of mitochondrial alternative oxidase in response to a cell signal pathway down-regulating the cytochrome pathway prevents programmed cell death. *Plant Physiol,* **129**: 1829-1842.

Vassileva V, Simova-Stoilova L, Demirevska K, Feller U. 2009. Variety-specific response of wheat (*Triticum aestivum* L.) leaf mitochondria to drought stress. *J Plant Res,* **122**: 445-54.

Velikova V, Yordanov I, Edreva A. 2000. Oxidative stress and some antioxidant systems in acid rain-treated bean plants: protective role of exogenous polyamines. *Plant Sci,* **151**: 59-66.

Vidal G, Ribas-Carbo M, Garmier M, Dubertret G, Rasmusson AG, Mathieu C, Foyer CH, De Paepe R. 2007. Lack of respiratory chain complex I impairs alternative oxidase engagement and modulates redox signaling during elicitor-induced cell death in tobacco. *Plant Cell,* **19**: 640-655.

Voss I, Sunil B, Scheibe R, Raghavendra AS. 2013. Emerging concept for the role of photorespiration as an important part of abiotic stress response. *Plant Biol,* **15**: 713-722.

Wagner AM, Krab K, Wagner MJ, Moore AL. 2008. Regulation of thermogenesis in flowering Araceae: the role of the alternative oxidase. *Biochim Biophys Acta,* **1777**: 993-1000.

Walker D, Walker R. 1987. The use of the oxygen electrode and fluorescence probes in simple measurements of photosynthesis. University of Sheffield Press.

Wang H, Huang J, Liang X, Bi Y. 2012. Involvement of hydrogen peroxide, calcium, and ethylene in the induction of the alternative pathway in chilling-stressed *Arabidopsis* callus. *Planta,* **235**: 53-67.

Wang H, Liang X, Huang J, Zhang D, Lu H, Liu Z, Bi Y. 2010. Involvement of ethylene and hydrogen peroxide in induction of alternative respiratory pathway in salt-treated *Arabidopsis* calluses. *Plant Cell Physiol*, **51**: 1754-65.

Wang J, Rajakulendran N, Amirsadeghi S, Vanlerberghe GC. 2011. Impact of mitochondrial alternative oxidase expression on the response of *Nicotiana tabacum* to cold temperature. *Physiol Plant,* **142**: 339-51.

Wang J, Vanlerberghe GC. 2013. A lack of mitochondrial alternative oxidase compromises capacity to recover from severe drought stress. *Physiol Plant,* **149**: 461-473.

Watanabe CK, Hachiya T, Takahara K, Kawai M, Uchimiya H, Uesono Y, Terashima I, Noguchi K. 2010. Effects of AOX1a deficiency on plant growth, gene expression of respiratory components, and metabolic profile under low-nitrogen stress in *Arabidopsis thaliana* plants. *Plant Cell Physiol,* **51**: 810-822.

Watanabe CK, Hachiya T, Terashima I, Noguchi K. 2008. The lack of alternative oxidase at low temperature leads to a disruption of the balance in carbon and nitrogen metabolism, and to an up-regulation of antioxidant defence systems in *Arabidopsis thaliana* leaves. *Plant Cell Environ,* **31**: 1190-1202.

Watling JR, Robinson SA, Seymour RS. 2006. Contribution of the alternative pathway to respiration during thermogenesis in flowers of the sacred lotus. *Plant Physiol,* **140**: 1367-73.

Weber AP, Linka N. 2011. Connecting the plastid: transporters of the plastid envelope and their role in linking plastidial with cytosolic metabolism. *Annu Rev Plant Biol,* **62**: 53-77.

Wheeler GL, Grant CM. 2004. Regulation of redox homeostasis in the yeast *Saccharomyces cerevisiae*. *Physiol Plant,* **120**: 12-20.

Xia D, Yu CA, Kim H, Xia JZ, Kachurin AM, Zhang L, Yu L, Deisenhofer J. 1997. Crystal structure of the cytochrome bc1 complex from bovine heart mitochondria. *Science,* **277**: 60-6.

Xu F, Yuan S, Lin HH. 2011. Response of mitochondrial alternative oxidase (AOX) to light signals. *Plant Signal Behav,* **6**: 55-8.

Xu F, Yuan S, Zhang D-W, Lv X, Lin H-H. 2012a. The role of alternative oxidase in tomato fruit ripening and its regulatory interaction with ethylene. *J Exp Bot,* **63**: 5705-5716.

Xu F, Zhang DW, Wang JH, Zhang ZW, Wen L, Du JB, Shang J, Yuan M, Yuan S, Lin HH. 2012b. n-propyl gallate is an inhibitor to tomato fruit ripening. *J Food Biochem,* **36**: 657-666.

Xu T, Yao F, Liang W-S, Li Y-H, Li D-R, Wang H, Wang Z-Y. 2012c. Involvement of alternative oxidase in the regulation of growth, development, and resistance to oxidative stress of *Sclerotinia sclerotiorum*. *J Microbiol,* **50**: 594-602.

Yabuta Y, Mieda T, Rapolu M, Nakamura A, Motoki T, Maruta T, Yoshimura K, Ishikawa T, Shigeoka S. 2007. Light regulation of ascorbate biosynthesis is dependent on the photosynthetic electron transport chain but independent of sugars in *Arabidopsis*. *J Exp Bot,* **58**: 2661-71.

Yeremenko N, Jeanjean R, Prommeenate P, Krasikov V, Nixon PJ, Vermaas WF, Havaux M, Matthijs HC. 2005. Open reading frame ssr2016 is required for

antimycin A-sensitive photosystem I-driven cyclic electron flow in the cyanobacterium *Synechocystis* sp. PCC 6803. *Plant Cell Physiol,* **46**: 1433-1436.

Yoshida K, Noguchi K. 2009. Differential gene expression profiles of the mitochondrial respiratory components in illuminated *Arabidopsis* leaves. *Plant Cell Physiol,* **50**: 1449-1462.

Yoshida K, Shibata M, Terashima I, Noguchi K. 2010. Simultaneous determination of in vivo plastoquinone and ubiquinone redox states by HPLC-based analysis. *Plant Cell Physiol,* **51**: 836-841.

Yoshida K, Terashima I, Noguchi K. 2006. Distinct roles of the cytochrome pathway and alternative oxidase in leaf photosynthesis. *Plant Cell Physiol,* **47**: 22-31.

Yoshida K, Terashima I, Noguchi K. 2007. Up-regulation of mitochondrial alternative oxidase concomitant with chloroplast over-reduction by excess light. *Plant Cell Physiol,* **48**: 606-14.

Yoshida K, Watanabe C, Kato Y, Sakamoto W, Noguchi K. 2008. Influence of chloroplastic photo-oxidative stress on mitochondrial alternative oxidase capacity and respiratory properties: a case study with *Arabidopsis* yellow variegated 2. *Plant Cell Physiol,* **49**: 592-603.

Yoshida K, Watanabe CK, Hachiya T, Tholen D, Shibata M, Terashima I, Noguchi K. 2011a. Distinct responses of the mitochondrial respiratory chain to long- and short-term high-light environments in *Arabidopsis thaliana*. *Plant Cell Environ,* **34**: 618-28.

Yoshida K, Watanabe CK, Terashima I, Noguchi K. 2011b. Physiological impact of mitochondrial alternative oxidase on photosynthesis and growth in *Arabidopsis thaliana*. *Plant Cell Environ,* **34**: 1890-9.

Young L, Shiba T, Harada S, Kita K, Albury MS, Moore AL. 2013. The alternative oxidases: simple oxidoreductase proteins with complex functions. *Biochem. Soc. Trans,* **41**: 1305-1311.

Yruela I. 2005. Copper in plants. *Braz J Plant Physiol,* **17**: 145-156.

Zhang DW, Xu F, Zhang ZW, Chen YE, Du JB, Jia SD, Yuan S, Lin HH. 2010. Effects of light on cyanide-resistant respiration and alternative oxidase function in *Arabidopsis* seedlings. *Plant Cell Environ,* **33**: 2121-31.

Zhang DW, Yuan S, Xu F, Zhu F, Yuan M, Ye HX, Guo HQ, Lv X, Yin Y, Lin HH. 2014. Light intensity affects chlorophyll synthesis during greening process by metabolite signal from mitochondrial alternative oxidase in *Arabidopsis*. *Plant Cell Environ*. doi: 10.1111/pce.12438.

Zhang L-T, Zhang Z-S, Gao H-Y, Meng X-L, Yang C, Liu J-G, Meng Q-W. 2012. The mitochondrial alternative oxidase pathway protects the photosynthetic apparatus against photodamage in *Rumex* K-1 leaves. *BMC Plant Biol,* **12**: 40.

Zhang LT, Zhang ZS, Gao HY, Xue ZC, Yang C, Meng XL, Meng QW. 2011. Mitochondrial alternative oxidase pathway protects plants against photoinhibition by alleviating inhibition of the repair of photodamaged PSII through preventing formation of reactive oxygen species in *Rumex* K-1 leaves. *Physiol Plant,* **143**: 396-407.

Zhang P, Battchikova N, Jansen T, Appel J, Ogawa T, Aro E-M. 2004. Expression and functional roles of the two distinct NDH-1 complexes and the carbon acquisition complex NdhD3/NdhF3/CupA/Sll1735 in *Synechocystis* sp PCC 6803. *Plant Cell,* **16**: 3326-3340.

Copyright Acknowledgements

Statement of Publications

The research presented in this thesis has appeared or has been submitted as a series of original publications in refereed journals.

Chapter 4

Vishwakarma A, Bashyam L, Senthilkumaran B, Scheibe R, Padmasree K (2014) Physiological role of AOX1a in photosynthesis and maintenance of cellular redox homeostasis under high light in *Arabidopsis thaliana*. Plant Physiol Biochem. 81: 44-53.

Chapter 5

Vishwakarma A, Tetali SD, Selinski J, Scheibe R, Padmasree K (2015) Importance of alternative oxidase pathway in regulating cellular redox and ROS homeostasis to optimize photosynthesis during restriction of cytochrome oxidase pathway in *Arabidopsis thaliana*. Ann Bot. 116: 555-569.

Chapter 6

Vishwakarma A, Dalal A, Tetali SD, Kirti PB, Padmasree K (2015) Genetic engineering of *AtAOX1a* in *Saccharomyces cerevisiae* prevents oxidative damage and maintains redox homeostasis (Submitted to FEBS Open Bio).

Conferences attended

Poster presentation

Vishwakarma A, Scheibe R and Padmasree K (2013) Physiological impact of alternative oxidase 1a against photoinhibition in *Arabidopsis thaliana*: Role of redox and ROS. Indo-Japan workshop on "Signal sensing and transduction in photosynthetic organisms – from cyanobacteria to land plant", University of Hyderabad, Hyderabad, 16-18 December.

Vishwakarma A, Scheibe R and Padmasree K (2013) Importance of AOX1a in sustaining photosynthesis and alleviating reactive oxygen species under high light in *Arabidopsis thaliana*. International conference on "Photosynthesis Research for Sustainability", Baku, Azerbaijan, 05 - 09 June.

Vishwakarma A, Dinakar C and Padmasree K (2010) Effects of AOX1a deficiency on Photosynthesis, Reactive Oxygen Species, Antioxidants and Redox metabolism in presence of Antimycin A in *Arabidopsis thaliana*. "National conference of Plant Physiology", Banaras Hindu University, India, 25-27 November.

Vishwakarma A, Dinakar C and Padmasree K (2009) Significance of ROS in mediating beneficial interactions between chloroplasts and mitochondria in light. National symposium on "Frontiers in Photobiology", Bhabha Atomic Research Centre, Mumbai, India, 24-26 August (**Best poster award**).

Oral presentation

Vishwakarma A and Padmasree K (2014) Physiological role of AOX1a in photosynthesis and maintenance of cellular redox homeostasis under high light in *Arabidopsis thaliana*. "Annual Research Awards 2013-14", Dr. K. V. Rao Scientific Society, Hyderabad, India, 22 March.

Vishwakarma A and Padmasree K (2012) Importance of AOX1A in optimizing photosynthesis in *Arabidopsis thaliana* under high light stress. "Plant Science Colloquium", University of Hyderabad, Hyderabad, India, 10 January.

Publications

1. **Vishwakarma A**, Tetali SD, Selinski J, Scheibe R, Padmasree K (2015) Importance of alternative oxidase pathway in regulating cellular redox and ROS homeostasis to optimize photosynthesis during restriction of cytochrome oxidase pathway in *Arabidopsis thaliana*. Ann Bot. 116: 555-569.
2. **Vishwakarma A**, Bashyam L, Senthilkumaran B, Scheibe R, Padmasree K (2014) Physiological role of AOX1a in photosynthesis and maintenance of cellular redox homeostasis under high light in *Arabidopsis thaliana*. Plant Physiol Biochem. 81: 44-53.
3. Dalal A, **Vishwakarma A**, Singh NK, Gudla T, Bhattacharyya MK, Padmasree K, Viehhauser A, Dietz KJ, Kirti PB (2014) Attenuation of hydrogen peroxide-mediated oxidative stress by *Brassica juncea* annexin-3 counteracts thiol-specific antioxidant (TSA1) deficiency in *Saccharomyces cerevisiae*. FEBS Lett. 588: 584-593.
4. Dinakar C, **Abhaypratap V**, Yearla SR, Raghavendra AS, Padmasree K (2010) Importance of ROS and antioxidant system during the beneficial interactions of mitochondrial metabolism with photosynthetic carbon assimilation. Planta 231: 461-474.
5. **Vishwakarma A**, Dalal A, Tetali SD, Kirti PB, Padmasree K (2015) Genetic engineering of *AtAOX1a* in *Saccharomyces cerevisiae* prevents oxidative damage and maintains redox homeostasis (under revision in FEBS Open Bio).